UNIVERSIDADE FEDERAL DE PERNAMBUCO
CENTRO DE BIOCIÊNCIAS
PROGRAMA DE PÓS-GRADUAÇÃO EM BIOQUÍMICA E FISIOLOGIA

DESENVOLVIMENTO DE BIOSSENSORES ELETROQUÍMICOS BASEADOS EM NANOESTRUTURAS PARA O DIAGNÓSTICO ULTRASSENSÍVEL DO ONCOGENE QUIMÉRICO BCR/ABL

KAREN YASMIM PEREIRA DOS SANTOS AVELINO

Orientadora: Profª. Drª. Maria Danielly Lima de Oliveira
Coorientador: Prof. Dr. César Augusto Souza de Andrade

RECIFE
2017

KAREN YASMIM PEREIRA DOS SANTOS AVELINO

DESENVOLVIMENTO DE BIOSSENSORES ELETROQUÍMICOS BASEADOS EM NANOESTRUTURAS PARA O DIAGNÓSTICO ULTRASSENSÍVEL DO ONCOGENE QUIMÉRICO BCR/ABL

Dissertação apresentada como um dos requisitos para o cumprimento parcial das exigências para obtenção do título de Mestre em Bioquímica e Fisiologia pela Universidade Federal de Pernambuco.

Orientadora: Prof[a]. Dr[a]. Maria Danielly Lima de Oliveira

Coorientador: Prof. Dr. César Augusto Souza de Andrade

RECIFE
2017

Catalogação na Fonte:
Bibliotecário Bruno Márcio Gouveia, CRB-4/1788

Avelino, Karen Yasmim Pereira dos Santos
Desenvolvimento de biossensores eletroquímicos baseados em nanoestruturas para o diagnóstico ultrassensível do oncogene quimérico BCRL/ABL / Karen Yasmim Pereira dos Santos Avelino. – Recife, 2017.

162 f.: il.

Orientadores: Maria Danielly Lima de Oliveira, César Augusto Souza de Andrade
Dissertação (mestrado) – Universidade Federal de Pernambuco. Centro de Biociências. Programa de Pós-graduação em Bioquímica e Fisiologia, 2017.
Inclui referências e anexos

1. Leucemia 2. Nanotecnologia 3. Materiais nanoestruturados I. Oliveira, Maria Danielly Lima de (orient.) II. Andrade, César Augusto Souza de (coorient.) III. Título.

616.99419 CDD (22.ed.) UFPE/CB-2017-466

KAREN YASMIM PEREIRA DOS SANTOS AVELINO

DESENVOLVIMENTO DE BIOSSENSORES ELETROQUÍMICOS BASEADOS EM NANOESTRUTURAS PARA O DIAGNÓSTICO ULTRASSENSÍVEL DO ONCOGENE QUIMÉRICO BCR/ABL

Dissertação apresentada como um dos requisitos para o cumprimento parcial das exigências para obtenção do título de Mestre em Bioquímica e Fisiologia pela Universidade Federal de Pernambuco.

Banca Examinadora

_____

Profª. Drª. Maria Danielly Lima de Oliveira (Presidente – Orientadora)
Universidade Federal de Pernambuco – UFPE/Departamento de Bioquímica

_____

Prof. Dr. César Augusto Souza de Andrade (1° Titular – Membro Externo)
Universidade Federal de Pernambuco – UFPE/Departamento de Bioquímica

_____

Profª. Drª. Adriana Fontes (2° Titular – Membro Externo)
Universidade Federal de Pernambuco – UFPE/Departamento de Biofísica e Radiobiologia

_____

Prof. Dr. Kleber Gonçalves Bezerra Alves (3° Titular – Membro Externo)
Universidade Federal de Pernambuco – UFPE/Departamento de Engenharia Mecânica

_____

Profª. Drª. Maria Tereza dos Santos Correia (1° Suplente – Membro Interno)
Universidade Federal de Pernambuco – UFPE/Departamento de Bioquímica

_____

Dr. Isaac Aarón Morales Frias (2° Suplente – Membro Externo)
Universidade Federal de Pernambuco – UFPE/Departamento de Bioquímica

Data: 23/02/2017

Àqueles que me ensinaram a caminhar com amor e dignidade para conquista dos meus sonhos, meus pais.

AGRADECIMENTOS

Em primeiro lugar, agradeço a Deus por ter me fortalecido em momentos difíceis, nos quais eu pensei que não iria conseguir, por guiar meus passos e me ensinar que em sua presença eu nunca estarei desamparada. Contigo quero estar todos os dias da minha vida, tu és meu eterno amigo e protetor. A Ele minha maior gratidão.

Aos meus pais, ***Paulo*** *e* ***Maria****, fonte inesgotável de amor e compreensão, que iluminaram meu caminho com afeto e me ensinaram a viver com honestidade, não bastaria um muito obrigada. Agradeço-lhes por terem me proporcionado o maior bem que um dia poderia desejar, a educação. Como vocês sempre mencionaram, através dela posso realizar todos os meus sonhos. Não há palavras que expressem este sentimento único de reconhecimento. Que o nosso Senhor me permita um dia retribuir tudo o que fazem por mim, amo vocês incondicionalmente.*

Ao meu irmão e cúmplice, ***Paulo Victor****. Obrigada por acreditar em minha vitória e estar sempre presente em minha vida. Amo-te em todas as circunstâncias.*

Aos meus familiares, em especial, ao meu avó ***José Lopes*** *(in memoriam), por todo amor e cuidado. Gostaria que o senhor estivesse comigo, mas tenho a certeza que estás zelando por mim ao lado do nosso Deus.*

Aos meus mestres, minha orientadora ***Profª. Drª. Maria Danielly*** *e ao* ***Prof. Dr. César Andrade****. Ao longo destes sete anos vocês exerceram um papel imprescindível em minha formação profissional e pessoal. Infelizmente não tenho como descrever de forma separada os ensinamentos e as influências que cada um teve em minha vida. Elas foram complementares e indissociáveis. Por cada ensinamento, oportunidade, reconhecimento, confiança e compreensão, serei eternamente grata*

Às minhas queridas amigas, ***Bárbara Nascimento****,* ***Bárbara Santos****,* ***Isabelly*** *e* ***Ruana*** *pela amizade duradoura e verdadeira, apoio e compreensão nos momentos de ausência. Desejo que estejamos sempre unidas, compartilhando as diferentes fases de nossas vidas, as conquistas e as dificuldades ao longo dos anos.*

Aos meus amigos, ***Alisson, Brenda, Ellyson****,* ***Flávia****,* ***Giselle, Jéssica****,* ***Marilena****,* ***Maurília****,* ***Natália****,* ***Pedro*** *e* ***Vinícius*** *por todo o carinho, incentivo, apoio e alegria plena.*

Aos companheiros do ***Grupo Biodispositivos Nanoestruturados****, Alberto, Érico, Estéfani, Felipe, Gustavo, Ítala, Kalline, Maryana, Rafael, Raíza, Raquel, Sandra e, especialmente, Isaac, por toda ajuda e conhecimento que tanto contribuíram para minha pesquisa.*

Ao ***Prof. Dr. Celso Pinto de Melo*** *do Laboratório de Polímeros Não-Convencionais do Departamento de Física/UFPE e à* ***Profª. Drª. Norma Lucena Cavalcanti Licinio da Silva*** *do Laboratório de Imunogenética do Centro de Pesquisas Aggeu Magalhães/Fiocruz pela colaboração e assistência, imprescindíveis para a conclusão deste objetivo.*

A todos os professores, alunos e funcionários do Programa de Pós-Graduação em Bioquímica e Fisiologia.

Ao Conselho Nacional de Desenvolvimento Científico e Tecnológico pelo apoio financeiro.

Enfim, a todos que incentivaram e me apoiaram a desenvolver este trabalho, meu muito obrigado.

É o tempo da travessia: e, se não ousarmos fazê-la, teremos ficado, para sempre, à margem de nós mesmos.

- Fernando Teixeira

RESUMO

A avaliação da presença do oncogene quimérico BCR/ABL possibilita um diagnóstico precoce do câncer e o monitoramento de células leucêmicas residuais, especialmente, após o transplante de medula óssea. O desenvolvimento de ensaios moleculares efetivos para a detecção do oncogene quimérico BCR/ABL é de grande interesse para a promoção da saúde de pacientes com leucemia. Diante desta problematização, esta dissertação tem o objetivo de desenvolver dois tipos de biossensores eletroquímicos utilizando diferentes nanomateriais com a finalidade de obter baixos limites de detecção, necessários para o diagnóstico ultrassensível e monitoramento do oncogene quimérico BCR/ABL. Os biossensores foram obtidos a partir das seguintes metodologias: a) imobilização eletrostática de uma sonda de DNA sobre uma superfície transdutora de ouro modificada com compósito híbrido de nanopartículas de ouro e polianilina (AuNpsPANI) e b) imobilização química de uma sonda de DNA aminada sobre uma superfície de ouro modificada com cisteína (Cys), nanotubos de carbono de paredes múltiplas com grupos carboxílicos (cMWCNT) e nanopartículas de óxido de zinco funcionalizadas com aminopropiltrietoxisilano (ZnONp/NH_2). As técnicas de voltametria cíclica (VC) e espectroscopia de impedância eletroquímica (EIE) foram utilizadas para a caracterização e compreensão dos processos físico-químicos interfaciais. Ao avaliar o desempenho analítico dos sistemas sensores com amostras de plasmídeos recombinantes contendo o oncogene quimérico BCR/ABL, foram observadas alterações nas correntes amperométricas e nos valores de resistência à transferência de carga (R_{CT}). Em oposição, nenhuma resposta significativa foi obtida durante o estudo de seletividade com sequências gênicas não-complementares. As micrografias de microscopia de força atômica (AFM) demonstraram mudanças nos perfis topográficos dos biossensores após sua exposição ao oncogene quimérico BCR/ABL. Apesar de ambos os biossensores apresentarem elevada reprodutibilidade, rápido tempo de resposta e efetividade para a identificação do oncogene quimérico BCR/ABL em amostras de cDNA de pacientes com leucemia, o biossensor baseado em Cys-cMWCNT-ZnONp/NH_2 demonstrou sensibilidade superior com um limite de detecção de 6,94 aM. Portanto, as plataformas biossensíveis desenvolvidas podem ser consideradas ferramentas promissoras para o diagnóstico do oncogene quimérico BCR/ABL e monitoramento de níveis mínimos de doença residual.

Palavras-chave: Biossensor. Nanopartículas. Nanotubos de carbono. Oncogene BCR/ABL.

ABSTRACT

The evaluation of the presence of the BCR/ABL fusion gene allows an early diagnosis of cancer and the monitoring of residual leukemic cells, especially after the bone marrow transplantation. The development of effective molecular assays for the detection of the BCR/ABL fusion gene is of great interest for the promotion of the health of patients with leukemia. In view of this problematization, this dissertation aims to develop two types of electrochemical biosensors using different nanomaterials in order to obtain low detection limits, necessary for the ultrasensitive diagnosis and monitoring of the BCR/ABL fusion gene. The biosensors were obtained from the following methodologies: a) electrostatic immobilization of a DNA probe on a gold transducer surface modified with hybrid composite of gold nanoparticles and polyaniline (AuNpsPANI) and b) chemical immobilization of an aminated DNA probe on a gold surface modified with) cysteine (Cys), carboxylated multiwalled carbon nanotubes (cMWCNT) and aminopropyltriethoxysilane functionalized zinc oxide nanoparticles (ZnONp/NH_2). The techniques of cyclic voltammetry (CV) and electrochemical impedance spectroscopy (EIS) were used for the characterization and understanding of the interfacial physico-chemical processes. When evaluating the analytical performance of the sensor systems with samples of recombinant plasmids containing the BCR/ABL fusion gene, were observed changes in the amperometric currents and in the charge transfer resistance (R_{CT}) values. In opposition, none significant response was obtained during the selectivity study with non-complementary gene sequences. The micrographs of atomic force microscopy (AFM) demonstrated modifications in the topographic profiles of the biosensors after their exposure to the BCR/ABL fusion gene. Although both biosensors showed high reproducibility, fast response time and effectiveness for the identification of the BCR/ABL fusion gene in cDNA samples of patients with leukemia, the biosensor based on Cys-cMWCNT-ZnONp/NH_2 demonstrated superior sensitivity with a detection limit of 6.94 aM. Hence, the developed biosensitive platforms can be considered promising tools for the identification of the BCR/ABL fusion gene and monitoring of minimum levels of residual disease.

Keywords: BCR/ABL oncogene. Biosensor. Carbon Nanotubes. Nanoparticles.

LISTA DE FIGURAS

LISTA DE ABREVIATURAS

as	Vibrações assimétricas
AFM	Microscopia de força atômica (do inglês *atomic force microscopy*)
APTES	Aminopropiltrietoxisilano
AuNps	Nanopartículas de ouro
AuNpsPANI	Compósito híbrido de nanopartículas de ouro e polianilina
cMWCNT	Nanotubos de carbono de múltiplas paredes com grupos carboxílicos (do ingês *carboxylated multiwalled carbon nanotubes*)
CNTs	Nanotubos de carbono (do ingles *carbon nanotubes*)
VC	Voltametria cíclica
Cys	Cisteína (do inglês *cysteine*)
dsDNA	DNA de cadeia dupla (do inglês *double-stranded DNA*)
EDC	1-etil-3-(3-dimetilaminopropil)carbodiimida
EIE	Espectroscopia de impedância eletroquímica
FISH	Hibridação *in situ* fluorescente (do inglês *fluorescent in situ hybridization*)
FTIR	Espectroscopia de infravermelho com transformada de Fourier (do inglês *Fourier Transform Infrared Spectroscopy*)
HIV	Vírus da imunodeficiência humana
ITO	Óxido de índio dopado com estanho (do inglês *indium tin oxide*)
LLA	Leucemia linfoide aguda
LMA	Leucemia mielóide aguda
LMC	Leucemia mielóide crônica
LNC	Leucemia neutrofílica crônica
MWCNTs	Nanotubos de carbono de múltiplas paredes (do inglês *multiwalled carbon nanotubes*)
NHS	N-hidroxissuccinimida
OMS	Organização Mundial da Saúde
PANI	Polianilina
PSA	Antígeno prostático específico (do inglês *prostate specific antigen*)
qRT-PCR	Transcrição reversa quantitativa em tempo real da reação em cadeia da polimerase (do inglês *quantitative real-time reverse-transcription*

	polymerase chain reaction)
s	Vibrações simétricas
ssDNA	DNA de cadeia simples (do inglês *single-stranded DNA*)
SWCNTs	Nanotubos de carbono de parede única (do inglês *single-walled carbon nanotubes*)
ZnONps	Nanopartículas de óxido de zinco (do inglês *zinc oxide nanoparticles*)
ZnONp/NH_2	Nanopartículas de óxido de zinco funcionalizadas com aminopropiltrietoxisilano
ZnONWs	Nanofios de óxido de zinco (do inglês *zinc oxide nanowires*)

LISTA DE SÍMBOLOS

C_{dl}	Capacitância da dupla camada
E	Potencial
I	Corrente elétrica
i_{pa}	Corrente de pico anódica
i_{pc}	Corrente de pico catódica
ne^-	Número de elétrons
O	Forma oxidada
R	Forma reduzida
R_{CT}	Resistência à transferência de carga (do inglês *resistance to charge transfer*)
R_S	Resistência da solução
Z	Impedância
Z'	Componente real da impedância
$-Z''$	Componente imaginária da impedância
Z_W	Impedância de Warburg
δ	Vibrações de flexão
ν	Vibrações de estiramento
ω	Frequência angular

SUMÁRIO

CAPÍTULO 1

1 INTRODUÇÃO

O câncer é um grupo de doenças caracterizadas pelo crescimento descontrolado e propagação de células anormais (KALIA, 2015). Entre os mais de 100 tipos de câncer, a leucemia é a principal desordem maligna que acomete crianças de até 15 anos de idade com uma prevalência de 30% sobre os casos de câncer diagnosticados (MILLER et al., 2016). Esta morbidade está relacionada às alterações cromossômicas que ocasionam transformações neoplásicas em células-tronco hematopoiéticas. O oncogene quimérico BCR/ABL é um biomarcador específico para casos de leucemia e sua identificação clínica determina a implementação de estratégias terapêuticas direcionadas e efetivas (SAWYERS, 2008). Este oncogene, comumente denominado de cromossomo *Philadelphia*, é obtido a partir da translocação recíproca entre os cromossomos 9 e 22 t(9;22) (HARRISON, 2001; CHEN et al., 2016). O oncogene quimérico BCR/ABL pode expressar três diferentes isoformas da proteína tirosino quinase ($p190^{BCR/ABL}$, $p210^{BCR/ABL}$ e $p230^{BCR/ABL}$) que estão associadas à patogênese de neoplasmas hematológicos, como a LMC e a leucemia linfoide aguda (LLA) (ADVANI; PENDERGAST, 2002; MULLIGHAN et al., 2008; BADGER-BROWN et al., 2013).

A avaliação da presença do oncogene quimérico BCR/ABL possibilita um diagnóstico precoce do câncer e o monitoramento da regressão da doença durante o tratamento. Além disso, torna possível a detecção de células leucêmicas residuais, especialmente após o transplante de medula óssea (WANG et al., 2014). Atualmente, os métodos de diagnóstico clínico e prognóstico utilizados para a identificação desta fusão gênica apresentam algumas limitações, como a necessidade de analistas especializados, experimentação dispendiosa e sensibilidade limitada (SHARMA et al., 2012). Logo, o desenvolvimento de novas metodologias para o diagnóstico e monitoramento do oncogene quimérico BCR/ABL é de suma relevância para os pacientes com leucemia.

Nos últimos anos, os avanços na nanociência e o desenvolvimento biotecnológico forneceram subsídios para a construção de novos testes de diagnóstico. Através da síntese de materiais em nanoescala, manipulação de material genético e imobilização de biomoléculas em superfícies sólidas, foi possível construir biossensores de DNA eletroquímicos (também denominados de genossensores eletroquímicos) (YANG; ZHANG, 2014). A estratégia funcional destes dispositivos é baseada na especificidade de sondas de DNA e na capacidade analítica dos métodos eletroquímicos de transdução de sinal (FRÍAS et al., 2015). Relatos na literatura indicam que os genossensores são tecnologias de última geração capazes de

melhorar o diagnóstico de doenças genéticas (CHEN; CHATTERJEE, 2013; JAYANTHI; DAS; SAXENA, 2016; RANJAN; ESIMBEKOVA; KRATASYUK, 2017). Estes permitem a detecção específica de sequências de nucleotídeos em concentrações mínimas com elevada sensibilidade e seletividade (COSTA et al., 2014; ROSARIO; MUTHARASAN, 2014).

Os principais desafios para a construção de biossensores eletroquímicos são a) a preservação da estrutura conformacional e a bioatividade das moléculas imobilizadas sobre superfícies transdutoras e b) melhoramento da sensibilidade para detectar mudanças sutis nas propriedades eletroquímicas do sensor, como por exemplo as alterações resultantes do processo de hibridação entre as sondas de DNA de cadeia simples (ssDNA) e a suas fitas complementares (alvo molecular) (PIVIDORI; MERKOCI; ALEGRET, 2000). Diante destes obstáculos, as plataformas nanoestruturadas surgem como uma alternativa inovadora para a obtenção de dispositivos com elevado desempenho analítico (PATEL et al., 2013; ROVINA; SIDDIQUEE, 2016).

Assumindo a premissa que as nanopartículas de ouro (AuNps), os nanotubos de carbono (CNTs) e as nanopartículas de óxido de zinco (ZnONps) compõe um grupo de elite das nanoestruturas com propriedades eletroquímicas altamente atrativas (HOLZINGER; LE GOFF; COSNIER, 2014; KUMAR et al., 2015; YÁÑEZ-SEDEÑO; CAMPUZANO; PINGARRÓN, 2017), novos biossensores de DNA foram desenvolvidos para o diagnóstico ultrassensível do oncogene quimérico BCR/ABL. Duas plataformas nanoestruturadas distintas baseadas em AuNpsPANI e Cys-cMWCNT-ZnONp/NH_2 foram construídas através das técnicas de automontagem e estruturação química, respectivamente. Em adição, ensaios clínicos foram realizados com amostras de cDNA de pacientes com leucemia para avaliação da bioatividade dos biossensores. Com base nos resultados obtidos e apresentados ao longo desta dissertação, as novas tecnologias desenvolvidas para a identificação do oncogene quimérico BCR/ABL podem ser consideradas ferramentas alternativas para caracterização de tumores hematológicos a nível molecular.

Para melhor compreensão, este trabalho foi estruturado em nove capítulos descritos a seguir.

- No primeiro capítulo foi apresentada a introdução, onde foi descrita a importância do desenvolvimento de novos dispositivos nanoestruturados para o diagnóstico molecular do oncogene quimérico BCR/ABL.
- No segundo capítulo foi apresentada a fundamentação teórica com a discussão dos seguintes tópicos: leucemia e o oncogene quimérico BCR/ABL; métodos convencionais de diagnóstico; avanços da nanotecnologia e o desenvolvimento

de biossensores; classificação dos biossensores quanto ao elemento receptor e transdutor; biossensores de DNA eletroquímicos; métodos de imobilização de DNA; plataformas nanoestruturas com ênfase nos seguintes materiais: compósito híbrido de AuNpsPANI, CNTs e ZnONps; técnicas eletroanalíticas (destaque para a voltametria cíclica e espectroscopia de impedância eletroquímica); microscopia de força atômica; e espectroscopia de infravermelho com transformada de Fourier.

- No terceiro capítulo estão descritos os objetivos geral e específicos.
- No quarto capítulo estão as referências da fundamentação teórica.
- No quinto e sexto capítulo foram apresentados os resultados obtidos no estudo em forma de dois artigos científicos intitulados de a) *Attomolar electrochemical detection of the BCR/ABL fusion gene based on an amplifying self-signal metal nanoparticle-conducting polymer hybrid composite* e b) *Nanostructured platform based on carbon nanotubes and zinc oxide nanoparticles for impedimetric determination of BCR/ABL fusion gene*.
- No sétimo e oitavo capítulo foram descritas, respectivamente, as conclusões e perspectivas da dissertação.
- No nono capítulo encontram-se os apêndices com os materiais suplementares dos artigos elaborados.
- Por fim, no décimo capítulo foram apresentadas as diretrizes da revista *Sensors and Actuators B: Chemical* utilizadas na formatação do artigo a ser submetido, intitulado de *Nanostructured platform based on carbon nanotubes and zinc oxide nanoparticles for impedimetric determination of BCR/ABL fusion gene*.

CAPÍTULO 2

2 FUNDAMENTAÇÃO TEÓRICA

2.1 Leucemia e o oncogene quimérico BCR/ABL

A leucemia é um dos tipos de câncer mais comum em todo o mundo com uma incidência anual de 250000 novos casos (FERLAY et al., 2012; MILLER et al., 2016). Esta morbidade é descrita como uma doença maligna que acomete células do sistema hematopoiético produzidas na medula óssea (CAZZOLA, 2016). Durante o desenvolvimento da leucemia ocorre uma produção exacerbada e descontrolada de células sanguíneas anormais e um aumento do número de células imaturas, como eritroblastos e linfoblatos (ADVANI; PENDERGAST, 2002). Como consequência, há uma diminuição das células sanguíneas saudáveis e funcionais, aumentando assim, a probabilidade da ocorrência de sangramentos, infecções e anemia grave (INAMDAR; BUESO-RAMOS, 2007). Ademais, as células leucêmicas podem realizar metástase através de um processo de infiltração, alcançando a circulação sistêmica e espalhando-se para outros órgãos como o baço, cérebro e linfonodos (INAMDAR; BUESO-RAMOS, 2007).

A designação leucemia compreende um grupo heterogêneo de doenças definidas por características clínicas, morfológicas, genotípicas e imunofenotípicas específicas (GUZMAN; ALLAN, 2014). Neste contexto, a prática clínica e a pesquisa científica proporcionam um suporte para a definição das doenças e obtenção de diagnósticos condizentes (VARDIMAN, 2010; EICHHORST et al., 2015; KOMANDURI; LEVINE, 2016).

A Organização Mundial da Saúde (OMS) classifica as leucemias de acordo com a linhagem da célula neoplásica em: mieloide, linfoide, histiocítica/dendrítica, neutrofílica, eosinofílica, mastocítica, basofílica, monoblástica, monocítica ou de linhagem ambígua. Em adição, as leucemias podem ser subclassificadas conforme sua evolução clínica em: agudas ou crônicas (ARBER et al., 2016).

As anormalidades genéticas são uma caraterística das neoplasias malignas humanas (GUARNERIO et al., 2016). Estas podem ser caracterizadas por variações no número de cópias de DNA e por aberrações na estrutura cromossômica decorrentes, por exemplo, de mutações e fusões gênicas (BOCHTLER, T.; FRÖHLING, S.; KRÄMER, 2015). A fusão gênica é uma recombinação de DNA que envolve a troca de material genético entre cromossomos ou entre regiões distintas de um mesmo cromossomo (GENT; HOEIJMAKERS; KANAAR, 2001). Os mecanismos moleculares responsáveis pela formação

de um gene híbrido são a translocação, deleção, inserção e inversão cromossômica (FEUK; CARSON; SCHERER, 2006). Frequentemente, em células neoplásicas ocorre a fusão oncogênica que inclui pelo menos um proto-oncogene no processo de recombinação de DNA. As proteínas derivadas da fusão oncogênica apresentam atividades anormais que contribuem para o desenvolvimento de câncer, como as leucemias (TEIXEIRA, 2006; MITELMAN et al., 2007; NERO et al., 2014).

O oncogene quimérico BCR/ABL é um dos principais biomarcadores para leucemia, sendo encontrado em mais de 90% dos pacientes adultos com LMC (NOWELL, 2007). Em crianças, esta anormalidade cromossômica é comum em casos de LLA de alto risco (NEUENDORFF et al., 2016). Através de um processo de translocação recíproca entre os braços longos do cromossomo 9 (que contém o proto-oncogene ABL) e o cromossomo 22 (que contém o gene BCR), gera-se o oncogene quimérico BCR/ABL (cromossomo *Philadelphia*) (Figura 1) (CHANDRA et al., 2011; HARRISON, 2001; CHEN et al., 2016). Durante este mecanismo molecular, ocorre a ativação do proto-oncogene ABL por meio de uma alteração estrutural. Como resultado, as células adquirem vantagens de crescimento e sobrevivência, tornando-se tumorais.

Figura 1. Mecanismo molecular da fusão gênica entre os cromossomos 9 e 22 e a formação do oncogene quimérico BCR/ABL

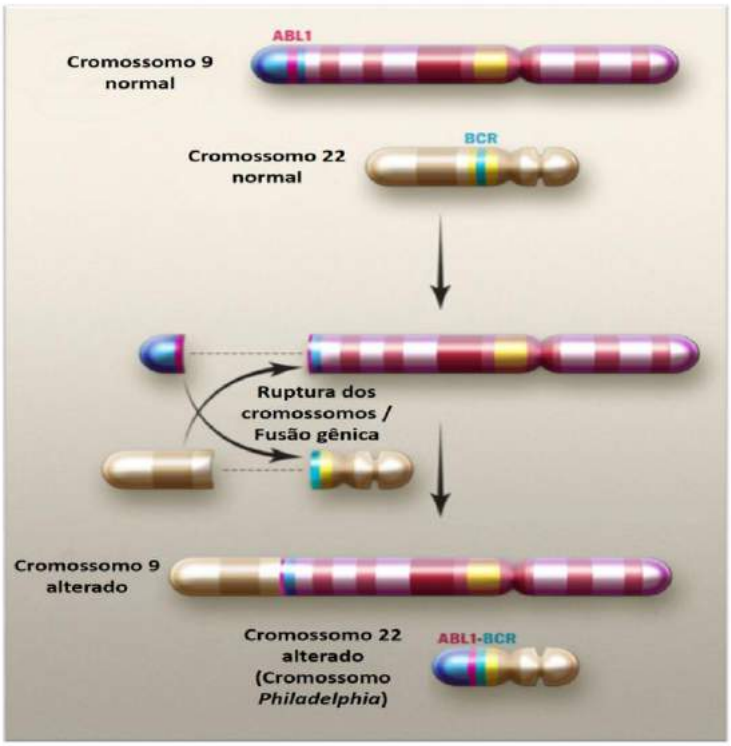

Fonte: adapatada de FAIRMAN STUDIOS, 2013.

O oncogene quimérico BCR/ABL codifica uma proteína tirosina quinase com atividade biológica desregulada (BEN-NERIAH, 1986; LI et al., 2017). Dependendo do ponto de ruptura no gene BCR, são produzidas três tipos de isoformas da oncoproteína, comumente denomidas de: $p190^{BCR/ABL}$, $p210^{BCR/ABL}$ e $p230^{BCR/ABL}$ (MELO, 1996; LYU et al., 2016). A $p190^{BCR/ABL}$ é uma isoforma pouco comum em pacientes com LMC, entretanto, é frequentemente encontrada em crianças com LLA. A $p210^{BCR/ABL}$ está presente na maioria dos pacientes com LMC em fase estável, sendo também identificada em alguns casos de LLA e leucemia mielóide aguda (LMA). A $p230^{BCR/ABL}$ é uma isoforma rara, no entanto, sua presença leva ao desenvolvimento de um quadro clínico distinto, designado de leucemia neutrofílica crônica (LNC) (LI; DU, 1998; MAURER et al., 1991; WINTER et al., 1999; LÓPEZ-ANDRADE et al., 2016).

No curso da leucemia, o oncogene quimérico BCR/ABL pode estar presente no organismo em variáveis concentrações. Por exemplo, um paciente com leucemia no momento do diagnóstico clínico apresenta, frequentemente, elevados níveis do oncogene quimérico BCR/ABL, responsável pelas alterações patológicas. Em contrapartida, após a implentação de estratégias terapêuticas contra o câncer, o paciente pode apresentar um quadro de doença residual mínima. Este quadro é caracterizado pela presença de células leucêmicas residuais sem evidências clínicas da doença (DEL PRINCIPE, et al., 2016). Nesta fase, há uma baixa concentração e expressão do oncogene quimérico BCR/ABL. O monitoramento da doença residual mínima é essencial para avaliar a resposta do paciente ao tratamento, delinear o risco de recorrência de leucemia e guiar decisões terapêuticas contra o câncer (SZCZEPANSKI, 2007; SUNG; LUGER, 2017). O monitoramento da doença residual mínima deve ser considerado pelos profissionais de saúde como uma prática clínica de rotina, uma vez que é um dos principais indicadores para o prognóstico de leucemia (VAN DONGEN et al., 2015; DEL PRINCIPE, et al., 2016). Assim, os métodos utilizados no monitoramento devem ter alta precisão e sensibilidade para detectar níveis mínimos da doença (VAN DONGEN et al., 2015).

2.1.1 Métodos convencionais de diagnóstico

O diagnóstico de leucemia pode ser obtido através de exames hematológicos, análises citogenéticas e ensaios moleculares (HALLEK et al., 2008; BENNOUR; SAAD; SENNANA, 2016). Inicialmente, o profissional habilitado, geralmente um médico, realiza a anamnese e o exame físico do paciente, considerando sua história clínica, sinais e sintomas. Posteriormente,

frente à uma suspeita de leucemia, uma amostra de sangue periférico será coletada para a realização de hemograma. Neste exame, através de um microscópio óptico, as células do sistema hematopoiético são avaliadas em relação à seu tipo, morfologia e número. Nos pacientes com leucemia são encontradas, frequentemente, células imaturas na corrente sanguínea, como os linfoblastos e eritroblastos. Em oposição, nota-se uma redução na quantidade de plaquetas e células maduras funcionais. Embora estes resultados possam sugerir um quadro leucemia, outros testes deverão ser realizados para a confirmação da doença, como por exemplo, a biópsia da medula óssea. Após a aspiração da medula óssea, a biópsia é realizada e os resultados obtidos poderão determinar o diagnóstico de leucemia. Entretanto, na maioria dos casos, análises citogenéticas e moleculares são requeridas para a identificação de biomarcadores específicos de leucemia, como o oncogene quimérico BCR/ABL (FEDERMANN et al., 2014; EICHHORST et al., 2015; AMERICAN CANCER SOCIETY, 2016).

Atualmente, os principais métodos usados para o diagnóstico do oncogene quimérico BCR/ABL compreendem a análise cromossômica (SOVERINI et al., 2011), hibridação *in situ* fluorescente (FISH) (CORBIN et al., 2011), citometria de fluxo (D'ALESSIO et al., 2011), análises de Southern blot (BENNOUR; SAAD; SENNANA, 2016) e transcrição reversa quantitativa em tempo real da reação em cadeia da polimerase (qRT-PCR) (BENNOUR et al., 2012). Apesar destes métodos de diagnóstico serem técnicas consolidadas que apresentam boa especificidade, algumas desvantagens, como a sensibilidade limitada, altos investimentos para aquisição e manutenção de equipamentos, protocolos experimentais complexos e longo tempo de análise, restringem seu amplo uso em áreas laboratoriais e hospitalares (SHARMA et al., 2012). Portanto, o desenvolvimento de ensaios moleculares simples e efetivos para a detecção do oncogene quimérico BCR/ABL é de grande interesse para a promoção da saúde de pacientes com leucemia (YEUNG; EGAN; RADICH, 2016).

2.2 Avanços da nanotecnologia e o desenvolvimento de biossensores

A nanociência tem um papel importante na inovação e no desenvolvimento de tecnologias, possibilitando a construção de novos testes de diagnóstico para inúmeras doenças. Esta atua em um campo de investigação multidisciplinar com a associação da biologia molecular, bioquímica, engenharia e física (PORTER; YOUTIE, 2009). Nas últimas duas décadas, foram descritas mais de 65000 citações e desde os anos 70, houve mais de 12000 invenções envolvendo a pesquisa nanotecnológica (KOSTOFF; KOYTCHEFF; LAU,

2007; CHEN et al., 2008a). Especialmente, na área de diagnósticos clínicos, o número de patentes relacionadas à nanotecnologia foi de 2200 entre os anos de 2000 e 2010. Além disso, espera-se que este valor duplique na próxima década (ANTUNES et al., 2012). Representando este progresso, os produtos nanotecnológicos disponíveis no mercado mundial movimentaram um capital de US$ 254 bilhões em 2009 (ROCO; MIRKIN; HERSAM, 2011). Em 2015, observou-se um crescimento nas operações financeiras de cerca de US$ 3 trilhões associadas à nanotecnologia (AITHAL, 2016).

A bionanotecnologia é uma subárea da nanotecnologia capaz de fornecer subsídios para o desenvolvimento de novos dispositivos de detecção baseados em componentes biológicos. Estes dispositivos são capazes de identificar uma grande variedade de microorganismos, vírus, enzimas e até mesmo anormalidades cromossômicas como o oncogene quimérico BCR/ABL (SUN; YU; SHEN, 2014; MATSISHIN et al., 2016; HWANG et al., 2017; JIN et al., 2017). Inúmeras são os campos de aplicação destes dispositivos que incluem a vida cotidiana, segurança alimentar, diagnósticos clínicos, monitoramento ambiental e controle de qualidade de produtos industriais (HENRY, 1990; ARDUINI et al., 2016). Em razão de sua grande aplicabilidade, um crescimento tem sido observado no número de estudos dedicados ao desenvolvimento de biossensores. Por exemplo, no ano 2000, o mercado global para os biossensores cresceu aproximadamente US$ 2 bilhões e espera-se um valor de US$ 17 bilhões em 2018 (TURNER, 2013; BAHADIR; SEZGINTÜRK, 2015; FADEL et al., 2016).

Neste cenário, define-se como biossensores os dispositivos eletrônicos capazes de fornecer informações analíticas específicas sobre alvos moleculares de forma quantitativa ou semi-quantitativa (SCHELLER et al., 2001). Estes dispositivos são constituídos por três unidades funcionais básicas: elemento receptor, transdutor e sistema de amplificação e processamento de sinal (SILVA et al., 2014) (Figura 2). O elemento receptor é representado por uma molécula biológica responsável pelo reconhecimento do alvo molecular através de interações intermoleculares específicas ou por meio de reações catalíticas. O transdutor é responsável por converter a resposta bioquímica oriunda do processo de biorreconhecimento em um sinal mensurável e proporcional à concentração do analito detectado. Por fim, o sistema eletrônico promove a amplificação e o processamento do sinal analítico, conduzindo-o para um monitor, onde o resultado é apresentado visualmente, podendo ser interpretado por analistas (D'ORAZIO, 2003; BAZIN et al., 2017).

Figura 2. Representação esquemática de um biossensor.

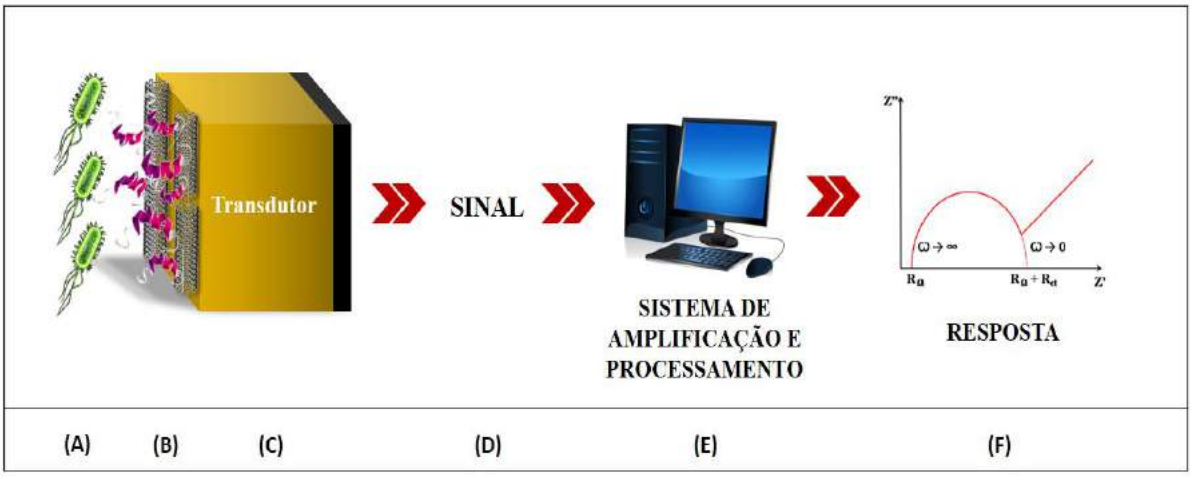

A detecção do analito (A) é realizada através de um componente biológico (B) associado a um transdutor (C). A superfície transdutora é responsável pela conversão da resposta bioquímica em um sinal mensurável (D) que será amplificado e processado por um software de computador (E), posteriormente, os dados experimentais serão apresentados na forma de gráficos (F). Fonte: adaptada de SILVA et al., 2014.

Dentre as várias características que definem um biossensor, destacam-se a funcionalidade, elevada sensibilidade, especificidade, seletividade, baixo limite de detecção, acurácia, precisão, linearidade, rápido tempo de resposta, reprodutibilidade, robustez, portabilidade, simplicidade, estabilidade, reusabilidade e baixo custo (LAZCKA; DEL CAMPO; MUNOZ, 2007; SCHMIDT et al., 2008; JUSTINO; ROCHA-SANTOS; DUARTE, 2010). Devido estas atrativas propriedades, os biossensores são considerados ferramentas promissoras para as análises clínicas e laboratoriais (JUSTINO; ROCHA-SANTOS; DUARTE, 2010). No entanto, estudos detalhados devem ser realizados para assegurar o potencial de uso e a comercialização destes métodos de biodetecção (HOBSON, 2016).

2.2.1 Classificação dos biossensores quanto ao elemento receptor

Diferentes elementos biológicos podem ser utilizados para a construção de sistemas biossensíveis, como por exemplo, tecidos vegetais ou animais, células, receptores celulares, organelas, enzimas, sistemas multienzimáticos, anticorpos, antígenos, ácidos nucléicos, aptâmeros, lectinas e microrganismos (GUAN; MIAO; ZHANG, 2004; OLIVEIRA et al., 2008; CAYGILL; BLAIR; MILLNER, 2010; SU et al., 2011; MITTAL et al., 2017). Apesar de haver inúmeros tipos de biorreceptores, a escolha adequada do elemento biológico é

essencial para assegurar a especificidade do biossensor a ser desenvolvido (VO-DINH; CULLUM, 2000).

Dentro deste contexto, os biossensores podem ser inicialmente classificados de acordo com o mecanismo de interação do elemento receptor com o analito e os eventos bioquímicos resultantes. Desta forma, designamos os biossensores em biocatalíticos ou de bioafinidade. Nos biossensores de bioafinidade, o receptor biológico reconhece o alvo molecular e forma um complexo estável capaz de gerar um sinal de transdução. Estes sistemas de biodetecção envolvem por exemplo, o uso de antígenos, anticorpos, lectinas e receptores proteicos. Assim, o equilíbrio é alcançado sem o consumo do analito pela molécula biológica imobilizada. Em oposição, nos biossensores catalíticos, o receptor biológico catalisa uma reação química caracterizada pela biotransformação do analito em subprodutos que serão posteriormente identificados. Neste caso, a interação receptor/analito é acompanhada por mudanças nas concentrações dos substratos ou produtos (THÉVENOT et al., 2001; MONOŠÍK; STREĎANSKÝ; ŠTURDÍK, 2012).

Os biossensores também podem ser classificados de acordo com a natureza do elemento receptor em:

- Biossensores enzimáticos: baseiam-se no uso de enzimas como elementos receptores. O princípio de detecção está relacionado ao consumo ou formação de substâncias químicas resultantes da interação enzima/analito (NEWMAN; SETFORD, 2006; SASSOLAS; BLUM; LECA-BOUVIER, 2012). Exemplos de enzimas utilizadas na construção de biossensores são a penicilinase (ZHI-ZHONG et al., 2016), urease (SAFITRI et al., 2017), álcool desidrogenase (BILGI; AYRANCI, 2016) e glicose oxidase (RAMANAVICIUS et al., 2017).

- Genossensores: são desenvolvidos a partir da imobilização de sequências de oligonucleotídeos capazes de viabilizar o reconhecimento molecular através de um processo específico de hibridação (PIVIDORI, M.I.; MERKOCI, A.; ALEGRET, 2000). Os fragmentos gênicos podem ser oriundos do ácido desoxirribonucleico (DNA) ou ácido ribonucleico (RNA) (JUSTINO et al., 2015). Entre as diversas aplicações dos genossensores, destaca-se o diagnóstico de doenças genéticas, neurológicas, infecciosas e neoplásicas, além das imunodeficiências (ABU-SALAH et al., 2015).

- Imunossensores: são baseados na imobilização de antígenos ou anticorpos na superfície do transdutor. O processo de biodetecção é caracterizado por uma reação imunológica que conduz a formação de complexos antígeno-anticorpo (LUPPA; SOKOLL; CHAN, 2001; PRODROMIDIS, 2010). Entre os analitos investigados pelos imunossensores destacam-se os hormônios protéicos ou esteroidais (CINCOTTO et al., 2016; MARTÍNEZ-GARCÍA, 2016), drogas (LEI, 2016), vírus (HAN et al., 2016), bactérias (PANDEY et al., 2017), toxinas alimentares (BAZIN et al., 2017) e poluentes ambientais, como os inseticidas (LI et al., 2016) e fungicidas (RAPINI; MARRAZZA, 2016).

- Aptassensores: nestes biodispositivos, aptâmeros são utilizados como elementos receptores (LIM; KOUZANI; DUAN, 2010). Aptâmeros são segmentos de oligonucleotídeos de fita simples (DNA ou RNA) que são sintetizados para adquirirem uma conformação estrutural com alta especificidade e afinidade para qualquer alvo de interesse farmacêutico ou biológico, como proteínas, íons e pequenas moléculas (FENG; DAI; WANG, 2014; MIODEK et al., 2014; LI et al., 2015; SONG et al., 2017). Em razão do elemento de biodetecção ser sintético e não possuir origem natural, os aptassensores são comumente chamados de biossensores miméticos ou artificiais (PERUMAL; HASHIM, 2014).

- Biossensores microbiológicos: são caracterizados pela imobilização de microrganismos sobre superfícies transdutoras. Nestes sistemas biossensíveis, as bactérias, leveduras e fungos atuam como elementos de biodetecção (LIM et al., 2015). As principais aplicações dos biossensores microbiológicos concentram-se, principalmente, no monitoramento ambiental e diagnóstico de doenças infecciosas (BEREZA-MALCOLM, L.T.; FRANKS, 2015; SUN et al., 2015).

- Biossensores celulares: baseiam-se no uso de células como elementos receptores. Muitos biossensores microbiológicos também são denominados de biossensores celulares. No entanto, a classe de biossensores celulares utiliza qualquer tipo de célula viva como elemento de biodetecção, seja ela oriunda de microrganismos ou não (LIU et al., 2014; PERUMAL; HASHIM, 2014). Em linhas gerais, estes biossensores apresentam uma versatilidade de uso, incluindo a detecção precoce de doenças crônicas, identificação de patógenos, monitoramento ambiental e testes toxicológicos.

Além destas aplicações, os biossensores celulares permitem a caracterização da ação de inúmeros fármacos sobre o sistema biológico, como o efeito das drogas antineoplásicas sobre as células do câncer (EDMONDSON et al., 2014; CHENG et al., 2015; HU et al., 2017).

2.2.2 Classificação dos biossensores quanto ao elemento transdutor

Conforme o sistema de transdução de sinal e o tipo de energia mensurada, os biossensores podem ser categorizados em:

- Biossensores ópticos: são biodispositivos que se baseiam em mudanças nas propriedades ópticas, com a finalidade de caracterizar o processo de construção de biossensores e monitorar a concentração do analito (DAMBORSKÝ; ŠVITEL; KATRLÍK, 2016). Entre as propriedades ópticas avaliadas, pode-se exemplificar a absorção e transmitância de energia eletromagnética, índice de refração, fluorescência, fosforescência e refletividade (ABDULHALIM; ZOUROB; LAKHTAKIA, 2008; ZHANG et al., 2017). Entre as vantagens destes biossensores, destacam-se a elevada sensibilidade, facilidade de integração de sinal, detecção livre de marcadores e obtenção de repostas em tempo real (BHATTA et al., 2010; NG et al., 2017). Nesta área, a técnica de ressonância de plásmons de superfície vem ganhando destaque no desenvolvimento de ensaios de biossensibilidade à base óptica (CAYGILL; BLAIR; MILLNER, 2010.

- Biossensores piezoelétricos: os biossensores baseados em piezoeletricidade utilizam cristais anisotrópicos como transdutores de sinal por apresentarem uma frequência de ressonância natural (como o cristal de quartzo, por exemplo) (JANSHOFF; GALLA; STEINEM, 2000; TICHÝ et al., 2010; POHANKA, 2017). Inicialmente, ao aplicar uma tensão alternada sobre o cristal, detecta-se uma frequência específica associada à massa e às constantes elásticas do material que o constitui (BUNDE; JARVI; ROSENTRETER, 1998; SKLÁDAL, 2016). Entretanto, ao imobilizar o elemento receptor na superfície do cristal e expor o biossensor ao analito, observa-se alterações nos valores de frequência. Estas mudanças na frequência do cristal poderão ser relacionadas à massa das substâncias em estudo (POHANKA, 2017). Entre as técnicas mais utilizadas para o desenvolvimento de biossensores piezoelétricos, ressalta-se a

microbalança de cristal de quartzo (ZHOU et al., 2016; DO NASCIMENTO et al., 2017).

- Biossensores térmicos: Os primeiros biossensores baseados em enzimas introduzidos por Clark e Lyons em 1962 inspiraram e atraíram o interesse dos pesquisadores no desenvolvimento de métodos de transdução baseados em calorimetria (CLARK; LYONS, 1962). A ideia geral fundamenta-se no princípio de que todas as reações bioquímicas envolvem a liberação ou absorção de energia na forma de calor. Partindo desta conjectura, biossensores térmicos (também denominados biossensores calorimétricos) foram desenvolvidos para detectar variações de calor/temperatura durante o processo de interação receptor-analito. Geralmente, estas variações são mensuradas por meio de termistores de alta sensibilidade (YAKOVLEVA; BHAND; DANIELSSON, 2013). As mudanças na quantidade de calor/temperatura podem ser correlacionados com a entalpia molar das substâncias e o número de reagentes consumidos ou produtos formados no sistema (RAMANATHAN, K.; DANIELSSON, 2001). As enzimas são os principais elementos de biodetecção usados para a construção de biossensores térmicos, no entanto, células, DNA e anticorpos também podem ser empregados (AHMAD et al., 2010; LEE et al., 2013). Os biossensores térmicos são instrumentos muito atraentes para estudos de hibridação com sequências específicas de DNA, ensaios enzimáticos, testes de controle de qualidade e vigilância ambiental (KIRCHNER et al. 2012; MASKOW et al., 2012; YAKOVLEVA; BHAND; DANIELSSON, 2013; BAI et al., 2017; LI et al., 2017).

- Biossensores eletroquímicos: estes dispositivos representam uma das principais classes de biossensores desenvolvidos nos dias atuais devido à sua alta sensibilidade e simplicidade para realização de ensaios analíticos (BANDODKAR; WANG, 2014; WANG; DAI, 2015). Os biossensores eletroquímicos são capazes de mensurar mudanças nas propriedades físico-químicas do meio, tais como a difusão de espécies eletroativas, transferência interfacial de elétrons e o armazenamento de cargas (THÉVENOT et al., 2001; WANG et al., 2008; KIMMEL et al., 2011). Nestes sistemas biossensíveis, os transdutores são eletrodos constituídos por materiais inertes, como por exemplo o ouro, carbono vítreo, platina, entre outros (PERUMAL; HASHIM, 2014). De acordo com a propriedade avaliada durante o processo de biorreconhecimento, os biossensores eletroquímicos podem ser subclassificados em:

a) biossensores amperométricos (medem o fluxo de corrente elétrica gerada pela reação de oxirredução de espécies eletroativas presentes na célula eletroquímica quando aplica-se uma variação de potencial) (GRIESHABER et al., 2008; VÁSQUEZ et al., 2017);

b) biossensores potenciométricos (quantificam o potencial gerado no eletrodo de trabalho em relação ao eletrodo de referência quando uma corrente é aplicada entre o eletrodo de trabalho e o eletrodo auxiliar) (DRAGHI; FERNANDES, 2017);

c) biossensores condutimétricos (mensuram a condutância da dupla camada elétrica, correlacionando-a com a concentração do analito detectado) (GRIESHABER et al., 2008; TANG et al., 2011; LEE et al., 2012);

d) biossensores impedimétricos (aferem a impedância gerada no sistema a partir da aplicação de um potencial senoidal no eletrodo de trabalho frente a uma determinada faixa de frequência, obtendo-se assim, uma corrente elétrica alternada que será associada à impedância total da interface eletrodo/solução) (RAMANATHAN et al., 2016; SHEIKHZADEH et al., 2016).

2.2.3 Biossensores de DNA eletroquímicos

Os biossensores de DNA eletroquímicos (também denominados de genossensores eletroquímicos) têm sido extensivamente utilizados como métodos moleculares para o diagnóstico de inúmeras doenças, tais como viroses (SINGHAL et al., 2017), infecções bacterianas (TAK; GUPTA; TOMAR, 2014) e desordens genéticas (ABU-SALAH, 2015). Os genossensores eletroquímicos são construídos a partir da imobilização de sequências de ácidos nucléicos sobre a superfície de transdutores eletroquímicos (KERMAN; KOBAYASHI; TAMIYA, 2003). A imobilização do ácido nucléico sobre a área transdutora é uma etapa crucial para obtenção de biossensores funcionais com maiores performances analíticas (SAGADEVAN; PERIASAMY, 2014). Por esta razão, a compreensão das estratégias de imobilização de DNA é essencial para assegurar a bioatividade da molécula ancorada e um efetivo processo de biorreconhecimento.

O elemento básico para obtenção de genossensores é um fragmento de oligonucleotídeo do tipo ssDNA (denominado de sonda) capaz de reconhecer a cadeia de DNA complementar (DNA alvo) com elevada especificidade e seletividade. Como resultado, obtêm-se uma estrutura de DNA de cadeia dupla (dsDNA) que caracteriza o processo hibridação molecular (PALEČEK, 2009) A estrutura molecular do DNA e as interações bioespecíficas entre suas bases nitrogenadas são apresentadas na Figura 3. Os genossensores apresentam amplo potencial de aplicabilidade para o diagnóstico clínico e laboratorial, pois, são dispositivos de biodetecção que permitem uma rápida análise de substâncias alvo a um baixo custo (DRUMMOND; HILL; BARTON, 2003). Em adição, o método eletroquímico de transdução de sinal apresenta elevada sensibilidade e o biossensor pode ser construído de forma simples, com a possibilidade de reusabilidade e miniaturização (KERMAN; KOBAYASHI; TAMIYA, 2003; SASSOLAS; LECA-BOUVIER; BLUM, 2008; CHAO et al., 2016). Em especial, destaca-se o crescente número de pesquisas científicas relacionadas ao desenvolvimento de genossensores eletroquímicos para a biodetecção do oncogene quimérico BCR/ABL (CHEN et al., 2008b; LIN et al., 2009; WANG et al., 2014; YANG; ZHANG, 2014; CHEN et al., 2015). As principais técnicas eletroquímicas utilizadas para o monitoramento do processo analítico de identificação do oncogene quimérico BCR/ABL são a VC (WANG et al., 2014), EIE (ZHONG et al., 2014; YANG; ZHANG, 2014), voltametria de pulso diferencial (LIN et al., 2007; SHARMA et al., 2012) e voltametria de redissolução anódica (HU et al., 2013). Apesar de biossensores já terem sido desenvolvidos para identificação do oncogene quimérico BCR/ABL, melhorias ainda devem ser alcançadas, como por exemplo, menores limites de detecção, o que viabilizará a aplicação destes dispositivos em estudos de doença residual mínima.

Figura 3. Estrutura molecular do DNA e as interações bioespecíficas entre suas bases nitrogenadas.

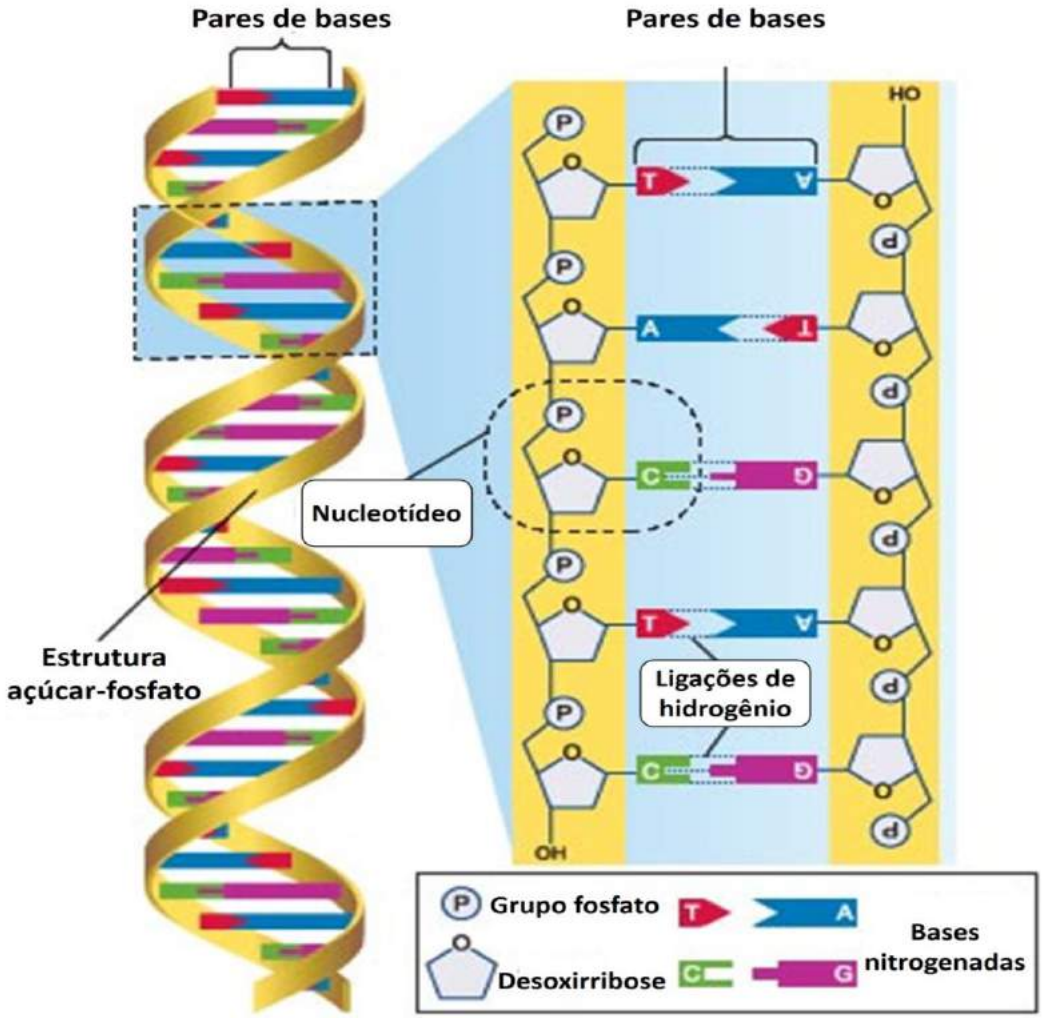

As letras T, A, C e G representam, respectivamente, as bases nitrogenadas timina, adenina, citosina e guanina. Fonte: adapatada de ENCYCLOPEDIA BRITANNICA, 2015.

2.2.4 Métodos de imobilização de DNA

Embora os biossensores de DNA sejam dispositivos aplicáveis ao diagnóstico de doenças clínicas em virtude de suas inúmeras características singulares (como a elevada especificidade e capacidade de discriminar alterações nas sequências de oligonucleotídeos na ordem de uma única base nitrogenada), alguns desafios ainda precisam ser superados, como a estabilidade da sonda imobilizada e a reprodutibilidade dos sistemas sensores (SASSOLAS; LECA-BOUVIER; BLUM, 2008; TELES; FONSECA, 2008; CHAO et al., 2016; JIA; DONG; WANG, 2016). Nestas circunstâncias, a arquitetura do biossensor de DNA e a

estratégia de ancoragem da molécula de biorreconhecimento são os postos-chaves para um processo de bioanálise eficaz (CHAO et al., 2016; JIA; DONG; WANG, 2016).

Como uma regra geral para a construção de biossensores de DNA, as sondas devem ser imobilizadas de maneira previsível, mantendo sua capacidade de biodetecção (DRUMMOND; HILL; BARTON, 2003; XU et al., 2009). Independente da identidade molecular, a adsorção não-específica deve ser minimizada e a estabilidade da biomolécula ancorada deve ser preservada (LUCARELLI et al., 2008; LIU et al., 2012; KURBANOGLU et al., 2016). Além disso, a orientação e acessibilidade da sonda de DNA são parâmetros essenciais para assegurar sua afinidade à molécula alvo e eficiência de hibridização (LUCARELLI et al., 2008). Portanto, o controle desses passos garante a alta sensibilidade e seletividade dos sistemas sensores (LIU et al., 2012).

As técnicas de imobilização empregadas no desenvolvimento de biossensores de DNA são baseadas em métodos físicos (por exemplo, adsorção), métodos químicos (via ligação covalente) e processos de biointeração (por exemplo, o uso de biotina e avidina para a ancoragem de biomoléculas). A adsorção física das sondas de DNA em superfícies sólidas fundamenta-se em interações iônicas entre os grupos fosfato das moléculas de DNA carregados negativamente e o substrato carregado positivamente (SASSOLAS; LECA-BOUVIER; BLUM, 2008; RAVAN et al., 2014). Esta técnica é um método simples para imobilização de DNA e não requer qualquer modificação na estrutura molecular do ácido nucleico (Figura 4A) (SASSOLAS; LECA-BOUVIER; BLUM, 2008; RAHMAN et al., 2015).

A imobilização química das sondas de DNA em diferentes suportes é uma das principais técnicas utilizadas na construção de biossensores (SONI et al., 2015; RASHEED; SANDHYARANI, 2016). Este tipo de ancoragem reduz o processo de lixiviação das moléculas de DNA, garantindo assim uma maior estabilidade e reprodutibilidade da camada sensora (SASSOLAS; LECA-BOUVIER; BLUM, 2008). Entre os métodos químicos, destaca-se a quimissorção para a ligação de sequências de DNA com grupos tióis terminais sobre superfícies de ouro (STEEL et al., 2000; MANNELLI et al., 2005; LIN et al., 2007; WANG et al., 2009; LI et al., 2013). A quimissorção é baseada na forte afinidade entre os átomos de enxofre e ouro, o que permite a formação de ligações covalentes (SASSOLAS; LECA-BOUVIER; BLUM, 2008). A imobilização covalente de sondas de DNA sobre superfícies funcionalizadas pode ser realizada através de agentes de acoplamento, tais como glutaraldeído, N-hidroxissuccinimida (NHS) e 1-etil-3-(3-dimetilaminopropil) carbodiimida (EDC) (STEEL et al., 2000; ZHONG et al., 2014; MCKENNA et al., 2016; THIPMANEE et

al., 2016). Neste caso, grupos químicos intrínsecos ou sintéticos da molécula de DNA reagem especificamente com grupos funcionais do substrato previamente ativados por agentes de acoplamento (Figura 4B) (SASSOLAS; LECA-BOUVIER; BLUM, 2008).

Outro método de ligação para sondas de DNA baseia-se na afinidade entre biomoléculas (RAHMAN et al., 2015). Por exemplo, as moléculas de biotina e avidina (ou estreptavidina) são amplamente utilizadas na construção de biossensores, uma vez que formam complexos com alta afinidade (TAKAHASHI; SATO; ANZAI, 2012; KIM; CHOI, 2014). As sondas de DNA podem ser biotiniladas por síntese química e subsequentemente imobilizadas em superfícies modificadas com avidina (ou estreptavidina). Assim, o processo de biointeração entre sondas de DNA biotiniladas e avidina (ou estreptavidina) permite uma orientação específica do DNA imobilizado (DONG et al., 2015). Diante das informações apresentadas, verifica-se que os segmentos de DNA podem ser ancorados por meio de diferentes estratégias. Entretanto, a determinação do protocolo experimental deve ser minuciosamente avaliado para garantir as propriedades bioquímicas e funcionais do DNA, bem como evitar o processo de dessorção (Figura 4C) (CAMPAS; KATAKIS, 2004; LUCARELLI et al., 2008).

Figura 4. Estratégias de imobilização de DNA em superfícies sólidas.

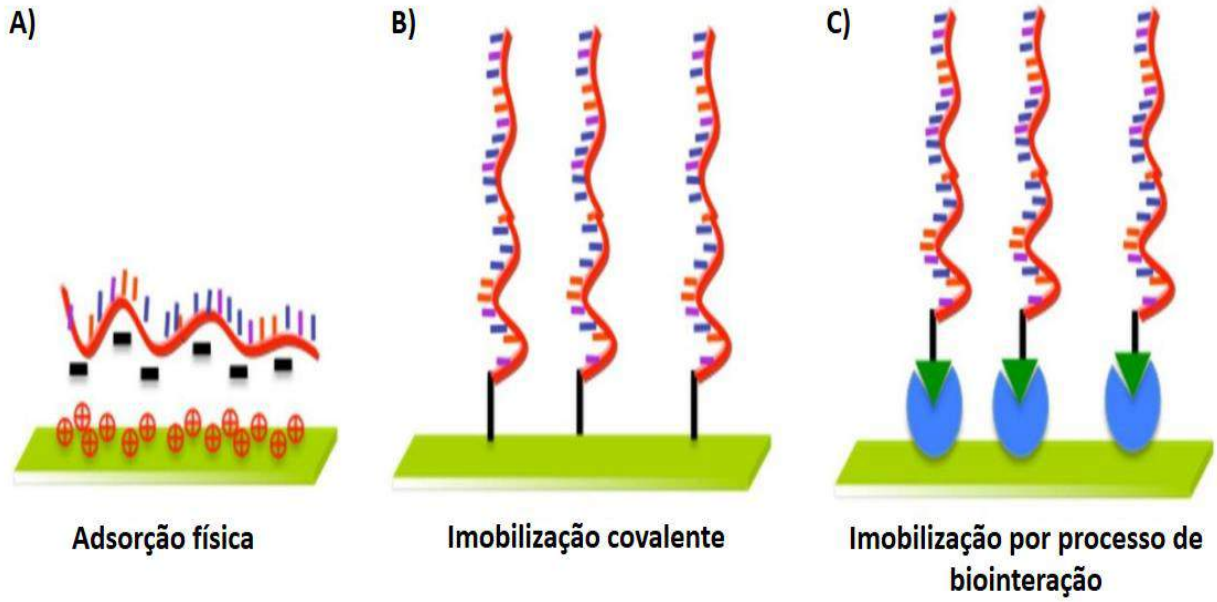

Fonte: Adapatada de NIMSE et al., 2014.

2.3 Plataformas nanoestruturadas

As plataformas nanoestruturadas são uma alternativa inovadora para a obtenção de dispositivos com elevado desempenho analítico (PATEL et al., 2013; ROVINA; SIDDIQUEE, 2016). No desenvolvimento de biossensores, estas plataformas atuam como interfaces entre as moléculas de biorreconhecimento e as superficies transdutoras. Além disso, podem apresentar grupos químicos funcionais que possibilitam a formação de ligações covalentes com sondas de DNA ou outras biomoléculas, o que assegura um processo estável de ancoragem molecular (FUENTES et al., 2004). Como descrito anteriormente, a imobilização química de sequências de DNA sobre substratos sólidos reduz a adsorção não específica e o processo de lixiviação da camada sensora (LUCARELLI et al., 2008; LIU et al., 2012; KURBANOGLU et al., 2016). Os protocolos de imobilização química também determinam uma orientação específica das biomoléculas e podem minimizar a repulsão eletrostática e o impedimento estérico entre as cadeias de DNA.

No entanto, o sucesso do método de imobilização é estritamente dependente das propriedades das superficies de transdução e dos materiais de interfaceamento (LUCARELLI et al., 2008; LIU et al., 2012). Por esta razão, um estudo detalhado das características físico-químicas dos materiais que constituem as plataformas nanoestruturadas (como nanopartículas, nanotubos, nanofios, nanobastões, nanoporos, quantum dots, nanocompósitos e biopolímeros) é essencial para assegurar a eficiência de hibridação, reprodutibilidade e robustez dos sistemas sensores (ZHU et al., 2012). Nas subseções seguintes, foi realizada uma discussão sobre os nanomateriais utilizados na construção das plataformas nanoestruturadas propostas.

2.3.1 Nanocompósito híbrido de nanopartículas de ouro e polianilina

Em um amplo sentido, o termo “nanocompósito híbrido” significa um material em escala nanométrica composto por duas ou mais substâncias com naturezas ou propriedades distintas. Estes materiais exibem propriedades únicas e sinérgicas de seus constituintes e versatilidade em termos de composição (LAINE; CHOI; LEE, 2001; SANCHEZ et al., 2005). Por exemplo, o uso de nanocompósitos híbridos constituídos por substâncias orgânicas e inorgânicas é uma estratégia inovadora e eficiente para o desenvolvimento de sistemas biológicos (WANG; HU, 2009; SAGADEVAN; PERIASAMY, 2014). Em particular, destaca-se a associação entre nanopartículas metálicas e polímeros condutores, como as

AuNps e polianilina (PANI), respectivamente, para a síntese de um nanocompósito híbrido com características diferenciadas (Figura 5) (SANTOS et al., 2013; AVELINO et al., 2014).

Figura 5. Representação do nanocompósito híbrido de AuNps e PANI.

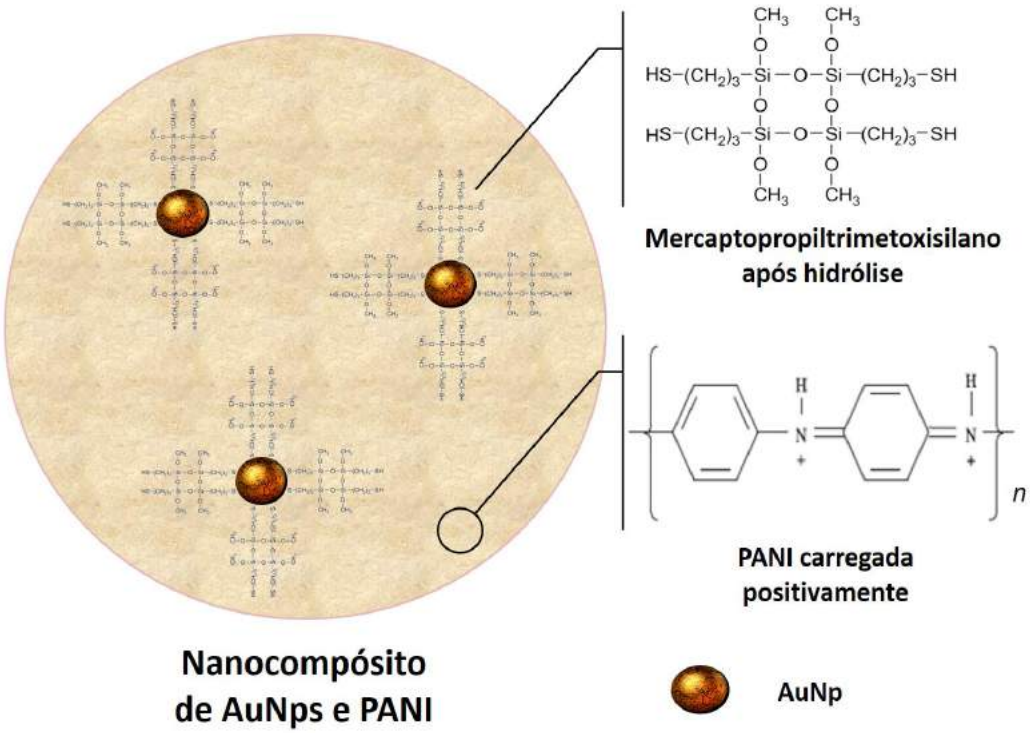

Durante a síntese deste nanocompósito híbrido pode-se utilizar substâncias químicas adicionais, como o mercaptopropiltrimetoxisilano, capaz de fornecer grupos sulfidrilas para a adsorção química do nanocompósito em superfícies de ouro, além de evitar a agregação das nanopartículas metálicas no interior da matriz polimérica (NASCIMENTO et al., 2011; SANTOS et al., 2013AVELINO et al., 2016). Fonte: Adapatada de AVELINO et al., 2016.

As AuNps possuem excelentes propriedades para o interfaceamento do reconhecimento biológico (DARAEE et al., 2016). Estas nanopartículas proporcionam um microambiente adequado para a imobilização de biomoléculas sem perda de atividade biológica ou mudança conformacional (LIU; LEECH; JU, 2003; YÁÑEZ-SEDEÑO; PINGARRÓN, 2005). As AuNps exibem elevada energia superficial e elevada razão entre área de superfície e volume, o que proporciona uma maior área eletroquimicamente ativa. Estas propriedades inerentes aos materiais em nanoescala são essenciais para a obtenção de biodispositivos com desempenho analítico superior (CHEN et al., 1998; NATH; CHILKOTI, 2004; BONANNI; PUMERA; MIYAHARA, 2011). Além disso, as AuNps atuam como agentes para a transferência direta e

efetiva de elétrons entre a superfície do eletrodo e a camada de biorreconhecimento (PINGARRÓN; YÁÑEZ-SEDEÑO; GONZÁLEZ-CORTÉS, 2008; KUMAR et al., 2015).

A PANI é um dos polímeros orgânicos mais explorados devido à sua estabilidade química sob condições ambientais, polimerização de baixo custo e capacidade de se conjugar a inúmeras estruturas (CAO; SMITH; HEEGER, 1992; SUCKEVERIENE et al., 2011). Além disso, a combinação de suas propriedades de transporte de carga, condutividade elétrica e taxa de transferência de energia pode conferir aos biodispositivos baseado em PANI uma sensibilidade amplificada (MCQUADE; PULLEN; SWAGER, 2000).

Em 2012, Dey et al. desenvolveram um imunossensor livre de marcador baseado em compósito híbrido de nanofios de PANI e AuNps para a detecção de antígeno prostático específico (PSA). Os resultados eletroquímicos demonstraram que as AuNps aumentam a superfície eletroativa da PANI, resultando em um transporte elevado de elétrons. Em adição, a PANI forneceu uma área eficaz para a imobilização do anticorpo anti-PSA. O imunossensor proposto apresentou elevada sensibilidade e um limite de detecção de 0,6 pg/mL (DEY et al., 2012). Recentemente, o genoma de *Leishmania infantum* foi identificado por um genossensor construído a partir da dispersão de AuNps em uma matriz polimérica de PANI (GARCIA et al., 2016). Os ensaios de VC e EIE evidenciaram a reprodutibilidade do sistema nanoestruturado e a capacidade de reconhecimento biológico em uma concentração tão baixa quanto 0,01 pg/mL. Além destas aplicações, o nanocompósito híbrido de AuNps e PANI tem sido utilizado para o desenvolvimento de interfaces sensoras com o objetivo de detectar glicoproteínas não estruturais do vírus da dengue (ANDRADE et al., 2011; NASCIMENTO et al., 2011; AVELINO et al., 2014). Diante destas aplicabilidades, verifica-se que o compósito híbrido de AuNps e PANI destaca-se entre os demais nanomateriais por apresentar características essenciais para a construção de plataformas biossensíveis (DEY et al., 2012; AVELINO et al., 2014; LIU et al., 2014).

2.3.2 Nanotubos de carbono

Entre os alótropos de carbono, os nanotubos tornaram-se o objeto de estudo de inúmeras pesquisas desde sua descoberta por Iijima em 1991 (IIJIMA, 1991). Os nanotubos de carbono (CNTs) possuem amplas aplicações em diferentes áreas de conhecimento devido à sua forte resistência mecânica, elevada razão entre superfície e volume, condutividade e estrutura eletrônica única (ZHU et al., 2012; DE VOLDER, 2013). Eles são compostos por uma rede hexagonal de átomos de carbono com hibridação sp^2 que dão origem as folhas de grafeno,

posteriormente, estas se enrolam na forma de cilindro para formarem os CNTs (UNWIN; GUELL; ZHANG, 2016). Os CNTs são considerados materiais de uma dimensão (2D) porque possuem seu diâmetro em escala nanométrica e comprimento variando de poucos micrômetros a centímetros. De acordo com o número de camadas em sua parede, podem ser classificados como a) nanotubos de carbono de parede única (SWCNTs) que são formados por folhas simples de grafeno e b) nanotubos de carbono de múltiplas paredes (MWCNTs) que são formados por folhas de grafeno enroladas concentricamente (Figura 6) (YANG et al., 2010). Os CNTs podem ser funcionalizados com grupos químicos (-COOH, -NH_2, -SH), tornando-se passíveis de imobilização covalente de biomoléculas e podendo ser associados à polímeros e partículas metálicas para obtenção novas estruturas (SUN et al., 2002; HARRIS, 2004; BALASUBRAMANIAN; BURGHARD, 2005; ZHAO et al., 2015).

Figura 6. Representação esquemática de um nanotubo de carbono de parede única (SWCNT), um nanotubo de carbono de múltiplas paredes (MWCNT) e exemplos de SWCNTs funcionalizados quimicamente.

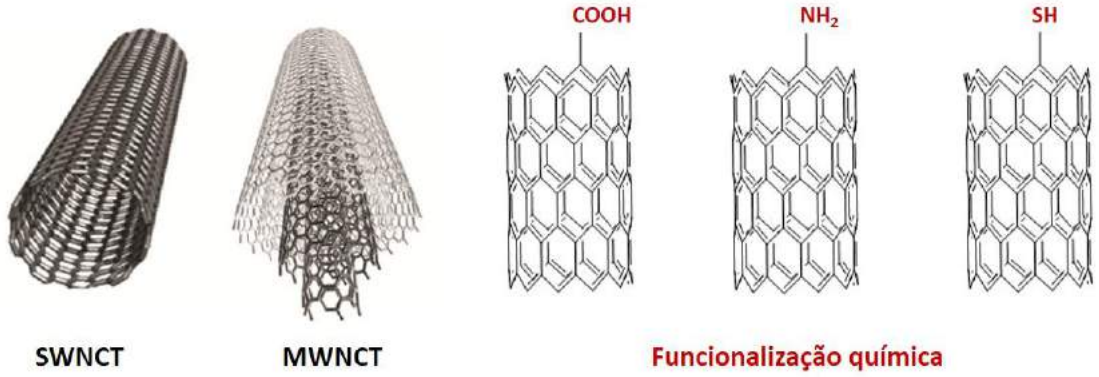

Fonte: Elaborada pelo autor.

No campo dos biossensores, os CNTs tem sido extensivamente empregados como mediadores de elétrons entre o eletrodo e a biomolécula, permitindo a amplificação do sinal eletroquímico (ANDRADE et al., 2015). Além de melhorar substancialmente o desempenho dos dispositivos sensores, os transdutores eletroquímicos baseados em CNTs diminuem o sobrepotencial e apresentam um limite de detecção mais baixo do que os biossensores convencionais (WANG, 2005; JACOBS; PEAIRS; VENTON, 2010; ZHU et al., 2012; TÎLMACIU; MORRIS, 2015).

Partindo do princípio da aplicação bionanotecnológica de CNTs, Hernández-Ibáñez et al. construíram um eletrodo impresso biomodificado baseado em compósito de MWCNTs e quitosana para a detecção de L-lactato em meios de cultura de células embrionárias. A enzima lactato oxidase foi utilizada como elemento receptor e as análises eletroquímicas demonstraram que o biossensor possui um limite de detecção de 22,6 µM, elevada reprodutibilidade e uma resposta enzimática superior a 82% após 5 meses de armazenamento a 4 °C (HERNÁNDEZ-IBÁÑEZ, 2016). Em adição, Ozkan-Ariksoysal et al. descreveram um novo protocolo para detecção eletroquímica do genoma de *Escherichia coli* em amostras de cDNA. Inicialmente, os MWCNTs foram envolvidos por sondas de biorreconhecimento através de interações do tipo "*π-stacking*". Posteriormente, os MWCNTs previamente modificados com as sondas de DNA foram imobilizados sobre a superfície de eletrodos descartáveis de grafite. Foi observado que a modificação dos eletrodos com MWCNTs proporciona uma maior adsorção das sondas de captura, oferecendo uma sensibilidade 3 vezes maior com um limite de detecção de 0,5 pM quando comparado ao biossensor fabricado na ausência dos MWCNTs. Em adição, o biossensor com MWCNTs exibiu elevada performance analítica, seletividade, reprodutibilidade e um rápido tempo de detecção (20 minutos) (OZKAN-ARIKSOYSAL et al., 2017). Portanto, verifica-se que os CNTs são nanoestruturas úteis para o desenvolvimento de genossensores.

2.3.3 Nanopartículas de óxido de zinco

As ZnONps destacam-se entre os óxidos de metais por possuírem excelentes propriedades físico-químicas para a construção de dispositivos eletrônicos biomoleculares (HAYAT et al., 2015; KARIM-NEZHAD et al., 2016). As ZnONps apresentam características físicas de um material semi-condutor com um baixo *band gap* de energia no valor de 3,37 eV. Este valor corresponde a energia requerida para os elétrons do óxido de zinco efetuarem a transição entre a banda de valência e a banda de condução, resultando assim, em um aumento da condutividade do material (KUMAR et al., 2015). Ademais, as ZnONps exibem elevada razão entre área superficial e volume, alta eficiência catalítica, estabilidade química, biocompatibilidade, não toxicidade e propriedades ópticas aplicáveis ao desenvolvimento de biossensores (KUMAR; CHEN, 2008; ROVINA; SIDDIQUEE, 2016).

Recentemente, estudos tem demonstrado mecanismos de síntese para a funcionalização química das ZnONps (GRASSET et al., 2003; HANG et al., 2015; RABIN et al., 2016). A presença de grupos químicos na superfície das nanopartículas pode contribuir diretamente

para a formação de ligações covalentes entre as ZnONps e biomoléculas ou outros nanomateriais, promovendo um processo específico de ancoragem molecular. Uma grande promessa para a construção de plataformas nanoestruturadas são as ZnONps funcionalizadas com aminopropiltrietoxisilano (APTES). Estas possuem propriedades intrínsecas do óxido metálico e características químicas do aminosilano (GRASSET et al., 2003; COSTENARO et al., 2013).

Durante o processo de funcionalização, os grupos hidroxilas (-OH) comumente existentes na superfície das ZnONps são utilizados como locais de partida para a reação química (NANAYAKKARA; LARISH; GRASSIAN, 2014). Os grupos trietóxi do agente aminosilano reagem com os grupos hidroxilas das ZnONps, levando à formação de ZnONps funcionalizadas com APTES e moléculas de etanol como subprodutos da reação (Figura 7) (MALLAKPOUR; MADANI, 2015). Apesar das ZnONps serem extensivamente utilizadas na construção de biossensores, as ZnONps funcionalizadas com APTES ainda não foram associadas à sistemas de biodetecção (SADEGHI et al., 2013; HWA; SUBRAMANI, 2014; WANG et al., 2014; EZHILAN et al., 2017). No entanto, devido suas características físicas e químicas descritas em trabalhos publicados na área de modificação superficial, acredita-se que elas podem desenvolver um importante papel no desenvolvimento de biodispositivos nanoestruturados (GRASSET et al., 2003, HANG, 2015).

As nanoestruturas de ZnO apresentam por si só uma elevada área de superfície e rugosidade, o que proporciona uma melhor imobilização de segmentos de oligonucleotídeos para a construção de genossensores (TERESHCHENKO et al., 2016). Neste contexto, Congur et al. desenvolveram um sistema eletroquímico para a detecção de ácidos nucléicos baseado em nanofios de óxido de zinco (ZnONWs). O estudo demonstrou que a modificação de eletrodos de grafite com ZnONWs proporciona um aumento da sensibilidade e seletividade dos sistemas sensores em comparação àqueles construídos sem os ZnONWs (CONGUR et al., 2015). Na pesquisa desenvolvida por Tak, Gupta e Tomar, uma sonda de biorreconhecimento foi imobilizada sobre um nanocompósito de óxido de zinco e CNTs, previamente adsorvido em superfície de óxido de índio dopado com estanho (ITO). O genossensor descrito foi utilizado para a detecção eletroquímica do genoma de *Neisseria meningitidis*. Este apresentou um rápido tempo de resposta (45 segundos) e uma faixa de linearidade para identificação do analito entre as concentrações de 5 e 180 ng/µL (TAK; GUPTA; TOMAR, 2016).

Figura 7. Reação esquemática do processo de funcionalização das ZnONps com APTES.

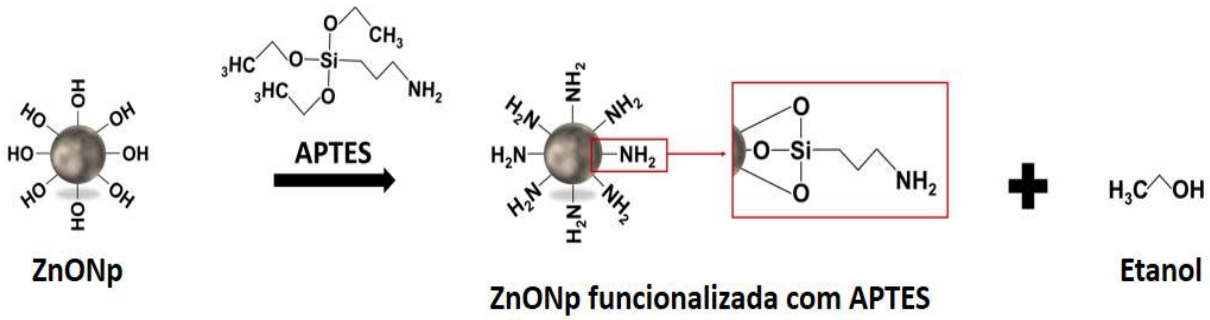

Fonte: Elaborada pelo autor.

2.4 Técnicas eletroanalíticas

2.4.1 Voltametria cíclica

A VC é uma das principais ferramentas utilizadas para a compreensão dos processos eletroquímicos interfaciais. Esta técnica destaca-se por sua eficiência em proporcionar informações sobre a cinética de transferência de carga, reversibilidade de reações eletroquímicas e potenciais redox de substâncias eletroativas (NICHOLSON, 1965; ENENGL, 2017; JARA-PALACIOS, 2017). Na pesquisa de biossensores, a VC é considerada uma técnica de ampla funcionalidade, podendo ser utilizada diretamente na construção de novos biodispositivos, por exemplo, através dos métodos de eletropolimerização e eletrodeposição. Além disso, é capaz de possibilitar a caracterização de fenômenos físico-químicos associados à imobilização de moléculas sobre o eletrodo de trabalho e ao processo de biorreconhecimento a nível molecular (LUNA et al., 2015; NIA et al., 2015; KISS et al., 2016; NESAKUMAR et al., 2016; POVEDANO et al., 2017).

A VC baseia-se nos eventos eletroquímicos que ocorrem na interface entre o eletrodo de trabalho e a camada adjacente de solução eletrolítica (CHEVION; ROBERTS; CHEVION, 2000). Os sinais de corrente mensurados pela voltametria estão associados às espécies eletroquímicas que realizam reações de oxirredução (Equação 1). Como resultado, estas reações fornecem elétrons para a passagem da corrente elétrica. No entanto, diversos fatores podem alterar a magnitude deste fluxo de carga, como o consumo ou a geração de espécies eletroquímicas, bem como a presença de moléculas e nanoestruturas na superfície do eletrodo que interferem na condutividade do sistema (WANG, 2006; RONKAINEN; HALSALL;

HEINEMAN, 2010). Logo, discriminando os principais fatores que influênciam na intensidade da corrente, informações específicas sobre o analito podem ser obtidas por meio de suas variações.

$$O + ne^- \leftrightarrow R$$

Equação 1

Onde *O* é a forma oxidada da espécie eletroativa, *R*, a forma reduzida e ne^- corresponde ao número de elétrons envolvido no processo de oxirredução (PACHECO et al., 2013).

Os experimentos voltamétricos são realizados uma célula eletroquímica composta por três eletrodos: eletrodo de trabalho, eletrodo auxiliar (também denominado de contra-eletrodo) e eletrodo de referência (Figura 8). A corrente gerada no sistema é mensurada entre o eletrodo de trabalho e o eletrodo auxiliar, enquanto a voltagem é aplicada entre o eletrodo de trabalho e o eletrodo de referência. Logo, o parâmetro ajustado é o potencial (*E*) e o parâmetro medido é a corrente resultante (*i*) (GRIESHABER, 2008). Por fim, os resultados de VC são representados graficamente por voltamogramas cíclicos (corrente *vs* potencial).

Figura 8. Representação esquemática de uma célula eletroquímica de compartimento único composta por três eletrodos: eletrodo de trabalho, eletrodo de auxiliar e eletrodo de referência.

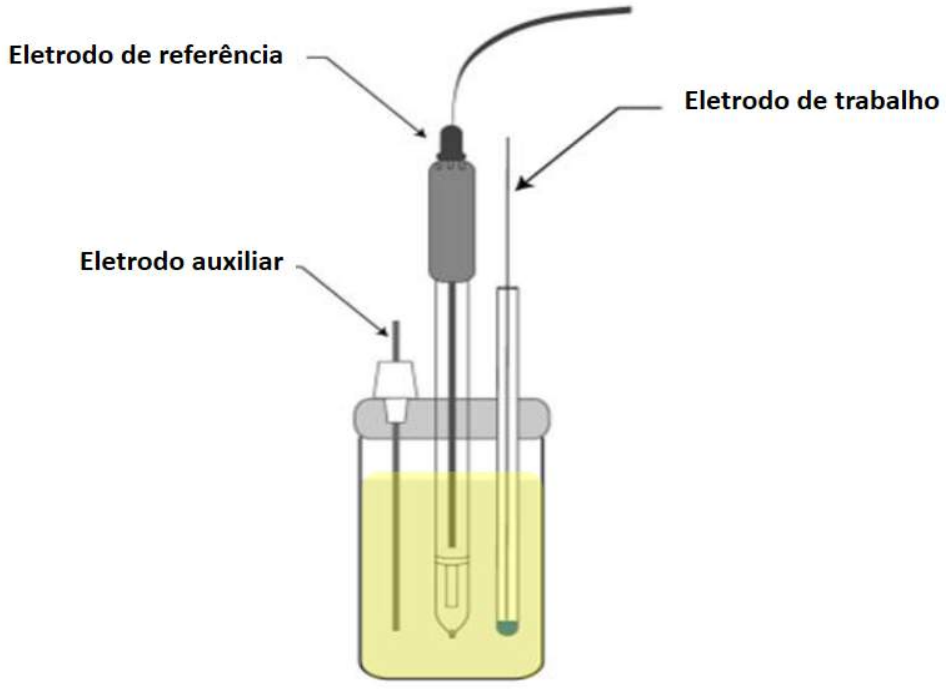

Fonte: Adapatada de LANDIM, 2014.

O que diferencia a VC das outras técnicas voltamétricas (como a voltametria de varredura linear, voltametria de pulso reverso, voltametria de pulso diferencial, voltametria de pulso normal, voltametria de redissolução e voltametria de onda quadrada) é a maneira como o potencial é aplicado ao sistema (GUPTA, 2011). Na VC, o potencial é varrido linearmente na forma de uma onda triangular em função do tempo (Figura 9A). A depender da finalidade do estudo eletroquímico, pode-se realizar ciclos simples ou ciclos múltiplos (PACHECO et al., 2013).

Figura 9. Gráfico de onda triangular demonstrado a forma em que o potencial é aplicado na técnica de VC (A) e o voltamograma cíclico resultante (V).

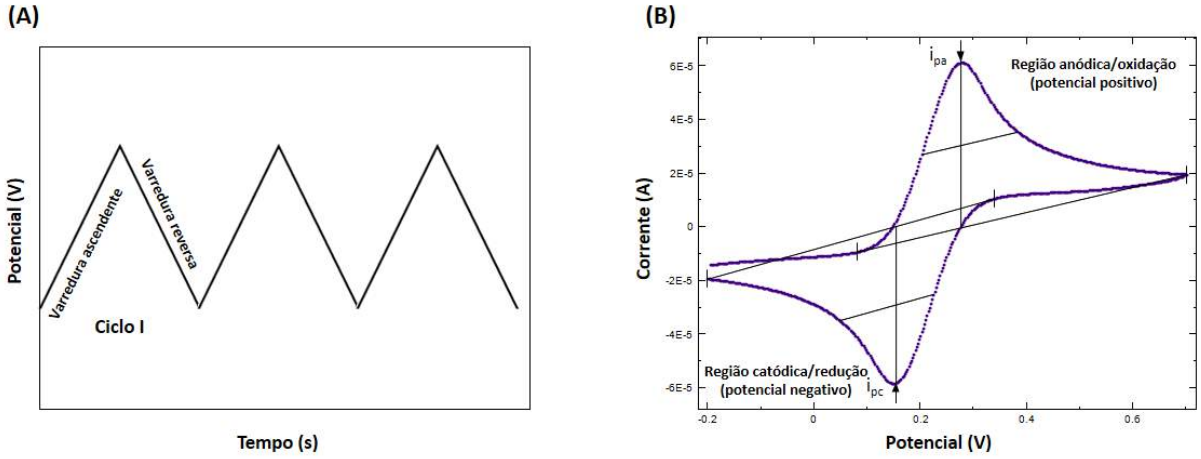

Fonte: Elaborada pelo autor.

O potencial aplicado no eletrodo de trabalho atua como uma força motriz para a reação eletroquímica. Inicialmente, é aplicado um valor de potencial que não causa nenhuma reação de oxirredução. Posteriormente, ocorre um aumento do potencial para regiões mais positivas (região anódica), favorecendo a oxidação das espécies em solução. Nesta etapa, forma-se uma corrente de pico anódica (i_{pa}) proporcional à concentração do analito. Mesmo com o aumento do potencial no sentido positivo, a corrente anódica começa a diminuir devido a depleção das espécies reduzidas passíveis de oxidação. Por conseguinte, quando as reações de oxidação decrescem a um valor mínimo e não verifica-se mudanças no valor da corrente anódica, o potencial é varrido no sentido inverso até o valor inicial. Neste momento, o potencial torna-se gradativamente mais negativo e as reações de redução são favorecidas. No caso de uma reação reversível, as espécies previamente oxidadas sofrerão redução, gerando uma corrente de pico catódica (i_{pc}) simétrica à i_{pa} (Figura 9B) (LOJOU; BIANCO, 2006; ROUNTREE et al., 2014).

Diante das informações descritas, verifica-se que o potencial exerce uma influência direta sobre o estado de oxirredução das espécies eletroativas próximas à superfície do eletrodo. À medida em que o potencial adquire um valor mais positivo, a oxidação das espécies é favorecida. Em oposição, em potenciais mais negativos, o eletrodo torna-se uma fonte de elétrons, favorecendo a redução das espécies na interface eletrodo/solução. Por esta razão, quando se faz uma varredura de potencial no sentido positivo usa-se a denominação de varredura anódica, enquanto que uma varredura de potencial no sentido negativo é chamada de varredura catódica (BRETT; BRETT, 1993; LOJOU; BIANCO, 2006; PACHECO et al., 2013).

Através de inúmeros trabalhos descritos na literatura, constata-se o grande potencial da técnica de VC para o desenvolvimento de biossensores eletroquímicos (JI et al., 2017; MAHADEVAN; FERNANDO, 2017; MOHAMED et al., 2017). Por exemplo, um sensor biológico foi construído para a identificação de acetilcolina por meio de análises de VC. O sistema de biodetecção foi baseado na imobilização de acetilcolinesterase e colina oxidase sobre uma superfície de óxido de índio dopado com flúor, previamente modificada com o compósito de nanopartículas de óxido de ferro e poli(3,4-etilenodioxitiofeno). O sensor apresentou uma ampla faixa de detecção de 4 nM a 800 µM com um tempo de resposta de 4 segundos. Diante desta aplicação, ressalta-se a efetividade da técnica de VC para caracterizar o processo de biorreconhecimento com elevada sensibilidade analítica (CHAUHAN et al., 2017). Com uma outra finalidade, WEN et al. utilizaram a VC para a montagem de um biossensor específico para estreptomicina. Neste estudo, o óxido de grafeno foi reduzido eletroquimicamente sobre um eletrodo de carbono vítreo e, em seguida, o ácido pirrol-3-carboxílico foi eletropolimerizado sobre o eletrodo modificado. Assim, a plataforma de interfaceamento foi construída (WEN et al., 2017). Portanto, verifica-se a ampla aplicabilidade da técnica de VC na área de biossensores eletroquímicos, viabilizando a construção e caracterização de novos sistemas de biodetecção.

2.4.2 Espectroscopia de impedância eletroquímica

A EIE é uma valiosa técnica para a investigação de superfícies modificadas e monitoramento de processos interfaciais (KATZ; WILLNER, 2003; GONG; WANG; YANG, 2017). Este método é capaz de fornecer um grande número de informações sobre as propriedades físico-químicas de sistemas em análise. Inúmeras são suas aplicações, como por exemplo, estudos de reações eletroquímicas, soluções iônicas, semicondutores, materiais

dielétricos, biossensores e mecanística (GUAN et al., 2004; ZHU et al., 2012; ZHANG et al., 2016; TURK; WALTERS; ROY, 2017).

A EIE fundamenta-se na aplicação de um estímulo elétrico a um sistema de eletrodos dispostos em uma célula eletroquímica e a observação da resposta resultante. Este estímulo frequentemente é um potencial contínuo de pequena amplitude na forma senoidal. Através da aplicação de um potencial de valor reduzido, o sistema sofrerá uma perturbação mínima, o que torna possível a investigação de fenômenos próximos ao estado de equilíbrio (DAMOS; MENDES; KUBOTA, 2004). No mesmo sistema de eletrodos é sobreposto um sinal alternado na forma de diferentes valores de frequência (MACDONALD, 1990; MACDONALD, 1992; BOTT, 2001). Consequentemente, uma corrente alternada de natureza senoidal é gerada na célula eletroquímica (SUNI, 2008). Mediante a monitorização das relações entre o potencial aplicado e a corrente resultante, a impedância do sistema é calculada (BARD et al., 2001; DAMOS; MENDES; KUBOTA, 2004). A partir de análises de EIE é possível avaliar a taxa de transferência de carga, condutividade de materiais, capacitância da dupla camada elétrica, entre outras propriedades (JIANG; KUCERNAK, 2002).

A impedância de um circuito elétrico é originalmente composta por três componentes: componente resistiva (ou simplesmente resistência), componente capacitiva (capacitância) e componente indutiva (indutância). A componente resistiva está associada a um elemento resistor responsável pela perda de energia elétrica na forma de calor. A componente capacitiva é originária de um elemento capacitor que armazena carga (energia eletrostática) em uma região específica do sistema, dificultando a passagem da corrente elétrica. A componente indutiva, resultante de um elemento indutor, é responsável pelo acúmulo de energia em um campo magnético (KATZ; WILLNER, 2003; LISDAT; SCHÄFER, 2008). A impedância (Z) é calculada como uma razão entre a voltagem e a corrente, ambas em função do tempo e levando em consideração as diferentes frequências de excitação (frequências angulares) (Equação 2) (WANG; YE; YING, 2012).

$$Z = \frac{V(t)}{i(t)}$$

Equação 2

Os valores de impededância correspondem a números complexos compostos por uma componente real (Z') e uma componente imaginária ($-Z''$), estando relacionadas, respectivamente, à resistência e a capacitância do circuito elétrico (MACDONALD, 1990;

SUNI, 2008; KATZ; WILLNER, 2003). Estes valores correlacionam-se de acordo com as equações 3 e 4 descritas abaixo.

$$Z' = R_S + \frac{R_{CT}}{1 + \omega^2 C_{dl}^2 R_{CT}^2}$$

Equação 3

$$-Z'' = \frac{\omega C_{dl} R_{CT}^2}{1 + \omega^2 C_{dl}^2 R_{CT}^2}$$

Equação 4

Onde, R_S - resistência da solução, R_{CT} - resistência à transferência de carga, ω - frequência angular e C_{dl} - capacitância da dupla camada elétrica (BARD et al., 2001).

A representação gráfica mais comum para avaliar os dados de EIE é o diagrama de Nyquist, também denominado de semicírculo de Cole-Cole, onde a componente real da impedância é plotada contra sua componente imaginária (Figura 10). No diagrama de Nyquist, cada ponto representa a impedância total do sistema em uma dada frequência. Em regiões de frequências mais altas forma-se um semicírculo que caracteriza os processos limitantes da transferência de carga, como a R_S e R_{CT}. Em regiões de frequências mais baixas observa-se uma linha reta que correlaciona-se com o processo difusional na dupla camada elétrica. O diagrama de Nyquist é um tipo de representação amplamente utilizada em estudos de eletroquímica por ser capaz de fornecer informações sobre a cinética de transferência de elétrons e ter fácil compreensão visual. Em processos muito rápidos de transferência de elétrons, o espectro de impedância inclui apenas a parte linear. Em contrapartida, os processos muito lentos de transferência de elétrons são caracterizados por uma grande região semicircular, na qual o diâmetro do semicírculo é igual à resistência à transferência de elétrons (ALVES; BRETT, 2002; WANG; YE; YING, 2012; BAHADIR; SEZGINTÜRK, 2016).

Figura 10. Representação de um diagrama de Nyquist.

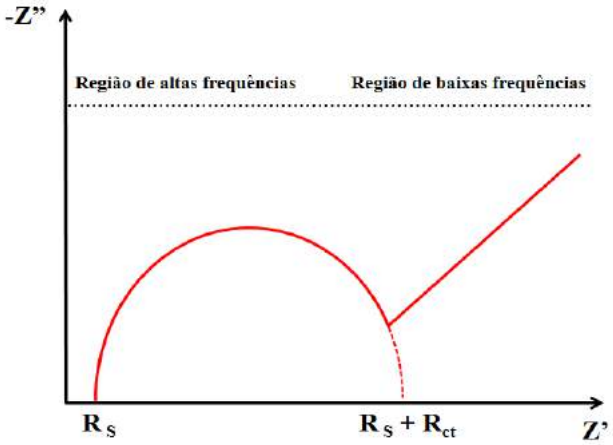

Fonte: Elaborada pelo autor.

Em estudos de espectroscopia de impedância, informações adicionais podem ser determinadas através do uso de circuitos equivalentes ou modelos matemáticos. Em razão dos sistemas eletroquímicos apresentarem constituintes similares a capacitores, resistores e indutores elétricos, os circuitos equivalentes podem ser utilizados para a simulação teórica dos dados experimentais e interpretação dos espectros de impedância (Figura 11A) (BOTT, 2001; MACDONALD, 1992; CHANG; PARK, 2010).

Figura 11. Representação esquemática demonstrando a similaridade da interface eletrodo/solução com um circuito elétrico (A). Circuito equivalente de Randles (B).

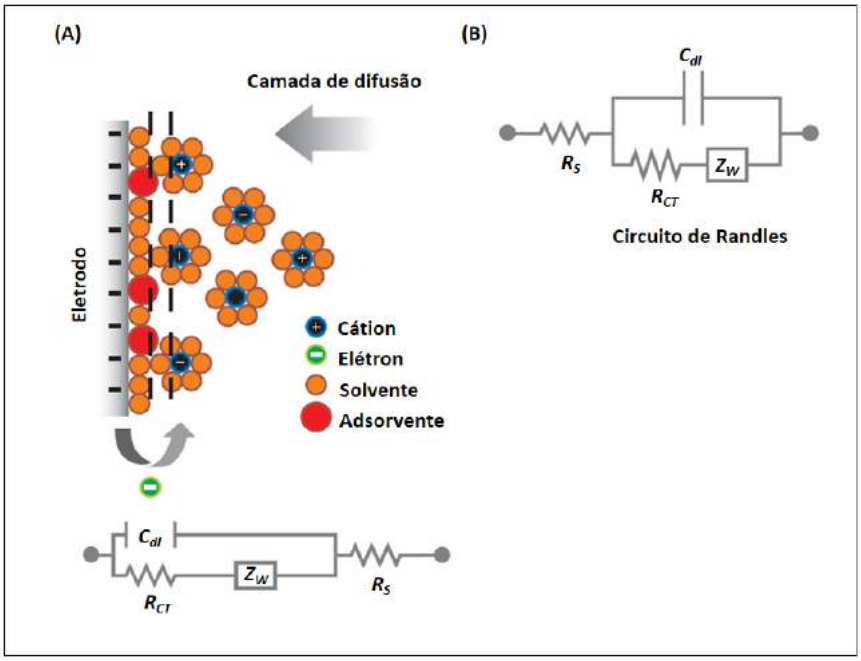

Fonte: Adaptada de CHANG; PARK, 2010.

Um dos circuitos equivalentes mais utilizados em estudos de biossensores é o circuito de Randles (Figura 11B). Através da aplicação deste circuito é possível analisar alguns elementos que estão associados aos processos físico-químicos que ocorrem na dupla camada elétrica. O circuito de Randles é constituído por: R_S, resistência da solução eletrolítica, relacionada à resistência da solução ao transporte de íons entre os eletrodos; R_{CT}, resistência à transferência de carga, associada aos processos de modificação do eletrodo que influenciam a passagem de elétrons na interface eletrodo/solução; Z_W, impedância de Warburg, representa a resistência ao transporte de massa das espécies eletroativas; e C_{dl}, capacitância da dupla camada resultante da distribuição de cargas na interface eletrodo/solução (CHANG; PARK, 2010; WANG; YE; YING, 2012).

A interface eletrodo/solução possui um comportamento similar a um capacitor de placas paralelas devido à distribuição de íons na dupla camada elétrica. Em decorrência do potencial aplicado, o eletrodo de trabalho adquire uma carga que pode ser positiva ou negativa em função da voltagem. Próximo a esta superfície, forma-se uma camada compacta de íons de carga oposta fortemente adsorvidos (camada de Helmholtz). Em regiões mais distantes da interface, os íons são ditos semiligados e estão distribuídos de forma difusa (camada de Gouy-Chapman). No seio da solução encontram-se os íons livres que são responsáveis pela condutividade iônica (Figura 12) (GUIDUCCI et al., 2002; YUQING; JIANGUO; JIANRONG, 2003; ZHANG; ZHAO, 2009).

Figura 12. Distribuição de íons na interface eletrodo/solução.

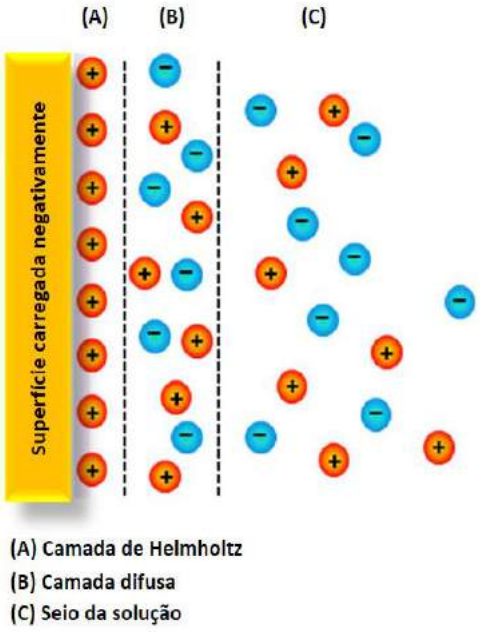

Fonte: Adaptada de LIN et al., 2012.

A EIE é uma técnica que destaca-se entre os demais métodos eletroquímicos em virtude de sua elevada sensibilidade. Apesar da espectroscopia de impedância ter sido originalmente desenvolvida no campo da engenharia elétrica, atualmente a técnica é utilizada em diversas áreas de pesquisa, como por exemplo, análises clínicas e biomédicas, tecnologia farmacêutica, ciência dos materiais, eletrônica, entre outras. Por ser capaz de monitorar propriedades físico-químicas, tais como a capacitância e a resistência à passagem de elétrons, a técnica de EIE possibilita a definição de eventos moleculares à nível da dupla camada elétrica. Ademais, a EIE permite a caracterização estrutural de biossensores e a compreensão de fenômenos interfaciais, como os processos de biodetecção na superfície dos eletrodos modificados (KATZ; WILLNER, 2003; GUAN; MIAO; ZHANG, 2004; PARK; PARK, 2009; BAHADIR; SEZGINTÜRK, 2016; GARCIA et al., 2016).

Recentemente, através da técnica de EIE foi possível desenvolver um biossensor para a detecção impedimétrica de sequências gênicas do vírus da imunodeficiência humana (HIV). O sistema sensor foi construído a partir da imobilização de sondas de DNA sobre um eletrodo de carbono vítreo modificado com compósito de nafion e grafeno. Foi verificado que a ancoragem das sondas de DNA carregadas negativamente repeliam o par redox $[Fe(CN)_6]^{3-/4-}$, levando a um aumento significativo da resistência à passagem de elétrons. Após o processo específico de hibridação com o genoma do HIV, houve a formação de moléculas de DNA de dupla-fita. Por conseguinte, estas moléculas se desprenderam da superfície do biossensor ocasionando uma diminuição na resistividade do sistema. Este decréscimo foi logaritimicamente proporcional à concentração do genoma de HIV. O biossensor exibiu repostas lineares na faixa de 1×10^{-10} a 1×10^{-13} M com um limite de detecção de $2{,}3\times10^{-14}$ M (GONG; WANG; YANG, 2017).

2.5 Microscopia de força atômica

A técnica AFM foi desenvolvida por Binning, Quate e Gerber em 1986 e até os dias atuais é considerada uma ferramenta valiosa para caracterização de superfícies à nível atômico, podendo ser aplicada ao estudo de inúmeras amostras, tais como materiais condutores, semi-condutores e dielétricos, biomoléculas, nanoestruturas, vidros, cerâmicas, polímeros e filmes orgânicos (BINNIG; QUATE; GERBER, 1986; ENDO; SUGIYAMA, 2014; HODEL et al., 2016; SCHÖNHERR, 2016; SILVA, et al., 2016). Em comparação a outras técnicas microscópicas, as principais vantagens da AFM são a maior resolução espacial aproximando-se de dimensões atômicas, a obtenção de imagens reais em três dimensões, a

não exigência de métodos específicos para a preparação das amostras nem a necessidade de recobrimento condutor, a medição direta da rugosidade das amostras, a determinação da espessura de filmes ultrafinos depositados em superfícies sólidas e a caracterização de superfícies imersas em líquidos (HANSMA et al., 1988; SANTOS; CASTANHO, 2004; NEUMAN; NAGY, 2008; EATON; WEST, 2010). Todas estas vantagens apresentadas pela técnica de AFM possibilitam sua aplicação em diferentes áreas de conhecimento, como a ciência dos materiais, nanobiotecnologia, biologia celular e engenharia de macromoléculas (MÜLLER; DUFRENE, 2008; CALZADO-MARTIN et al., 2016; MIYAGI et al., 2016).

Os principais componentes de um microscópio de força atômica são a) o cantilever com uma sonda integrada, b) o laser que está focalizado na parte de trás do cantilever, c) o fotodiodo capaz de detectar mudanças no feixe do laser e d) o scanner piezoelétrico responsável pelo posicionamento tridimensional da amostra com alta resolução (Figura 13). O princípio de funcionamento desta técnica microscópica baseia-se nas forças de interação (atrativas ou repulsivas) entre os átomos da superfície da amostra e os átomos que constituem a ponta da sonda (também denominada de "*tip*"). Quando a sonda se aproxima da amostra, os átomos de sua ponta interagem com os átomos que compõe a superfície da amostra. Ao longo da varredura, o cantilever sofre deflexões por causa da interação atômica, desviando o feixe do laser incidente. Este desvio é detectado por um fotodiodo que conduz a informação para um computador, onde a topografia digitalizada da superfície é construída (DUFRÊNE, 2002; HINTERDORFER, P.; DUFRÊNE, 2006; WHITED; PARK, 2014).

Figura 13. Esquema ilustrativo do mecanismo de funcionamento de um microscópio de força atômica.

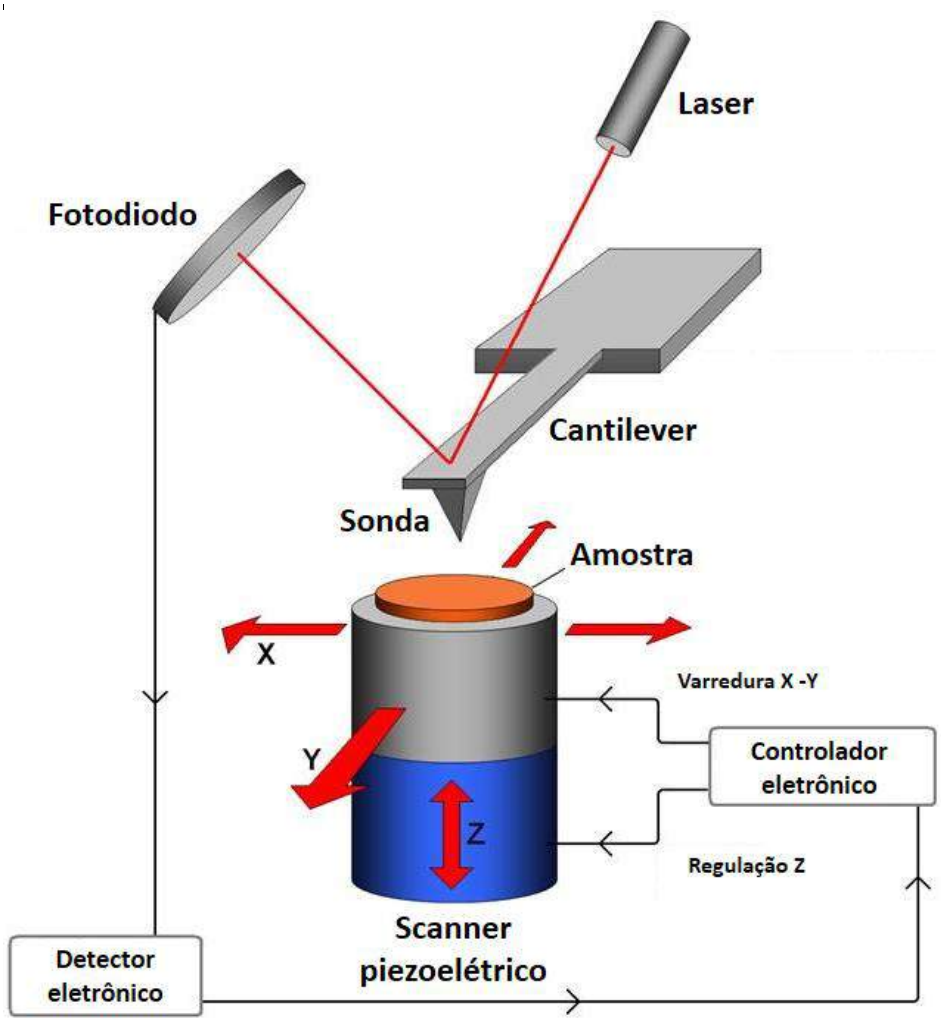

Fonte: Adapatada de DEPARTMENT OF PHARMACOLOGY/UNIVERSITY OF VIRGINIA SCHOOL OF MEDICINE, 2017.

Quando a ponta da sonda está próxima da amostra, ela é primeiramente atraída pela superfície devido a existência de forças atrativas na região, como as forças de Van der Waals, interações eletrostáticas, forças químicas e forças capilares. À medida que esta distância diminui, há o predomínio de forças repulsivas que ocasionam o enfraquecimento das forças atrativas. O fenômeno de repulsão acontece quando os átomos que constituem a ponta da sonda e o átomos da amostra estão tão próximos que seus orbitais eletrônicos começam a se repelir. As forças anulam-se quando a distância entre os átomos está na ordem de alguns ângströms (a qual corresponde a distância característica que uma ligação química) (ZLATANOVA; LINDSAY; LEUBA, 2000; BUTT; CAPPELLA; KAPPL, 2005).

Na Figura 14 está descrita a curva teórica para a energia potencial resultante das interações entre os átomos da sonda e os átomos da amostra em função da distância de separação. Uma força de interação positiva corresponde a uma força repulsiva que empurra a ponta da sonda para longe da amostra. Neste caso, o cantilever sofrerá deflexão positiva em uma direção vertical. Em oposição, uma força de interação negativa representa uma força atrativa que puxa a ponta da sonda em direção à amostra, o que resulta em uma deflexão negativa do cantilever (CAPPELLA; DIETLER, 1999; BUTT; CAPPELLA; KAPPL, 2005; CAPPELLA, 2016).

Figura 14. Efeito da distância entre a sonda e a amostra sobre o regime de forças do sistema.

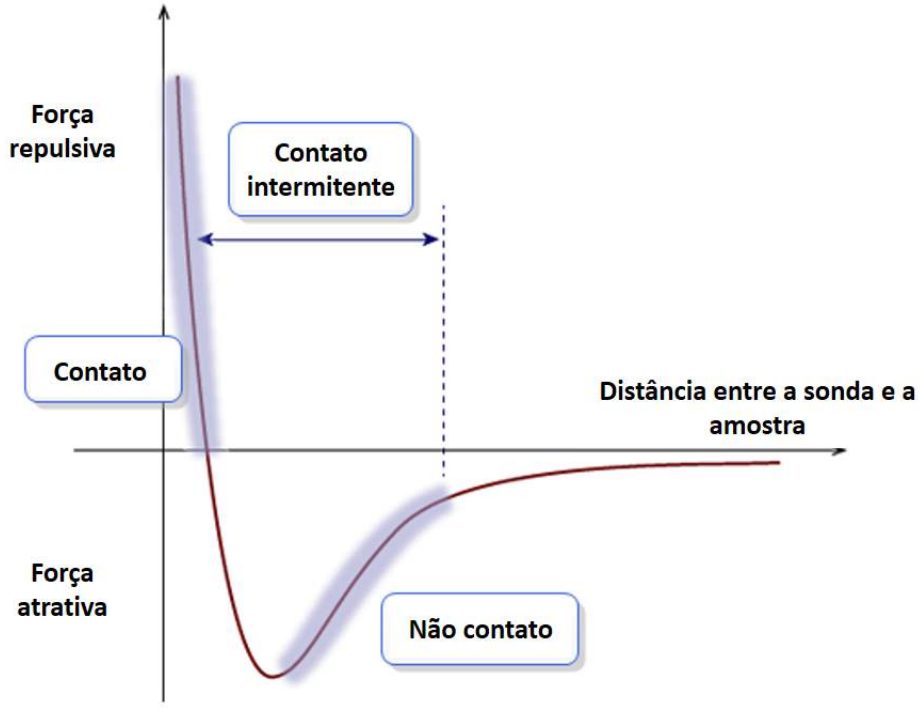

Fonte: Adapatada de SPM TRAINING GUIDE, 2011.

O microscópio de força atômica funciona em três modos distintos de operação: modo de contato, modo de não contato e modo de contato intermitente. As forças de interação entre a sonda e a amostra variam de acordo com o modo de operação em uso, como será destacado a seguir (DUFRÊNE, 2002; SANTOS; CASTANHO, 2004).

a) Modo de contato: a ponta da sonda é colocada em contato físico com a amostra, de tal forma que o regime de forças é repulsivo. Por esta razão, a constante elástica do cantilever utilizado neste modo de operação deve ter o menor valor possível para conseguir uma boa flexão e não danificar a amostra. O modo de contato pode ser realizado de duas formas

diferentes para obtenção da imagem. Na primeira forma, a distância relativa entre a ponta da sonda e a superfície da amostra é mantida constante durante o processo de análise. Através de deflexões no cantilever (resultante de variações nas forças de interação atômica) e por meio do registro das coordenadas x e y, a imagem topográfica é construída. Na segunda forma, o cantilever é mantido a uma deflexão constante e a amostra é movida ao longo do plano x e y, de tal maneira que a altura (distância) e os valores de x e y são registrados para a montagem da topografia da amostra (Figura 15A) (JALILI; LAXMINARAYANA, 2004; KASAS; LONGO; DIETLER, 2013).

b) Modo de não contato: quando operado neste modo, a ponta da sonda oscila a uma distância na ordem de nanômetros entre a superfície da amostra. O cantilever vibra em uma frequência de ressonância com baixa amplitude para garantir que a amostra não seja tocada. Neste tipo de operação prevalecem as forças atrativas, logo, o cantilever deve ser suficientemente rígido com uma constante elástica de alto valor (Figura 15B) (MORITA et al., 2015).

c) Modo de contato intermitente: neste modo de operação, também denominado de modo dinâmico ou *tapping mode*, o cantilever oscila em sua frequência natural de ressonância, sendo posto em contato intermitente com a amostra (a superfície da amostra é tocada de forma periódica). Assim, o microscópio atua em dois regimes de forças: ora atrativa e ora repulsiva. Em cada ciclo, a ponta da sonda entra em contato com a amostra durante um tempo finito. Quando a ponta da sonda varre diferentes alturas ocorre uma variação na amplitude de oscilação, possibilitando a formação da imagem (Figura 15C) (GARCIA; PEREZ, 2002; JONES et al., 2016).

Figura 15. Modos de operação de um microscópio de força atômica: modo de contato (A), modo de não contato (B) e modo de contato intermitente (C).

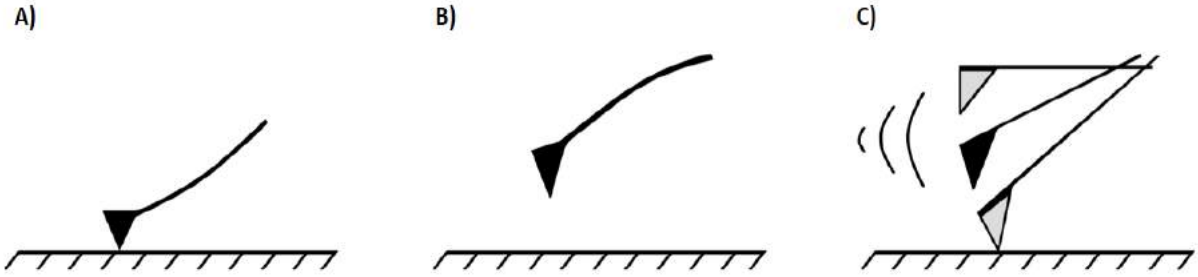

Fonte: Adaptada de WIKIMEDIA COMMONS, 2016.

Apesar da AFM ser uma técnica de caracterização precisa e com elevada sensibilidade para monitorização de superfícies, alguns aspectos podem interferir na qualidade da imagem. Por exemplo, cita-se a presença de impurezas na amostra, a umidade relativa do ar, os materiais que compõem a amostra e a sonda, bem como a geometria e as dimensões da sonda. Logo, todos estes fatores em associação com a experiência do analista irá determinar a qualidade da micrografia. Em casos de baixa qualidade, podem aparecer artefatos na imagem que encobrem a verdadeira morfologia da superfície da amostra (CAPPELLA, B.; DIETLER, 1999; ZANETTE et al., 2000; NEUMAN; NAGY, 2008; MORITA et al., 2015).

As análises de AFM tem sido cada vez mais utilizadas no estudo de biossensores, possibilitando uma caracterização topográfica tridimensional de eletrodos biomodificados, observação direta de plataformas nanoestruturadas e avaliação de processos de biorreconhecimento (BOUGRINI et al., 2016; NGUYEN et al., 2016; POVEDANO et al., 2017). Recentemente, Chen et al. utilizaram a técnica de AFM para monitorar a imobilização de sondas de DNA com grupos tióis terminais sobre um eletrodo de carbono vítreo modificado com folhas de grafeno, PANI e AuNps. Foi observado que o eletrodo modificado com folhas de grafeno, PANI e AuNps apresenta uma topografia rugosa e granular. Entretanto, após a ancoragem dos segmentos de DNA, verifica-se uma alteração na aparência do sistema nanoestruturado. Este passa a exibir um maior número de agragados, o que evidencia a imobilização efetiva das sondas de DNA específicas para a biodetecção do oncogene quimérico BCR/ABL (CHEN et al., 2015). Em adição, HUSHEGYI et al. desenvolveram um biossensor impedimétrico baseado em glicanos para a detecção do vírus influenza H3N2 com um limite de detecção de 13 partículas virais/µL. As análises de AFM possibilitaram a caracterização topográfica de cada etapa de montagem do biossensor e a avaliação do processo de captura de partículas virais (HUSHEGYI et al., 2016). Diante destas aplicações, constata-se o potencial da técnica de AFM para o desenvolvimento de sistemas biossensíveis (WANG et al., 2014; LI, et al., 2016).

2.6 Espectroscopia de infravermelho com transformada de Fourier

A espectroscopia de infravermelho é um tipo de espectroscopia de absorção em que a energia absorvida encontra-se na região do infravermelho do espectro eletromagnético. Esta técnica é amplamente utilizada para identificação de substâncias químicas e análise da composição de diferentes amostras (JAWAID et al., 2013; HAMEED; IBRAHEAM; KADHIM, 2015; CEBI et al., 2016). Sabe-se que a uma temperatura superior ao zero

absoluto, todos os átomos e moléculas encontram-se sob vibração constante. Partindo deste princípio, a espectroscopia de infravermelho fundamenta-se no fato de que as frequências vibracionais são específicas para cada ligação atômica. Por exemplo, ao incidir uma radiação infravermelha com energia correspondente a frequência vibracional da molécula, ocorrerá a absorção da radiação. No entanto, este fenômeno de absorção ocorre apenas em moléculas ativas ao infravermelho. Estas moléculas possuem ligações atômicas que vibram ritmicamente e apresentam um momento dipolar elétrico. O campo elétrico alternado, produzido pela distribuição de cargas ao longo da vibração molecular, acopla o campo magnético oscilante da radiação eletromagnética, o que resulta na absorção de energia radiante no infravermelho. Como resultado, a molécula é excitada a um estado energético superior. Apesar deste processo de absorção no infravermelho ser quantizado (apenas certas frequências são absorvidas), o espectro é composto por uma série de bandas ao invés de linhas como apresentado na Figura 16. Este fato ocorre porque cada mudança de nível vibracional está associado a uma série de alterações nos níveis rotacionais. As vibrações moleculares podem ser classificadas em deformações axiais (também denominadas de deformações de estiramento) e deformações angulares. Em adição, estas vibrações podem ser simétricas ou assimétricas. As vibrações de deformação axial correspondem à movimentos rítmicos ao longo do eixo interatômico que aumenta e diminui alternadamente. As vibrações de deformação angular envolvem a alteração do ângulo entre duas ligações químicas (STUART, 2005; BAKER et al., 2014; SATHYANARAYANA, 2015).

Figura 16. Espectro de absorbância no infravermelho para as principais macromoléculas biológicas.

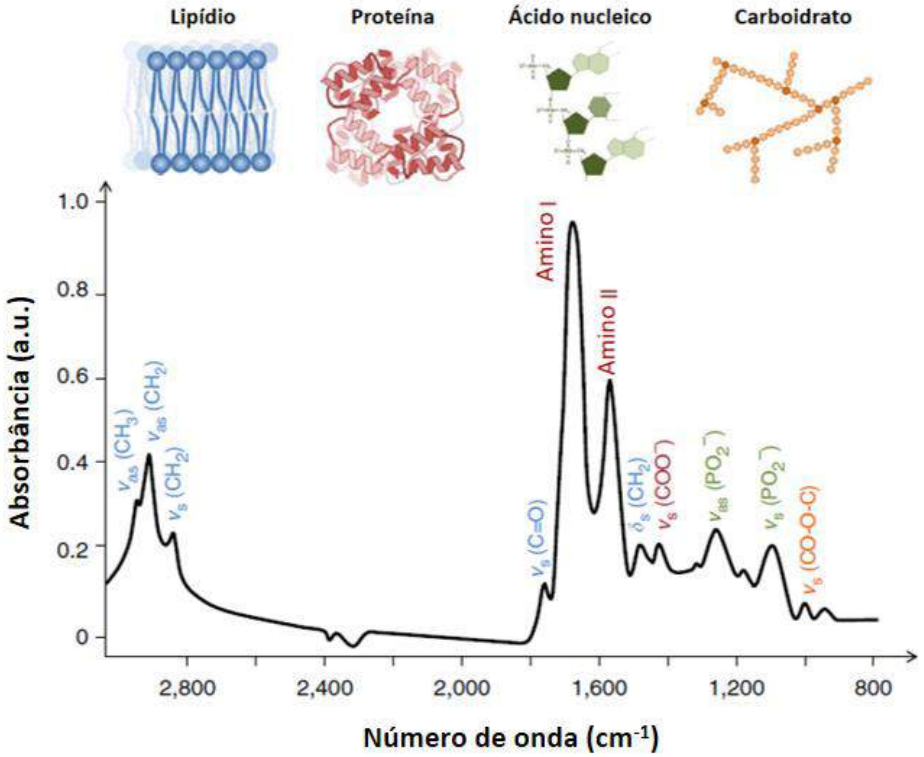

Onde, ν - vibrações de estiramento, δ - vibrações de flexão (angulares), s - vibrações simétricas e as - vibrações assimétricas. Fonte: BAKER et al., 2014.

A espectroscopia de infravermelho com transformada de Fourier (FTIR) é uma técnica variante da espectroscopia de infravermelho que baseia-se na mesma premissa dos estados moleculares vibracionais. A técnica de FTIR possibilita uma otimização das funções da espectroscopia de infravermelho convencional, assegurando uma maior sensibilidade, resolução e velocidade de análise. Durante o funcionamento do equipamento de FTIR, a radiação infravermelha contendo todos os comprimentos de onda de interesse (proveniente de uma fonte) é separada em dois feixes eletromagnéticos. Um destes feixes percorre uma distância específica até o espelho fixo e o outro feixe percorre uma distância variável até o espelho móvel. Após a reflexão nas superfícies dos espelhos, os dois feixes se encontram e sofrem interferências, sendo estas construtivas ou destrutivas e dependentes da trajetória da luz em função do espelho móvel. Posteriormente, o detector é capaz de identificar estas variações na intensidade da radiação infravermelha. A diferença no caminho percorrido entre os dois feixes eletromagnéticos é chamada de “atraso” e o gráfico da intensidade da radiação em função do atraso é chamado de interferograma. Por meio da transformada de Fourier, o

interferograma que encontra-se no domínio de tempo/distância pode ser convertido em um interferograma de domínio de frequências. Logo, através de variações sucessivas na posição do espelho móvel, é possível obter, pela transformada de Fourier, o espectro completo na região do infravermelho (Figura 17) (SMITH, 1996; GRIFFITHS; DE HASETH, 2007; LASCH; NAUMANN, 2015).

Figura 17. Componentes básicos de um espectrofotômetro de FTIR e o processo analítico para obtenção dos espectros de absorção.

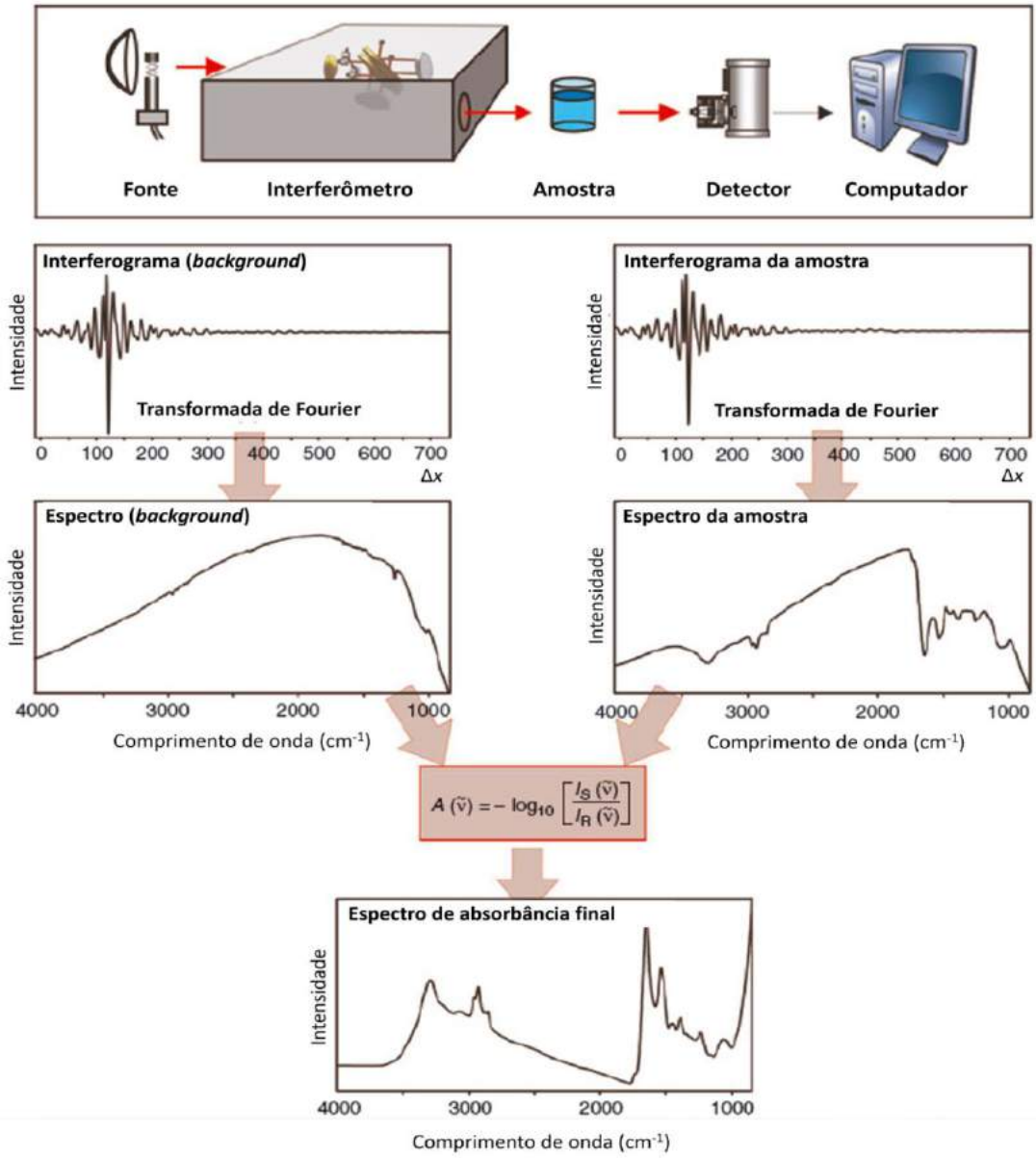

Após apresentar os componentes básicos de um espectrofotômetro de FTIR, o princípio de funcionamento da técnica é descrita graficamente. Primeiramente, obtêm-se os interferogramas (de background e amostra) que serão convertidos em espectros através da transformada de Fourier. Por meio de uma fórmula específica, os dois espectros (de background e amostra) são utilizados para calcular o espectro de absorbância final de FTIR. Fonte: Adapatada de LASCH; NAUMANN, 2015.

CAPÍTULO 3

3 OBJETIVOS

3.1 Objetivo geral

- Construir dois biossensores eletroquímicos baseados em AuNpsPANI e Cys-cMWCNT-ZnONp/NH_2 para a detecção ultrassensível do oncogene quimérico BCR/ABL.

3.2 Objetivos específicos

Biossensor baseado em AuNpsPANI-sonda

- Avaliar as propriedades interfaciais do compósito híbrido AuNpsPANI adsorvido em eletrodo de ouro através das técnicas de VC e EIE.
- Analisar o processo de adsorção eletrostática da sonda de DNA sobre o eletrodo de ouro modificado com AuNpsPANI.
- Verificar a capacidade de reconhecimento bioespecífico e a sensibilidade do biossensor AuNpsPANI-sonda após sua interação com plasmídeos contendo o oncogene quimérico BCR/ABL em variáveis concentrações (controle positivo).
- Avaliar a seletividade do biossensor AuNpsPANI-sonda frente à plasmídeos contendo segmentos de DNA não complementares (controle negativo).
- Determinar o limite de detecção do biossensor AuNpsPANI-sonda e realizar ensaios de biodetecção em amostras clínicas de pacientes com leucemia e doença residual mínima (amostras de cDNA).
- Realizar análise topográfica do filme biológico AuNpsPANI-sonda e avaliar as características morfológicas de sua superfície após o processo de biodetecção por meio da técnica de AFM.

Biossensor baseado em Cys-cMWCNT-ZnONp/NH_2-sonda

- Funcionalizar quimicamente as ZnONp com APTES e realizar análise de FTIR.
- Estudar a formação da camada auto-montada de Cys sobre eletrodo de ouro e avaliar suas propriedades eletroquímicas através das técnicas de VC e EIE.

- Avaliar o processo de conjugação química dos cMWCNT sobre o eletrodo de ouro modificado com Cys e verificar sua influência sobre a condutividade do sistema nanoestruturado.
- Analisar o comportamento físico-químico das ZnONp/NH_2 adsorvidas quimicamente sobre o eletrodo de ouro modificado com Cys e cMWCNT.
- Imobilizar a sonda de DNA com grupos amino funcionais sobre a plataforma nanoestruturada de Cys-cMWCNT-ZnONp/NH_2 através de ligações covalentes específicas.
- Verificar a capacidade de reconhecimento bioespecífico e a sensibilidade do biossensor Cys-cMWCNT-ZnONp/NH_2-sonda após sua interação com plasmídeos contendo o oncogene quimérico BCR/ABL em variáveis concentrações (controle positivo).
- Avaliar a seletividade do biossensor Cys-cMWCNT-ZnONp/NH_2-sonda frente à plasmídeos contendo segmentos de DNA não complementares (controle negativo).
- Determinar o limite de detecção do biossensor Cys-cMWCNT-ZnONp/NH_2-sonda e realizar ensaios de biodetecção em amostras clínicas de pacientes com leucemia e doença residual mínima (amostras de cDNA).
- Realizar análise topográfica do filme biológico Cys-cMWCNT-ZnONp/NH_2-sonda e avaliar as características morfológicas de sua superfície após o processo de biodetecção por meio da técnica de AFM.

CAPÍTULO 4

4 REFERÊNCIAS DA FUNDAMENTAÇÃO TEÓRICA

ABDULHALIM, I.; ZOUROB, M.; LAKHTAKIA, A. Overview of optical biosensing techniques. **Handbook of Biosensors and Biochips**, 2008.

ABU-SALAH, K. M. et al. DNA-based nanobiosensors as an emerging platform for detection of disease. **Sensors**, v. 15, n. 6, p. 14539-14568, 2015.

ADVANI, A. S.; PENDERGAST, A. M. BCR-ABL variants: biological and clinical aspects. **Leukemia Research**, v. 26, p. 713-720, 2002.

AHMAD, L. M. et al. Binding event measurement using a chip calorimeter coupled to magnetic beads. **Sensors and Actuators B: Chemical**, v. 145, n. 1, p. 239-245, 2010.

AITHAL, P. S. Nanotechnology Innovations & Business Opportunities: A Review. **International Journal of Management, IT and Engineering**, v.6, n.1, p. 182-204, 2016.

ALVES, V. A.; BRETT, C. M. A. Characterisation of passive films formed on mild steels in bicarbonate solution by EIS. **Electrochimica Acta**, v. 47, n. 13, p. 2081-2091, 2002.

AMERICAN CANCER SOCIETY. **How Is Acute Lymphocytic Leukemia Diagnosed?**. 2016. Disponível em: <https://www.cancer.org/cancer/acute-lymphocytic-leukemia/detection-diagnosis-staging/how-diagnosed.html>. Acesso em: 02 fev. 2017.

ANDRADE, C. A. S. et al. Diagnosis of dengue infection using a modified gold electrode with hybrid organic–inorganic nanocomposite and Bauhinia monandra lectin. **Journal of Colloid and Interface Science**, v. 362, n. 2, p. 517-523, 2011.

ANDRADE, C. A. S. et al. Nanostructured sensor based on carbon nanotubes and clavanin A for bacterial detection. **Colloids and Surfaces B: Biointerfaces**, v. 135, p. 833-839, 2015.

ANTUNES, A. M. S. et al. Trends in nanotechnology patents applied to the health sector. **Recent patents on nanotechnology**, v. 6, n. 1, p. 29-43, 2012.

ARBER, D. A. et al. The 2016 revision to the World Health Organization (WHO) classification of myeloid neoplasms and acute leukemia. **Blood**, p. 1-45, 2016.

ARDUINI, F. et al. Electrochemical biosensors based on nanomodified screen-printed electrodes: Recent applications in clinical analysis. **TrAC Trends in Analytical Chemistry**, v. 79, p. 114-126, 2016.

AVELINO, K. Y. P. S. et al. Biosensor based on hybrid nanocomposite and CramoLL lectin for detection of dengue glycoproteins in real samples. **Synthetic Metals**, v. 194, p. 102-108, 2014.

BADGER-BROWN, K. M. et al. CBL-B is required for leukemogenesis mediated by BCR-ABL through negative regulation of bone marrow homing. **Leukemia**, v. 27, n. 5, p. 1146-1154, 2013.

BAHADIR, E. B.; SEZGINTÜRK, M. K. A review on impedimetric biosensors. **Artificial Cells, Nanomedicine, and Biotechnology**, v. 44, n. 1, p. 248-262, 2016.

BAHADIR, E. B.; SEZGINTÜRK, M. K. Applications of commercial biosensors in clinical, food, environmental, and biothreat/biowarfare analyses. **Analytical Biochemistry**, v. 478, p. 107-120, 2015.

BAI, S. et al. A novel colorimetric biosensor for detecting target DNA and human alpha thrombin based on associative toehold activation concatemer induced catalyzed hairpin assembly amplification. **Sensors and Actuators B: Chemical**, v. 239, p. 447-454, 2017.

BAKER, M. J. et al. Using Fourier transform IR spectroscopy to analyze biological materials. **Nature Protocols**, v. 9, n. 8, p. 1771-1791, 2014.

BALASUBRAMANIAN, K.; BURGHARD, M. Chemically functionalized carbon nanotubes. **Small**, v. 1, n. 2, p. 180-192, 2005.

BANDODKAR, A. J.; WANG, J. Non-invasive wearable electrochemical sensors: a review. **Trends in Biotechnology**, v. 32, n. 7, p. 363-371, 2014.

BARD, A. J. et al. Fundamentals and applications. **Electrochemical Methods**, v. 2, 2001.

BAZIN, I. et al. New biorecognition molecules in biosensors for the detection of toxins. **Biosensors and Bioelectronics**, v. 87, p. 285-298, 2017.

BEN-NERIAH, Y. et al. The chronic myelogenous leukemis-specific P210 protein is the product of the bcr-abl hybrid gene. **Science**, v. 233, p. 212-215, 1986.

BINNIG, G.; QUATE, C. F.; GERBER, C. Atomic force microscope. **Physical Review Letters**, v. 56, n. 9, p. 930, 1986.

BENNOUR, A. et al. Comprehensive analysis of BCR/ABL variants in chronic myeloid leukemia patients using multiplex RT-PCR. **Clinical Laboratory**, v. 58, p. 433-439, 2012.

BENNOUR, A.; SAAD, A.; SENNANA, H. Chronic myeloid leukemia: Relevance of cytogenetic and molecular assays. **Critical Reviews in Oncology/Hematology**, v. 97, p. 263-274, 2016.

BEREZA-MALCOLM, L. T.; FRANKS, A. E. Coupling anaerobic bacteria and microbial fuel cells as whole-cell environmental biosensors. **Microbiology Australia**, v. 36, n. 3, p. 129-132, 2015.

BHATTA, D. et al. Label-free monitoring of antibody–antigen interactions using optical microchip biosensors. **Journal of Immunological Methods**, v. 362, n. 1, p. 121-126, 2010.

BILGI, M.; AYRANCI, E. Biosensor application of screen-printed carbon electrodes modified with nanomaterials and a conducting polymer: Ethanol biosensors based on alcohol dehydrogenase. **Sensors and Actuators B: Chemical**, v. 237, p. 849-855, 2016.

BOCHTLER, T.; FRÖHLING, S.; KRÄMER, A. Role of chromosomal aberrations in clonal diversity and progression of acute myeloid leukemia. **Leukemia**, v. 29, n. 6, p. 1243-1252, 2015.

BONANNI, A.; PUMERA, M.; MIYAHARA, Y. Influence of gold nanoparticle size (2–50 nm) upon its electrochemical behavior: an electrochemical impedance spectroscopic and voltammetric study. **Physical Chemistry Chemical Physics**, v. 13, n. 11, p. 4980-4986, 2011.

BOTT, A. W. Electrochemical techniques for the characterization of redox polymers. **Current Separations**, v. 19, n. 3, p. 71-75, 2001.

BOUGRINI, M. et al. Development of a novel capacitance electrochemical biosensor based on silicon nitride for ochratoxin A detection. **Sensors and Actuators B: Chemical**, v. 234, p. 446-452, 2016.

BRETT, C. M. A.; BRETT, A. M. O. **Electrochemistry: principles, methods, and applications**. Oxford university press, 1993.

BUNDE, R. L.; JARVI, E. J.; ROSENTRETER, J. J. Piezoelectric quartz crystal biosensors. **Talanta**, v. 46, n. 6, p. 1223-1236, 1998.

BUTT, H. J.; CAPPELLA, B.; KAPPL, M. Force measurements with the atomic force microscope: Technique, interpretation and applications. **Surface Science Reports**, v. 59, n. 1, p. 1-152, 2005.

CALZADO-MARTIN, A. et al. Effect of actin organization on the stiffness of living breast cancer cells revealed by peak-force modulation atomic force microscopy. **ACS Nano**, v. 10, n. 3, p. 3365-3374, 2016.

CAMPAS, M.; KATAKIS, I. DNA biochip arraying, detection and amplification strategies. **TrAC Trends in Analytical Chemistry**, v. 23, n. 1, p. 49-62, 2004.

CAO, Y.; SMITH, P.; HEEGER, A. J. Counter-ion induced processibility of conducting polyaniline and of conducting polyblends of polyaniline in bulk polymers. **Synthetic Metals**, v. 48, n. 1, p. 91-97, 1992.

CAPPELLA, B. Physical Principles of Force - Distance Curves by Atomic Force Microscopy. In: **Mechanical Properties of Polymers Measured through AFM Force-Distance Curves**. Springer International Publishing, 2016. p. 3-66.

CAPPELLA, B.; DIETLER, G. Force-distance curves by atomic force microscopy. **Surface Science Reports**, v. 34, n. 1-3, p. 15-3104, 1999.

CAYGILL, R. L.; BLAIR, G. E.; MILLNER, P. A. A review on viral biosensors to detect human pathogens. **Analytica Chimica Acta**, v. 681, p. 8-15, 2010.

CAZZOLA, M. **Introduction to a review series on myeloproliferative neoplasms**. 2016.

CEBI, N. et al. An evaluation of Fourier transforms infrared spectroscopy method for the classification and discrimination of bovine, porcine and fish gelatins. **Food Chemistry**, v. 190, p. 1109-1115, 2016.

CHANDRA, H. S.et al. Philadelphia Chromosome Symposium: commemoration of the 50th anniversary of the discovery of the Ph chromosome. **Cancer Genetics**, v. 204, n. 4, p. 171-179, 2011.

CHANG, B. Y.; PARK, S. M. Electrochemical impedance spectroscopy. **Annual Review of Analytical Chemistry**, v. 3, p. 207-229, 2010.

CHAO, J. et al. DNA nanotechnology-enabled biosensors. **Biosensors and Bioelectronics**, v. 76, p. 68-79, 2016.

CHAUHAN, N. et al. An electrochemical sensor for detection of neurotransmitter-acetylcholine using metal nanoparticles, 2D material and conducting polymer modified electrode. **Biosensors and Bioelectronics**, v. 89, p. 377-383, 2017.

CHEN, A.; CHATTERJEE, S. Nanomaterials based electrochemical sensors for biomedical applications. **Chemical Society Reviews**, v. 42, n. 12, p. 5425-5438, 2013.

CHEN, H. et al. Trends in nanotechnology patents. **Nature nanotechnology**, v. 3, n. 3, p. 123-125, 2008a.

CHEN, J. et al. Electrochemical biosensor for detection of BCR/ABL fusion gene using locked nucleic acids on 4-aminobenzenesulfonic acid-modified glassy carbon electrode. **Analytical chemistry**, v. 80, n. 21, p. 8028-8034, 2008b.

CHEN, L. et al. A novel e8a2 BCR-ABL1 intronic fusion through insertion of a chromosome 22 BCR gene fragment into chromosome 9 in an atypical Philadelphia (Ph) chromosome chronic myeloid leukemia patient. **Leukemia & lymphoma**, v. 57, n. 12, p. 2930-2933, 2016.

CHEN, S. et al. Gold nanoelectrodes of varied size: transition to molecule-like charging. **Science**, v. 280, n. 5372, p. 2098-2101, 1998.

CHEN, X. et al. Coupling a universal DNA circuit with graphene sheets/polyaniline/AuNPs nanocomposites for the detection of BCR/ABL fusion gene. **Analytica Chimica Acta**, v. 889, p. 90-97, 2015.

CHEN, X. Y. et al. A new step to the mechanism of the enhancement effect of gold nanoparticles on glucose oxidase. **Biochemical and Biophysical Research Communications**, v. 245, n. 2, p. 352-355, 1998.

CHENG, M. S. et al. Impedimetric cell-based biosensor for real-time monitoring of cytopathic effects induced by dengue viruses. **Biosensors and Bioelectronics**, v. 70, p. 74-80, 2015.

CHEVION, S.; ROBERTS, M. A.; CHEVION, M. The use of cyclic voltammetry for the evaluation of antioxidant capacity. **Free Radical Biology and Medicine**, v. 28, n. 6, p. 860-870, 2000.

CLARK, L. C.; LYONS, C. Electrode systems for continuous monitoring in cardiovascular surgery. **Annals of the New York Academy of sciences**, v. 102, n. 1, p. 29-45, 1962.

CINCOTTO, F. H. et al. Electrochemical immunosensor for ethinylestradiol using diazonium salt grafting onto silver nanoparticles-silica–graphene oxide hybrids. **Talanta**, v. 147, p. 328-334, 2016.

CONGUR, G. et al. Zinc Oxide Nanowire Decorated Single-Use Electrodes for Electrochemical DNA Detection. **Journal of the American Ceramic Society**, v. 98, n. 2, p. 663-668, 2015.

COSTA, M. P. et al. Self-assembled monolayers of mercaptobenzoic acid and magnetite nanoparticles as an efficient support for development of tuberculosis genosensor. Journal of **Colloid and Interface Science**, v. 433, p. 141-148, 2014.

COSTENARO, D. et al. Preparation of luminescent ZnO nanoparticles modified with aminopropyltriethoxy silane for optoelectronic applications. **New Journal of Chemistry**, v. 37, n. 7, p. 2103-2109, 2013.

DAMBORSKÝ, P.; ŠVITEL, J.; KATRLÍK, J. Optical biosensors. **Essays in Biochemistry**, v. 60, n. 1, p. 91-100, 2016.

DAMOS, F. S.; MENDES, R. K.; KUBOTA, L. T. Applications of QCM, EIS and SPR in the investigation of surfaces and interfaces for the development of (bio)sensors. **Química Nova**, v. 27, n. 6, p. 970-979, 2004.

DARAEE, H. et al. Application of gold nanoparticles in biomedical and drug delivery. **Artificial Cells, Nanomedicine, and Biotechnology**, v. 44, n. 1, p. 410-422, 2016.

DEL PRINCIPE, M. I. et al. Minimal residual disease in acute myeloid leukemia of adults: determination, prognostic impact and clinical applications. **Mediterranean Journal of Hematology and Infectious Diseases**, v. 8, n. 1, 2016.

DEPARTMENT OF PHARMACOLOGY/UNIVERSITY OF VIRGINIA SCHOOL OF MEDICINE. **Atomic Force Microscope (AFM)**. 2017. Disponível em: <https://pharm.virginia.edu/facilities/atomic-force-microscope-afm/>. Acesso em: 02 fev. 2017.

DE VOLDER, M. F. L. et al. Carbon nanotubes: present and future commercial applications. **Science**, v. 339, n. 6119, p. 535-539, 2013.

DEY, A. et al. Mediator free highly sensitive polyaniline-gold hybrid nanocomposite based immunosensor for prostate-specific antigen (PSA) detection. **Journal of Materials Chemistry**, v. 22, p. 14763-14772, 2012.

DO NASCIMENTO, N. M. et al. Label-free piezoelectric biosensor for prognosis and diagnosis of Systemic Lupus Erythematosus. **Biosensors and Bioelectronics**, v. 90, p. 166-173, 2017.

DONG, S. et al. Electrochemical DNA biosensor based on a tetrahedral nanostructure probe for the detection of avian influenza A (H7N9) virus. **ACS Applied Materials & Interfaces**, v. 7, n. 16, p. 8834-8842, 2015.

D'ORAZIO, P. Biosensors in clinical chemistry. **Clinica Chimica Acta**, v. 334, p. 41-69, 2003.

DRAGHI, P. F.; FERNANDES, J. C. B. Label-free potentiometric biosensor based on solid-contact for determination of total phenols in honey and propolis. **Talanta**, v. 164, p. 413-417, 2017.

DRUMMOND, T. G.; HILL, M. G.; BARTON, J. K. Electrochemical DNA sensors. **Nature Biotechnology**, v. 21, p. 1192-1199, 2003.

DUFRÊNE, Y. F. Atomic force microscopy, a powerful tool in microbiology. **Journal of Bacteriology**, v. 184, n. 19, p. 5205-5213, 2002.

EATON, P.; WEST, P. **Atomic force microscopy**. Oxford University Press, 2010.

EDMONDSON, R. et al. Three-dimensional cell culture systems and their applications in drug discovery and cell-based biosensors. **Assay and Drug Development Technologies**, v. 12, n. 4, p. 207-218, 2014.

EICHHORST, B. et al. Chronic lymphocytic leukaemia: ESMO Clinical Practice Guidelines for diagnosis, treatment and follow-up. **Annals of Oncology**, v. 26, n. suppl 5, p. v78-v84, 2015.

ENCYCLOPAEDIA BRITANNICA. **DNA Chemical Compound.** 2015. Disponível em: <https://global.britannica.com/science/DNA>. Acesso em: 30 jan. 2017.

ENDO, M.; SUGIYAMA, H. Single-molecule imaging of dynamic motions of biomolecules in DNA origami nanostructures using high-speed atomic force microscopy. **Accounts of Chemical Research**, v. 47, n. 6, p. 1645-1653, 2014.

ENENGL, C. et al. Explaining the Cyclic Voltammetry of a Poly (1, 4-phenylene-ethynylene)-alt-poly (1, 4-phenylene-vinylene) Copolymer upon Oxidation by using Spectroscopic Techniques. **ChemPhysChem**, v. 18, n. 1, p. 93-100, 2017.

FADEL, T. R. et al. Toward the Responsible Development and Commercialization of Sensor Nanotechnologies. **ACS Sensors**, v. 1, n. 3, p. 207-216, 2016.

FAIRMAN STUDIOS. **The Philadelphia chromosome**. 2013. Disponível em: <http://www.fairmanstudios.com/the-philadelphia-chromosome/>. Acesso em: 31 jan. 2017.

FEDERMANN, B. et al. The detection of SRSF2 mutations in routinely processed bone marrow biopsies is useful in the diagnosis of chronic myelomonocytic leukemia. **Human Pathology**, v. 45, n. 12, p. 2471-2479, 2014.

FENG, C.; DAI, S.; WANG, L. Optical aptasensors for quantitative detection of small biomolecules: A review. **Biosensors and Bioelectronics**, v. 59, p. 64-74, 2014.

FERLAY, J. et al. Breast and cervical cancer in 187 countries between 1980 and 2010. **The Lancet**, v. 379, n. 9824, p. 1390-1391, 2012.

FEUK, L.; CARSON, A. R.; SCHERER, S. W. Structural variation in the human genome. **Nature Reviews Genetics**, v. 7, p. 85-97, 2006.

FRÍAS, I. A. M. et al. Trends in biosensors for HPV: identification and diagnosis. **Journal of Sensors**, v. 2015, p. 1-16, 2015.

FUENTES, M. et al. Directed covalent immobilization of aminated DNA probes on aminated plates. **Biomacromolecules**, v. 5, n. 3, p. 883-888, 2004.

GARCIA, M. F. K. S. et al. Impedimetric sensor for Leishmania infantum genome based on gold nanoparticles dispersed in polyaniline matrix. **Journal of Chemical Technology and Biotechnology**, v. 91, n. 11, p. 2810-2816, 2016.

GARCIA, R; PEREZ, R. Dynamic atomic force microscopy methods. **Surface Science Reports**, v. 47, n. 6, p. 197-301, 2002.

GENT, D. C. V; HOEIJMAKERS, J. H. J.; KANAAR, R. Chromosomal stability and the DNA double-stranded break connection. **Nature Reviews Genetics**, v. 2, p. 196-206, 2001.

GONG, Q.; WANG, Y.; YANG, H. A sensitive impedimetric DNA biosensor for the determination of the HIV gene based on graphene-Nafion composite film. **Biosensors and Bioelectronics**, v. 89, p. 565-569, 2017.

GRASSET, F. et al. Surface modification of zinc oxide nanoparticles by aminopropyltriethoxysilane. **Journal of Alloys and Compounds**, v. 360, n. 1, p. 298-311, 2003.

GRIESHABER, D. et al. Electrochemical biosensors-sensor principles and architectures. **Sensors**, v. 8, n. 3, p. 1400-1458, 2008.

GRIFFITHS, P. R.; DE HASETH, J. A. **Fourier transform infrared spectrometry**. John Wiley & Sons, 2007.

GUAN, J. G.; MIAO, Y. Q.; ZHANG, Q. J. Impedimetric biosensors. **Journal of Bioscience and Bioengineering**, v. 97, p.219-226, 2004.

GUARNERIO, J. et al. Oncogenic role of fusion-circRNAs derived from cancer-associated chromosomal translocations. **Cell**, v. 165, n. 2, p. 289-302, 2016.

GUIDUCCI, C. et al. A biosensor for direct detection of DNA sequences based on capacitance measurements. In: **Proceeding of the 32nd European Solid-State Device Research Conference**. 2002. p. 24-26.

GUPTA, V. K. et al. Voltammetric techniques for the assay of pharmaceuticals - a review. **Analytical Biochemistry**, v. 408, n. 2, p. 179-196, 2011.

GUZMAN, M. L.; ALLAN, J. N. Concise review: leukemia stem cells in personalized medicine. **Stem Cells**, v. 32, n. 4, p. 844-851, 2014.

HALLEK, M. et al. Guidelines for the diagnosis and treatment of chronic lymphocytic leukemia: a report from the International Workshop on Chronic Lymphocytic Leukemia updating the National Cancer Institute – Working Group 1996 guidelines. **Blood**, v. 111, n. 12, p. 5446-5456, 2008.

HAMEED, I. H.; IBRAHEAM, I. A.; KADHIM, H. J. Gas chromatography mass spectrum and fourier-transform infrared spectroscopy analysis of methanolic extract of Rosmarinus oficinalis leaves. **Journal of Pharmacognosy and Phytotherapy**, v. 7, n. 6, p. 90-106, 2015.

HAN, J. H. et al. A multi-virus detectable microfluidic electrochemical immunosensor for simultaneous detection of H1N1, H5N1, and H7N9 virus using ZnO nanorods for sensitivity enhancement. **Sensors and Actuators B: Chemical**, v. 228, p. 36-42, 2016.

HANG, T. T. X. et al. Effect of silane modified nano ZnO on UV degradation of polyurethane coatings. **Progress in Organic Coatings**, v. 79, p. 68-74, 2015.

HANSMA, P. K. et al. Scanning tunneling microscopy and atomic force microscopy: application to biology and technology. **Science**, v. 242, n. 4876, p. 209, 1988.

HARRIS, P. J. F. Carbon nanotube composites. **International Materials Reviews**, v. 49, n. 1, p. 31-43, 2004.

HARRISON, C. J. Acute lymphoblastic leukaemia. **Best Practice & Research Clinical Haematology**, v. 14, n.3, p. 593-607, 2001.

HAYAT, A. et al. Colorimetric cholesterol sensor based on peroxidase like activity of zinc oxide nanoparticles incorporated carbon nanotubes. **Talanta**, v. 143, p. 157-161, 2015.

HENRY, J. B. The impact of biosensors on the clinical laboratory. **MLO: Medical Laboratory Observer**, v. 22, n. 7, p. 32-35, 1990.

HERNÁNDEZ-IBÁÑEZ, N. et al. Electrochemical lactate biosensor based upon chitosan/carbon nanotubes modified screen-printed graphite electrodes for the determination of lactate in embryonic cell cultures. **Biosensors and bioelectronics**, v. 77, p. 1168-1174, 2016.

HINTERDORFER, P.; DUFRÊNE, Y. F. Detection and localization of single molecular recognition events using atomic force microscopy. **Nature Methods**, v. 3, n. 5, p. 347-355, 2006.

HOBSON, D. W. The Commercialization of Medical Nanotechnology for Medical Applications. In: Intracellular Delivery III. **Springer International Publishing**, p. 405-449, 2016.

HODEL, A. W. et al. Atomic force microscopy of membrane pore formation by cholesterol dependent cytolysins. **Current Opinion in Structural Biology**, v. 39, p. 8-15, 2016.

HOLZINGER, M.; LE GOFF, A.; COSNIER, S. Nanomaterials for biosensing applications: a review. **Frontiers in Chemistry**, v. 2, p. 63, 2014.

HU, L. et al. A novel label-free bioengineered cell-based biosensor for salicin detection. **Sensors and Actuators B: Chemical**, v. 238, p. 1151-1158, 2017.

HU, L. et al. Ultrasensitive electrochemical detection of BCR/ABL fusion gene fragment based on polymerase assisted multiplication coupling with quantum dot tagging. **Electrochemistry Communications**, v. 35, p. 104-107, 2013.

HUSHEGYI, A. et al. Ultrasensitive detection of influenza viruses with a glycan-based impedimetric biosensor. **Biosensors and Bioelectronics**, v. 79, p. 644-649, 2016.

HWANG, H. J. et al. High sensitive and selective electrochemical biosensor: Label-free detection of human norovirus using affinity peptide as molecular binder. **Biosensors and Bioelectronics**, v. 87, p. 164-170, 2017.

IIJIMA, S. et al. Helical microtubules of graphitic carbon. **Nature**, v. 354, n. 6348, p. 56-58, 1991.

INAMDAR, K. V.; BUESO-RAMOS, C. E. Pathology of chronic lymphocytic leukemia: an update. **Annals of Diagnostic Pathology**, v. 11, n. 5, p. 363-389, 2007.

JACOBS, C. B.; PEAIRS, M. J.; VENTON, B. J. Review: Carbon nanotube based electrochemical sensors for biomolecules. **Analytica Chimica Acta**, v. 662, n. 2, p. 105-127, 2010.

JALILI, N.; LAXMINARAYANA, K. A review of atomic force microscopy imaging systems: application to molecular metrology and biological sciences. **Mechatronics**, v. 14, n. 8, p. 907-945, 2004.

JANSHOFF, A.; GALLA, H. J.; STEINEM, C. Piezoelectric Mass-Sensing Devices as Biosensors - An Alternative to Optical Biosensors?. **Angewandte Chemie International Edition**, v. 39, n. 22, p. 4004-4032, 2000.

JARA-PALACIOS, M. J. et al. Cyclic voltammetry to evaluate the antioxidant potential in winemaking by-products. **Talanta**, v. 165, p. 211-215, 2017.

JAWAID, S. et al. Rapid detection of melamine adulteration in dairy milk by SB-ATR–Fourier transform infrared spectroscopy. **Food Chemistry**, v. 141, n. 3, p. 3066-3071, 2013.

JAYANTHI, V. S. P. K. S. A.; DAS, A. B.; SAXENA, U. Recent advances in biosensor development for the detection of cancer biomarkers. **Biosensors and Bioelectronics**, v., 91, p. 15-23, 2016.

JI, D. et al. Smartphone-based cyclic voltammetry system with graphene modified screen printed electrodes for glucose detection. **Biosensors and Bioelectronics**, v. 98, n. 15, p. 449-456, 2017.

JIA, X.; DONG, S.; WANG, E. Engineering the bioelectrochemical interface using functional nanomaterials and microchip technique toward sensitive and portable electrochemical biosensors. **Biosensors and Bioelectronics**, v. 76, p. 80-90, 2016.

JIANG, J.; KUCERNAK, A. Nanostructured platinum as an electrocatalyst for the electrooxidation of formic acid. **Journal of Electroanalytical Chemistry**, v. 520, n. 1, p. 64-70, 2002.

JIN, B. et al. Upconversion nanoparticles based FRET aptasensor for rapid and ultrasenstive bacteria detection. **Biosensors and Bioelectronics**, v. 90, p. 525-533, 2017.

JONES, O. G. Developments in dynamic atomic force microscopy techniques to characterize viscoelastic behaviors of food materials at the nanometer-scale. **Current Opinion in Food Science**, v. 9, p. 77-83, 2016.

JUSTINO, C. I. L. et al. Recent developments in recognition elements for chemical sensors and biosensors. **TrAC Trends in Analytical Chemistry**, v. 68, p. 2-17, 2015.

JUSTINO, C. I. L.; ROCHA-SANTOS, T. A.; DUARTE, A. C. Review of analytical figures of merit of sensors and biosensors in clinical applications. TrAC Trends in **Analytical Chemistry**, v. 29, n. 10, p. 1172-1183, 2010.

KALIA, M. Biomarkers for personalized oncology: recent advances and future challenges. **Metabolism**, v. 64, n. 3, p. S16-S21, 2015.

KARIM-NEZHAD, G. et al. Voltammetric sensor for tartrazine determination in soft drinks using poly (p-aminobenzenesulfonic acid)/zinc oxide nanoparticles in carbon paste electrode. **Journal of Food and Drug Analysis**, p. 1-9, 2016.

KASAS, S.; LONGO, G.; DIETLER, G. Mechanical properties of biological specimens explored by atomic force microscopy. **Journal of Physics D: Applied Physics**, v. 46, n. 13, p. 133001, 2013.

KATZ, E.; WILLNER, I. Probing biomolecular interactions at conductive and semiconductive surfaces by impedance spectroscopy: routes to impedimetric immunosensors, DNA-sensors, and enzyme biosensors. **Electroanalysis**, v. 15, n. 11, p. 913-947, 2003.

KERMAN, K.; KOBAYASHI, M.; TAMIYA, E. Recent trends in electrochemical DNA biosensor technology. **Measurement Science and Technology**, v. 15, n. 2, p. R1-R11, 2003.

KIM, S.; CHOI, S. J. A lipid-based method for the preparation of a piezoelectric DNA biosensor. **Analytical Biochemistry**, v. 458, p. 1-3, 2014.

KIMMEL, D. W. et al. Electrochemical sensors and biosensors. **Analytical Chemistry**, v. 84, n. 2, p. 685-707, 2011.

KIRCHNER, P. et al. Realisation of a calorimetric gas sensor on polyimide foil for applications in aseptic food industry. **Sensors and Actuators B: Chemical**, v. 170, p. 60-66, 2012.

KISS, L. et al. Electropolymerized molecular imprinting on glassy carbon electrode for voltammetric detection of dopamine in biological samples. **Talanta**, v. 160, p. 489-498, 2016.

KOMANDURI, K. V.; LEVINE, R. L. Diagnosis and therapy of acute myeloid leukemia in the era of molecular risk stratification. **Annual Review of Medicine**, v. 67, p. 59-72, 2016.

KOSTOFF, R. N.; KOYTCHEFF, R. G.; LAU, C. G. Y. Global nanotechnology research literature overview. **Technological Forecasting and Social Change**, v. 74, n. 9, p. 1733-1747, 2007.

KUMAR, S. A.; CHEN, S. M. Nanostructured zinc oxide particles in chemically modified electrodes for biosensor applications. **Analytical Letters**, v. 41, n. 2, p. 141-158, 2008.

KUMAR, S. et al. Graphene, carbon nanotubes, zinc oxide and gold as elite nanomaterials for fabrication of biosensors for healthcare. **Biosensors and Bioelectronics**, v. 70, p. 498-503, 2015.

KURBANOGLU, S. et al. Advances in electrochemical DNA biosensors and their interaction mechanism with pharmaceuticals. **Journal of Electroanalytical Chemistry**, v. 775, p. 8-26, 2016.

LAINE, R. M.; CHOI, J.; LEE, I. Organic–inorganic nanocomposites with completely defined interfacial interactions. **Advanced Materials**, v. 13, n. 11, p. 800-803, 2001.

LANDIM, V. P. A. **Desenvolvimento de imunossensor eletroquímico empregando nanohíbrido Pirrol – nanotubos de haloisita para detecção da troponina T cardíaca humana.** 2014. 71 f. Dissertação (Mestrado em Engenharia Biomédica) – Centro de Tecnologia e Geociência, Universidade Federal de Pernambuco, Recife, 2014.

LASCH, P.; NAUMANN, D. Infrared spectroscopy in microbiology. **Encyclopedia of Analytical Chemistry**, 2015.

LAZCKA, O.; DEL CAMPO, F. J.; MUNOZ, F. X. Pathogen detection: a perspective of traditional methods and biosensors. **Biosensors and Bioelectronics**, v. 22, n. 7, p. 1205-1217, 2007.

LEE, I. et al. Detection of cardiac biomarkers using single polyaniline nanowire-based conductometric biosensors. **Biosensors**, v. 2, n. 2, p. 205-220, 2012.

LEE, S. et al. Bi nanowire-based thermal biosensor for the detection of salivary cortisol using the Thomson effect. **Applied Physics Letters**, v. 103, n. 14, p. 143114, 2013.

LEI, Y. Application of Electrochemical Immuno-sensor Based on Ketamine Hydrochloride for the Detection of Sports Illicit Drugs. **Journal of New Materials for Electrochemical System**s, v. 19, n. 3, 2016.

LI, Q. et al. AFM-based force spectroscopy for bioimaging and biosensing. **RSC Advances**, v. 6, n. 16, p. 12893-12912, 2016.

LI, Q. et al. A novel aptasensor based on single-molecule force spectroscopy for highly sensitive detection of mercury ions. **Analyst**, v. 140, n. 15, p. 5243-5250, 2015.

LI, S. et al. Electrochemical determination of BCR/ABL fusion gene based on in situ synthesized gold nanoparticles and cerium dioxide nanoparticles. **Colloids and Surfaces B: Biointerfaces**, v. 112, p. 344-349, 2013.

LI, S. et al. Supramolecular imprinted electrochemical sensor for the neonicotinoid insecticide imidacloprid based on double amplification by Pt-In catalytic nanoparticles and a Bromophenol blue doped molecularly imprinted film. **Microchimica Acta**, v. 183, n. 12, p. 3101-3109, 2016.

LI, W.; DU, C. Construction of a competitor for bcr-abl cDNA by recombinant PCR. **Chinese Journal of Medical Genetics**, v. 15, n. 3, p. 143-146, 1998.

LI, Z. M. et al. The colorimetric assay of DNA methyltransferase activity based on strand displacement amplification. **Sensors and Actuators B: Chemical**, v. 238, p. 626-632, 2017.

LI, Y. F. et al. Tyrosine kinase c-Abl regulates the survival of plasma cells. **Scientific Reports**, v. 7, 2017.

LIM, J. W. et al. Review of micro/nanotechnologies for microbial biosensors. **Frontiers in Bioengineering and Biotechnology**, v. 3, p. 1-13, 2015.

LIM, Y. C.; KOUZANI, A. Z.; DUAN, W. Aptasensors: a review. **Journal of biomedical nanotechnology**, v. 6, n. 2, p. 93-105, 2010.

LIN, K. W. et al. Sub-20nm node photomask cleaning enhanced by controlling zeta potential. **Spie Newsroom**, 2012.

LIN, L. et al. Electrochemical biosensor for detection of BCR/ABL fusion gene based on hairpin locked nucleic acids probe. **Electrochemistry Communications**, v. 11, n. 8, p. 1650-1653, 2009.

LIN, X. H. et al. Electrochemical DNA biosensor for the detection of short DNA species of Chronic Myelogenous Leukemia by using methylene blue. **Talanta**, v. 72, n. 2, p. 468-471, 2007.

LISDAT, F.; SCHÄFER, D. The use of electrochemical impedance spectroscopy for biosensing. **Analytical and Bioanalytical Chemistry**, v. 391, n. 5, p. 1555, 2008.

LIU, A. et al. Development of electrochemical DNA biosensors. **TrAC Trends in Analytical Chemistry**, v. 37, p. 101-111, 2012.

LIU, Q. et al. Cell-based biosensors and their application in biomedicine. **Chemical Reviews**, v. 114, n. 12, p. 6423-6461, 2014.

LIU, S.; LEECH, D.; JU, H. Application of colloidal gold in protein immobilization, electron transfer, and biosensing. **Analytical Letters**, v. 36, n. 1, p. 1-19, 2003.

LÓPEZ-ANDRADE, B. et al. Acute lymphoblastic leukemia with e1a3 BCR/ABL fusion protein. A report of two cases. **Experimental Hematology & Oncology**, v. 5, n. 1, p. 21, 2016.

LOJOU, E.; BIANCO, P. Application of the electrochemical concepts and techniques to amperometric biosensor devices. **Journal of Electroceramics**, v. 16, n. 1, p. 79-91, 2006.

LUCARELLI, F. et al. Electrochemical and piezoelectric DNA biosensors for hybridisation detection. **Analytica Chimica Acta**, v. 609, n. 2, p. 139-159, 2008.

LUNA, D. M. N. et al. Electrochemical immunosensor for dengue virus serotypes based on 4-mercaptobenzoic acid modified gold nanoparticles on self-assembled cysteine monolayers. **Sensors and Actuators B: Chemical**, v. 220, p. 565-572, 2015.

LUPPA, P. B.; SOKOLL, L. J.; CHAN, D. W. Immunosensors - principles and applications to clinical chemistry. **Clinica Chimica Acta**, v. 314, n. 1, p. 1-26, 2001.

LYU, X. et al. A novel BCR-ABL1 fusion gene identified by next-generation sequencing in chronic myeloid leukemia. **Molecular Cytogenetics**, v. 9, n. 1, p. 47, 2016.

MACDONALD, D. D. Review of mechanistic analysis by electrochemical impedance spectroscopy. **Electrochimica Acta**, v. 35, n. 10, p. 1509-1525, 1990.

MACDONALD, J. R. Impedance spectroscopy. **Annals of Biomedical Engineering**, v. 20, n. 3, p. 289-305, 1992.

MAHADEVAN, A.; FERNANDO, S. An improved glycerol biosensor with an Au-FeS-NAD-glycerol-dehydrogenase anode. **Biosensors and Bioelectronics**, v. 92, p. 417-424, 2017.

MANNELLI, I. et al. Direct immobilisation of DNA probes for the development of affinity biosensors. **Bioelectrochemistry**, v. 66, n. 1, p. 129-138, 2005.

MARTÍNEZ-GARCÍA, G. et al. Multiplexed electrochemical immunosensing of obesity-related hormones at grafted graphene-modified electrodes. **Electrochimica Acta**, v. 202, p. 209-215, 2016.

MASKOW, T. et al. Rapid analysis of bacterial contamination of tap water using isothermal calorimetry. **Thermochimica Acta**, v. 543, p. 273-280, 2012.

MATSISHIN, M. J. et al. SPR Detection and Discrimination of the Oligonucleotides Related to the Normal and the Hybrid bcr-abl Genes by Two Stringency Control Strategies. **Nanoscale Research Letters**, v. 11, n. 1, p. 19, 2016.

MAURER, J. et al. Detection of chimeric BCR-ABL genes in acute lymphoblastic leukaemia by the polymerase chain reaction. **The Lancet**, v. 337, n. 8749, p. 1055-1058, 1991.

MCQUADE, D. T.; PULLEN, A. E.; SWAGER, T. M. Conjugated polymer-based chemical sensors. **Chemical Reviews**, v. 100, n. 7, p. 2537-2574, 2000.

MCKENNA, M. et al. Click chemistry as an immobilization method to improve oligonucleotide hybridization efficiency for nucleic acid assays. **Sensors and Actuators B: Chemical**, v. 236, p. 286-293, 2016.

MELO, J. V. **The diversity of BCR-ABL fusion proteins and their relationship to leukemia phenotype** [editorial; comment]. 1996.

MILLER, K. D. et al. Cancer treatment and survivorship statistics, 2016. **CA: a cancer Journal for Clinicians**, v. 66, n. 4, p. 271-289, 2016.

MIODEK, A. et al. Electrochemical aptasensor of cellular prion protein based on modified polypyrrole with redox dendrimers. **Biosensors and Bioelectronics**, v. 56, p. 104-111, 2014.

MITELMAN, F.; JOHANSSON, B.; MERTENS, F. The impact of translocations and gene fusions on cancer causation. **Nature Reviews Cancer**, v. 7, p. 233-245, 2007.

MITTAL, S. et al. Biosensors for breast cancer diagnosis: A review of bioreceptors, biotransducers and signal amplification strategies. **Biosensors and Bioelectronics**, v. 88, p. 217-231, 2017.

MOHAMED, M. A. et al. Novel MWCNTs/graphene oxide/pyrogallol composite with enhanced sensitivity for biosensing applications. **Biosensors and Bioelectronics**, v. 89, p. 1034-1041, 2017.

MONOŠÍK, R.; STREĎANSKÝ, M.; ŠTURDÍK, E. Biosensors-classification, characterization and new trends. **Acta Chimica Slovaca**, v. 5, n. 1, p. 109-120, 2012.

MÜLLER, D. J.; DUFRENE, Y. F. Atomic force microscopy as a multifunctional molecular toolbox in nanobiotechnology. **Nature Nanotechnology**, v. 3, n. 5, p. 261-269, 2008.

MULLIGHAN, C. G. et al. BCR–ABL1 lymphoblastic leukaemiais characterized by the deletion of Ikaros. **Nature**, v. 453, p. 110-114, 2008.

MIYAGI, A. et al. High-speed atomic force microscopy shows that annexin V stabilizes membranes on the second timescale. **Nature Nanotechnology**, 2016.

MORITA, S. et al. (Ed.). **Noncontact atomic force microscopy**. Springer, 2015.

NASCIMENTO, H.P.O. et al. An impedimetric biosensor for detection of dengue serotype at picomolar concentration based on gold nanoparticles-polyaniline hybrid composites. **Colloids and Surfaces B: Biointerfaces**, v. 86, n. 2, p. 414-419, 2011.

NASEEM, S.; AGARWAL, Pallavi; VARMA, Neelam. Acute Leukemia Cytochemically Myeloid and Immunophenotypically T Lymphoid. **Journal of Pediatric Hematology/Oncology**, v. 36, n. 6, p. e387-e388, 2014.

NATH, N.; CHILKOTI, A. Label-free biosensing by surface plasmon resonance of nanoparticles on glass: optimization of nanoparticle size. **Analytical Chemistry**, v. 76, n. 18, p. 5370-5378, 2004.

NERO, T. L. et al. Oncogenic protein interfaces: small molecules, big challenges. **Nature Reviews Cancer**, v. 14, n. 4, p. 248-262, 2014.

NESAKUMAR, N. et al. Electrochemical acetylcholinesterase biosensor based on ZnO nanocuboids modified platinum electrode for the detection of carbosulfan in rice. **Biosensors and Bioelectronics**, v. 77, p. 1070-1077, 2016.

NEUENDORFF, N. R. et al. BCR-ABL-positive acute myeloid leukemia: a new entity? Analysis of clinical and molecular features. **Annals of hematology**, v. 95, n. 8, p. 1211-1221, 2016.

NEUMAN, K. C.; NAGY, A. Single-molecule force spectroscopy: optical tweezers, magnetic tweezers and atomic force microscopy. **Nature Methods**, v. 5, n. 6, p. 491, 2008.

NEWMAN, J. D.; SETFORD, S. J. Enzymatic biosensors. **Molecular Biotechnology**, v. 32, n. 3, p. 249-268, 2006.

NG, S. P. et al. Label-free detection of 3-nitro-l-tyrosine with nickel-doped graphene localized surface plasmon resonance biosensor. **Biosensors and Bioelectronics**, v. 89, p. 468-476, 2017.

NGUYEN, B. H. et al. Development of label-free electrochemical lactose biosensor based on graphene/poly (1, 5-diaminonaphthalene) film. **Current Applied Physics**, v. 16, n. 2, p. 135-140, 2016.

NIA, P. M. et al. Electrodeposition of copper oxide/polypyrrole/reduced graphene oxide as a nonenzymatic glucose biosensor. **Sensors and Actuators B: Chemical**, v. 209, p. 100-108, 2015.

NICHOLSON, R. S. Theory and application of cyclic voltammetry for measurement of electrode reaction kinetics. **Analytical Chemistry**, v. 37, n. 11, p. 1351-1355, 1965.

NIMSE, S. B. et al. Immobilization techniques for microarray: challenges and applications. **Sensors**, v. 14, n. 12, p. 22208-22229, 2014.

NOWELL, P. C. Discovery of the Philadelphia chromosome: a personal perspective**. The Journal of Clinical Investigation**, v. 117, n. 8, p. 2033-2035, 2007.

OLIVEIRA, M. D. L. et al. Electrochemical evaluation of lectin–sugar interaction on gold electrode modified with colloidal gold and polyvinyl butyral. **Colloids and Surfaces B: Biointerfaces**, v. 66, n. 1, p. 13-19, 2008.

OZKAN-ARIKSOYSAL, D. et al. DNA-wrapped multi-walled carbon nanotube modified electrochemical biosensor for the detection of Escherichia coli from real samples. **Talanta**, 2017.

PACHECO, W. F. et al. Voltametrias: Uma breve revisão sobre os conceitos. **Revista Virtual de Química**, v. 5, n. 4, p. 516-537, 2013.

PALEČEK, E. Fifty years of nucleic acid electrochemistry. **Electroanalysis**, v. 21, n. 3-5, p. 239-251, 2009.

PANDEY, C. M. et al. Highly sensitive electrochemical immunosensor based on graphene-wrapped copper oxide-cysteine hierarchical structure for detection of pathogenic bacteria. **Sensors and Actuators B: Chemical**, v. 238, p. 1060-1069, 2017.

PARK, J. Y.; PARK, S. M. DNA hybridization sensors based on electrochemical impedance spectroscopy as a detection tool. **Sensors**, v. 9, n. 12, p. 9513-9532, 2009.

PATEL, M. K. et al. Biocompatible nanostructured magnesium oxide-chitosan platform for genosensing application. **Biosensors and Bioelectronics**, v. 45, p. 181-188, 2013.

PERUMAL, V.; HASHIM, U. Advances in biosensors: Principle, architecture and applications. **Journal of Applied Biomedicine**, v. 12, n. 1, p. 1-15, 2014.

PINGARRÓN, J. M.; YÁÑEZ-SEDEÑO, P.; GONZÁLEZ-CORTÉS, A. Gold nanoparticle-based electrochemical biosensors. **Electrochimica Acta**, v. 53, p. 5848-5866, 2008.

PIVIDORI, M. I.; MERKOCI, A.; ALEGRET, S. Electrochemical genosensor design: immobilisation of oligonucleotides onto transducer surfaces and detection methods. **Biosensors and Bioelectronics**, v. 15, n. 5, p. 291-303, 2000.

POHANKA, M. The Piezoelectric Biosensors: Principles and Applications. **International Journal of Electrochemical Science**, v. 12, p. 496-506, 2017.

PORTER, A. L.; YOUTIE, J. How interdisciplinary is nanotechnology?. **Journal of Nanoparticle Research**, v. 11, n. 5, p. 1023-1041, 2009.

POVEDANO, E. et al. Decoration of reduced graphene oxide with rhodium nanoparticles for the design of a sensitive electrochemical enzyme biosensor for 17β-estradiol. **Biosensors and Bioelectronics**, v. 89, p. 343-351, 2017.

PRODROMIDIS, M. I. Impedimetric immunosensors - A review. **Electrochimica Acta**, v. 55, n. 14, p. 4227-4233, 2010.

RABIN, N. N. et al. Surface modification of the ZnO nanoparticles with γ-aminopropyltriethoxysilane and study of their photocatalytic activity, optical properties and antibacterial activities. **International Journal of Chemical Reactor Engineering**, v. 14, n. 3, p. 785-794, 2016.

RAHMAN, M M. et al. Electrochemical DNA hybridization sensors based on conducting polymers. **Sensors**, v. 15, n. 2, p. 3801-3829, 2015.

RAMANAVICIUS, A. et al. Single-step procedure for the modification of graphite electrode by composite layer based on polypyrrole, Prussian blue and glucose oxidase. **Sensors and Actuators B: Chemical**, v. 240, p. 220-223, 2017.

RAMANATHAN, K.; DANIELSSON, B. Principles and applications of thermal biosensors. **Biosensors and Bioelectronics**, v. 16, n. 6, p. 417-423, 2001.

RAMANATHAN, M. et al. Gold-coated carbon nanotube electrode arrays: Immunosensors for impedimetric detection of bone biomarkers. **Biosensors and Bioelectronics**, v. 77, p. 580-588, 2016.

RANJAN, R.; ESIMBEKOVA, E. N.; KRATASYUK, V. A. Rapid biosensing tools for cancer biomarkers. **Biosensors and Bioelectronics**, v. 87, p. 918-930, 2017.

RAPINI, R.; MARRAZZA, G. Biosensor Potential in Pesticide Monitoring. **Comprehensive Analytical Chemistry**, v. 74, p. 3-31, 2016.

RASHEED, P. A.; SANDHYARANI, N. Quartz crystal microbalance genosensor for sequence specific detection of attomolar DNA targets. **Analytica Chimica Acta**, v. 905, p. 134-139, 2016.

RAVAN, H. et al. Strategies for optimizing DNA hybridization on surfaces. **Analytical Biochemistry**, v. 444, p. 41-46, 2014.

ROCO, M. C.; MIRKIN, C. A.; HERSAM, M. C. Nanotechnology research directions for societal needs in 2020: summary of international study. **Journal of Nanoparticle Research**, v. 3, n. 3, p. 897-919, 2011.

RONKAINEN, N. J.; HALSALL, H. B.; HEINEMAN, W. R. Electrochemical biosensors. **Chemical Society Reviews**, v. 39, n. 5, p. 1747-1763, 2010.

ROSARIO, R.; MUTHARASAN, R. Nucleic acid electrochemical and electromechanical biosensors: a review of techniques and developments. **Reviews in Analytical Chemistry**, v. 33, n. 4, p. 213-230, 2014.

ROUNTREE, E. S. et al. Evaluation of homogeneous electrocatalysts by cyclic voltammetry. **Inorganic Chemistry**, 2014.

ROVINA, K.; SIDDIQUEE, S. Electrochemical sensor based rapid determination of melamine using ionic liquid/zinc oxide nanoparticles/chitosan/gold electrode. **Food Control**, v. 59, p. 801-808, 2016.

SAFITRI, E. et al. Fluorescence bioanalytical method for urea determination based on water soluble ZnS quantum dots. **Sensors and Actuators B: Chemical**, v. 240, p. 763-769, 2017.

SAGADEVAN, S.; PERIASAMY, M. Recent trends in nanobiosensors and their applications - a review. **Reviews on Advanced Materials Science**, v. 36, p. 62-69, 2014.

SANCHEZ, C. et al. Applications of hybrid organic – inorganic nanocompósitos. **Journal of Materials Chemistry**, v. 15, p. 3559-3592, 2005.

SANTOS, N. C.; CASTANHO, M. A. An overview of the biophysical applications of atomic force microscopy. **Biophysical chemistry**, v. 107, n. 2, p. 133-149, 2004.

SANTOS, R. F. S. et al. Visible luminescence in polyaniline/(gold nanoparticle) composites. **Journal of Nanoparticle Research**, v. 15, p. 1408-1418, 2013.

SASSOLAS, A.; BLUM, L. J.; LECA-BOUVIER, B. D. Immobilization strategies to develop enzymatic biosensors. **Biotechnology Advances**, v. 30, n. 3, p. 489-511, 2012.

SASSOLAS, A.; LECA-BOUVIER, B. D.; BLUM, L. J. DNA biosensors and microarrays. **Chemical Reviews**, v. 108, n. 1, p. 109-139, 2008.

SATHYANARAYANA, D. N. **Vibrational spectroscopy: theory and applications**. New Age International, 2015.

SAWYERS, C. L. The cancer biomarker problem. **Nature**, v. 452, n. 7187, p. 548-552, 2008.

SCHELLER, F. W. et al. Research and development in biosensors. **Current Opinion in Biotechnology**, v. 12, n. 1, p. 35-40, 2001.

SCHMIDT, H. L. et al. Specific features of biosensors. **Sensors Set: A Comprehensive Survey**, p. 717-817, 2008.

SCHÖNHERR, H. Imaging Polymer Morphology using Atomic Force Microscopy. **Polymer Morphology: Principles, Characterization, and Processing**, p. 100-117, 2016.

SHARMA, A. et al. Chitosan encapsulated quantum dots platform for leukemia detection. **Biosensors and Bioelectronics**, v. 38, n. 1, p. 107-113, 2012.

SHEIKHZADEH, E. et al. Label-free impedimetric biosensor for Salmonella Typhimurium detection based on poly [pyrrole-co-3-carboxyl-pyrrole] copolymer supported aptamer. **Biosensors and Bioelectronics**, v. 80, p. 194-200, 2016.

SILVA, M. S. et al. Conductive atomic force microscopy characterization of PTCR-BaTiO 3 laser-sintered ceramics. **Journal of the European Ceramic Society**, v. 36, n. 6, p. 1385-1389, 2016.

SILVA, R. R. et al. Optical and dielectric sensors based on antimicrobial peptides for microorganism diagnosis. **Frontiers in Microbiology**, v. 5, p. 443, 2014.

SINGHAL, C. et al. Impedimetric genosensor for detection of hepatitis C virus (HCV1) DNA using viral probe on methylene blue doped silica nanoparticles. **International Journal of Biological Macromolecules**, 2017.

SKLÁDAL, P. Piezoelectric biosensors. **TrAC Trends in Analytical Chemistry**, v. 79, p. 127-133, 2016.

SMITH, B.C. **Fourier transform infrared spectroscopy**. CRC, Boca Raton, FL, 1996.

SPM Training Guide. **Atomic Force Microscopy**. 2011. Disponível em: <http://www.nanophys.kth.se/nanophys/facilities/nfl/afm/icon/bruker-help/Content/SPM%20Training%20Guide/Atomic%20Force%20Microscopy%20(AFM)/Atomic%20Force%20Microscopy%20(AFM).htm>. Acesso em: 02 fev. 2017.

SONG, Q. et al. A nuclease-assisted label-free aptasensor for fluorescence turn-on detection of ATP based on the in situ formation of copper nanoparticles. **Biosensors and Bioelectronics**, v. 87, p. 760-763, 2017.

SONI, D. K. et al. Label-free impedimetric detection of Listeria monocytogenes based on poly-5-carboxy indole modified ssDNA probe. **Journal of Biotechnology**, v. 200, p. 70-76, 2015.

STUART, B. **Infrared spectroscopy**. John Wiley & Sons, Inc., 2005.

SU, L. et al. Microbial biosensors: a review. **Biosensors and Bioelectronics**, v. 26, n. 5, p. 1788-1799, 2011.

SUCKEVERIENE, R. Y. et al. Literature review: conducting carbon nanotube/polyaniline nanocomposites. **Reviews in Chemical Engineering**, v. 27, n. 1-2, p. 15-21, 2011.

SUN, J. et al. Microbial fuel cell-based biosensors for environmental monitoring: a review. **Water Science and Technology**, v. 71, n. 6, p. 801-809, 2015.

SUN, L.; YU, L.; SHEN, W. DNA nanotechnology and its applications in biomedical research. **Journal of Biomedical Nanotechnology**, v. 10, p. 2350-2370, 2014.

SUN, Y. P. et al. Functionalized carbon nanotubes: properties and applications. **Accounts of Chemical Research**, v. 35, n. 12, p. 1096-1104, 2002.

SUNG, P. J.; LUGER, S. M. Minimal Residual Disease in Acute Myeloid Leukemia. **Current Treatment Options in Oncology**, v. 18, n. 1, p. 1, 2017.

SUNI, I. I. Impedance methods for electrochemical sensors using nanomaterials. **TrAC Trends in Analytical Chemistry**, v. 27, n. 7, p. 604-611, 2008.

STEEL, A. B. et al. Immobilization of nucleic acids at solid surfaces: effect of oligonucleotide length on layer assembly. **Biophysical Journal**, v. 79, n. 2, p. 975-981, 2000.

SZCZEPANSKI, Tomasz. Why and how to quantify minimal residual disease in acute lymphoblastic leukemia?. **Leukemia**, v. 21, n. 4, p. 622-626, 2007.

TAK, M.; GUPTA, V.; TOMAR, M. Flower-like ZnO nanostructure based electrochemical DNA biosensor for bacterial meningitis detection. **Biosensors and Bioelectronics**, v. 59, p. 200-207, 2014.

TAKAHASHI, S.; SATO, K.; ANZAI, J. I. Layer-by-layer construction of protein architectures through avidin-biotin and lectin-sugar interactions for biosensor applications. **Analytical and Bioanalytical Chemistry**, v. 402, n. 5, p. 1749-1758, 2012.

TANG, J. et al. Sandwich-type conductometric immunoassay of alpha-fetoprotein in human serum using carbon nanoparticles as labels. **Biochemical Engineering Journal**, v. 53, n. 2, p. 223-228, 2011.

TEIXEIRA, M. R. Recurrent Fusion Oncogenes in Carcinomas. **Critical Reviews™ in Oncogenesis**, v. 12, p. 3-4, 2006.

TELES, F. R. R.; FONSECA, L. P. Trends in DNA biosensors. **Talanta**, v. 77, n. 2, p. 606-623, 2008.

TERESHCHENKO, A. et al. Optical biosensors based on ZnO nanostructures: advantages and perspectives. A review. **Sensors and Actuators B: Chemical**, v. 229, p. 664-677, 2016.

THÉVENOT, D. R. et al. Electrochemical biosensors: recommended definitions and classification. **Biosensors and Bioelectronics**, v. 16, n. 1, p. 121-131, 2001.

THIPMANEE, O. et al. Enhancing capacitive DNA biosensor performance by target overhang with application on screening test of HLA-B* 58: 01 and HLA-B* 57: 01 genes. **Biosensors and Bioelectronics**, v. 82, p. 99-104, 2016.

TICHÝ, J. et al. **Fundamentals of piezoelectric sensorics: mechanical, dielectric, and thermodynamical properties of piezoelectric materials**. Springer Science & Business Media, 2010.

TÎLMACIU, C. M.; MORRIS, M. C. Carbon nanotube biosensors. **Frontiers in Chemistry**, v. 3, p. 1-21, 2015.

TURK, M. C.; WALTERS, M. J.; ROY, D. Experimental considerations for using electrochemical impedance spectroscopy to study chemical mechanical planarization systems. **Electrochimica Acta**, v. 224, p. 355-368, 2017.

TURNER, A. P. F. Biosensors: sense and sensibility. **Chemical Society Reviews**, v. 42, n. 8, p. 3184-3196, 2013.

UNWIN, P. R.; GUELL, A. G.; ZHANG, G. Nanoscale electrochemistry of sp2 carbon materials: from graphite and graphene to carbon nanotubes. **Accounts of Chemical Research**, v. 49, n. 9, p. 2041-2048, 2016.

VAN DONGEN, J. J. M. et al. Minimal residual disease diagnostics in acute lymphoblastic leukemia: need for sensitive, fast, and standardized technologies. **Blood**, v. 125, n. 26, p. 3996-4009, 2015.

VARDIMAN, J. W. The World Health Organization (WHO) classification of tumors of the hematopoietic and lymphoid tissues: an overview with emphasis on the myeloid neoplasms. **Chemico-Biological Interactions**, v. 184, n. 1, p. 16-20, 2010.

VÁSQUEZ, G. et al. Amperometric biosensor based on a single antibody of dual function for rapid detection of Streptococcus agalactiae. **Biosensors and Bioelectronics**, v. 87, p. 453-458, 2017.

VO-DINH, T.; CULLUM, B. Biosensors and biochips: advances in biological and medical diagnostics. **Fresenius' Journal of Analytical Chemistry**, v. 366, n. 6, p. 540-551, 2000.
WANG, F.; HU, S. Electrochemical sensors based on metal and semiconductor nanoparticles. **Microchimica Acta**, v. 165, p. 1-22, 2009.

WANG, J. **Analytical electrochemistry**. John Wiley & Sons, 2006.

WANG, J. Carbon-nanotube based electrochemical biosensors: A review. **Electroanalysis**, v. 17, n. 1, p. 7-14, 2005.

WANG, K. et al. A Sandwich-Type Electrochemical Biosensor for Detection of BCR/ABL Fusion Gene Using Locked Nucleic Acids on Gold Electrode. **Electroanalysis**, v. 21, n. 10, p. 1159-1166, 2009.

WANG, L. et al. Graphene sheets, polyaniline and AuNPs based DNA sensor for electrochemical determination of BCR/ABL fusion gene with functional hairpin probe. **Biosensors and Bioelectronics**, v. 51, p. 201-207, 2014.

WANG, Z.; DAI, Z. Carbon nanomaterial-based electrochemical biosensors: an overview. **Nanoscale**, v. 7, n. 15, p. 6420-6431, 2015.

WANG, Y. et al. Electrochemical sensors for clinic analysis. **Sensors**, v. 8, n. 4, p. 2043-2081, 2008.

WANG, Y.; YE, Z.; YING, Y. New trends in impedimetric biosensors for the detection of foodborne pathogenic bacteria. **Sensors**, v. 12, n. 3, p. 3449-3471, 2012.

WEN, Y. et al. Imprinted voltammetric streptomycin sensor based on a glassy carbon electrode modified with electropolymerized poly (pyrrole-3-carboxy acid) and electrochemically reduced graphene oxide. **Microchimica Acta**, p. 1-7, 2017.

WHITED, A. M.; PARK, P. S. H. Atomic force microscopy: a multifaceted tool to study membrane proteins and their interactions with ligands. **Biochimica et Biophysica Acta (BBA)-Biomembranes**, v. 1838, n. 1, p. 56-68, 2014.

WIKIMEDIA COMMONS. **AFM modes**. 2016. Disponível em: <https://commons.wikimedia.org/wiki/File:Afm_modes_12-10.svg>. Acesso em: 02 fev. 2017.

WINTER, S. S. et al. Pre-B acute lymphoblastic leukemia with b3a2 (p210) and e1a2 (p190) BCR-ABL fusion transcripts relapsing as chronic myelogenous leukemia with a less differentiated b3a2 (p210) clone. **Leukemia (08876924)**, v. 13, n. 12, 1999.

XU, K. et al. Recent development of nano-materials used in DNA biosensors. **Sensors**, v. 9, n. 7, p. 5534-5557, 2009.

YAKOVLEVA, M.; BHAND, S.; DANIELSSON, B. The enzyme thermistor - A realistic biosensor concept. A critical review. **Analytica Chimica Acta**, v. 766, p. 1-12, 2013.

YÁÑEZ-SEDEÑO, P.; CAMPUZANO, S.; PINGARRÓN, J. M. Carbon Nanostructures for Tagging in Electrochemical Biosensing: A Review. **Journal of Carbon Research**, v. 3, n. 1, p. 3, 2017.

YÁÑEZ-SEDEÑO, P.; PINGARRÓN, J. M. Gold nanoparticle-based electrochemical biosensors. **Analytical and Bioanalytical Chemistry**, v. 382, n. 4, p. 884-886, 2005.

YANG, J.; ZHANG, W. Indicator-free impedimetric detection of BCR/ABL fusion gene based on ordered FePt nanoparticle-decorated electrochemically reduced graphene oxide. **Journal of Solid State Electrochemistry**, v. 18, n. 10, p. 2863-2868, 2014.

YANG, W. et al. Carbon nanomaterials in biosensors: should you use nanotubes or graphene?. **Angewandte Chemie International Edition**, v. 49, n. 12, p. 2114-2138, 2010.

YEUNG, C. C. S.; EGAN, D.; RADICH, J. P. Molecular monitoring of chronic myeloid leukemia: present and future. **Expert Review of Molecular Diagnostics**, v. 16, n. 10, p. 1083-1091, 2016.

YUQING, M.; JIANGUO, G.; JIANRONG, C. Ion sensitive field effect transducer-based biosensors. **Biotechnology Advances**, v. 21, n. 6, p. 527-534, 2003.

ZANETTE, S. I. et al. Theoretical and experimental investigation of the force–distance relation for an atomic force microscope with a pyramidal tip. **Surface Science**, v. 453, n. 1, p. 75-82, 2000.

ZHANG, H. et al. Fluorescent biosensors enabled by graphene and graphene oxide. **Biosensors and Bioelectronics**, v. 89, p. 96-106, 2017.

ZHANG, L. et al. An impedimetric biosensor for the diagnosis of renal cell carcinoma based on the interaction between 3-aminophenyl boronic acid and sialic acid. **Biosensors and Bioelectronics**, 2016.

ZHANG, L. L.; ZHAO, X. S. Carbon-based materials as supercapacitor electrodes. **Chemical Society Reviews**, v. 38, n. 9, p. 2520-2531, 2009.

ZHAO, M. Q. et al. Flexible MXene/carbon nanotube composite paper with high volumetric capacitance. **Advanced Materials**, v. 27, n. 2, p. 339-345, 2015.

ZHI-ZHONG, H. A. N. et al. A Low Detection Limit Penicillin Electrochemical Biosensor Based on Penicillinase-Hematein Au/ZnO/Single Graphene Nanosheets. **Chinese Journal of Analytical Chemistry**, p. 377-384, 2016.

ZHONG, G. X. et al. Electrochemical biosensor for detection of BCR/ABL fusion gene based on isorhamnetin as hybridization indicator. **Sensors and Actuators B: Chemical**, v. 204, p. 326-332, 2014.

ZHOU, L. et al. Silver nanocluster based sensitivity amplification of a quartz crystal microbalance gene sensor. **Microchimica Acta**, v. 183, n. 2, p. 881-887, 2016.

ZHU, Z. et al. A critical review of glucose biosensors based on carbon nanomaterials: carbon nanotubes and graphene. **Sensors**, v. 12, n. 5, p. 5996-6022, 2012.

ZHU, Z. W. et al. Electrochemical impedance spectroscopy and atomic force microscopic studies of electrical and mechanical properties of nano-black lipid membranes and size dependence. **Langmuir**, v. 28, n. 41, p. 14739-14746, 2012.

ZLATANOVA, J.; LINDSAY, S. M.; LEUBA, S. H. Single molecule force spectroscopy in biology using the atomic force microscope. **Progress in Biophysics and Molecular Biology**, v. 74, n. 1, p. 37-61, 2000.

CAPÍTULO 5

5 ARTIGO 1

Artigo publicado na revista *Colloids and Surfaces B: Biointerfaces*

Attomolar electrochemical detection of the BCR/ABL fusion genebased on an amplifying self-signal metal nanoparticle-conductingpolymer hybrid composite

Colloids and Surfaces B: Biointerfaces 148 (2016) 576–584

Contents lists available at ScienceDirect

Colloids and Surfaces B: Biointerfaces

journal homepage: www.elsevier.com/locate/colsurfb

Attomolar electrochemical detection of the BCR/ABL fusion gene based on an amplifying self-signal metal nanoparticle-conducting polymer hybrid composite

Karen Y.P.S. Avelino[a], Isaac A.M. Frias[b], Norma Lucena-Silva[c,d], Renan G. Gomes[c,d], Celso P. de Melo[e], Maria D.L. Oliveira[a,b], César A.S. Andrade[a,b,*]

[a] Programa de Pós-Graduação em Bioquímica e Fisiologia, Universidade Federal de Pernambuco, 50670-901 Recife, PE, Brazil
[b] Programa de Pós-Graduação em Inovação Terapêutica, Universidade Federal de Pernambuco, 50670-901 Recife, PE, Brazil
[c] Centro de Pesquisas Aggeu Magalhães, Fundação Osvaldo Cruz (Fiocruz), 50670-420 Recife, PE, Brazil
[d] Laboratório de Biologia Molecular, Departamento de Oncologia Pediátrica, Instituto de Medicina Integral Professor Fernando Figueira (IMIP), 50070-550 Recife, PE, Brazil
[e] Departamento de Física, Universidade Federal de Pernambuco, 50670-901 Recife, PE, Brazil

ARTICLE INFO

Article history:
Received 10 June 2016
Received in revised form 5 September 2016
Accepted 21 September 2016
Available online 22 September 2016

Keywords:
BCR/ABL fusion gene
Biosensor
Electrochemistry
Hybrid nanoparticles
Leukemia

ABSTRACT

In the last ten years, conjugated polymers started to be used in the immobilization of nucleic acids via non-covalent interactions. In the present study, we describe the construction and use of an electrochemical DNA biosensor based on a nanostructured polyaniline-gold composite, specifically developed for the detection of the BCR/ABL chimeric oncogene. This chromosome translocation is used as a biomarker to confirm the clinical diagnosis of both chronic myelogenous leukemia (CML) and acute lymphocytic leukemia (ALL). The working principle of the biosensor rests on measuring the conductivity resulting from the non-covalent interactions between the hybrid nanocomposite and the DNA probe. The nanostructured platform exhibits a large surface area that enhances the conductivity. Positive cases, which result from the hybridization between DNA probe and targeted gene, induce changes in the amperometric current and in the charge transfer resistance (R_{CT}) responses. Atomic force microscopy (AFM) images showed changes in the genosensor surface after exposure to cDNA sample of patient with leukemia, evidencing the hybridization process. This new hybrid sensing-platform displayed high specificity and selectivity, and its detection limit is estimated to be as low as 69.4 aM. The biosensor showed excellent analytical performance for the detection of the BCR/ABL oncogene in clinical samples of patients with leukemia. Hence, this electrochemical sensor appears as a simple and attractive tool for the molecular diagnosis of the BCR/ABL oncogene even in early-stage cases of leukemia and for the monitoring of minimum levels of residual disease.

1. Introduction

The occurrence of genetic disorders related to BCR/ABL chimeric oncogene represents a risk factor for the development of both CML in adults and ALL in children [1–4]. Prompt identification of BCR/ABL oncogene would enable an early diagnosis as well as the monitoring of the disease's remission [5,6]. Currently, however, leukemia diagnosis is mainly performed in a qualitative manner and the concentration of the BCR/ABL fusion gene is not determined. While most patients are diagnosed by hematological examination [7], molecular methods to confirm clinical diagnosis include chromosome analysis [8], fluorescence *in situ* hybridization [9], flow cytometry [10] and quantitative real-time reverse-transcription polymerase chain reaction (qRT-PCR) [11]. We stress that in spite of their high sensitivity these techniques face major limitations for a more widespread application, which are associated to time-consuming protocols and high acquisition costs [12,13]. Therefore, at present the development of a simple and effective molecular assay capable to detect the BCR/ABL fusion gene continues to be of great interest for allowing the effective implementation of adequate early-stage therapeutic strategies.

In recent years, significant advances in nanoscience and biotechnology have allowed a substantial improvement of the electrochemical DNA detection devices [14–16]. Covalent and non-

* Corresponding author at: Departamento de Bioquímica, UFPE, 50670-901, Recife, PE, Brazil.
E-mail addresses: csrandrade@pq.cnpq.br, csrandrade@gmail.com (C.A.S. Andrade).

http://dx.doi.org/10.1016/j.colsurfb.2016.09.029
0927-7765/

covalent methods have been used in genosensors to immobilize small nucleic acid segments on numerous transducing materials [17]. However, the main challenge still relies on improving the ability of the transducer to detect small changes in the electrochemical properties of the sensor interface caused by the hybridization between the single-stranded DNA probes (ssDNA) and their complementary targets. For the most part, a secondary amplification of the signal needs to be implemented in the form of electrochemical, chromatic, magnetic or metallic reporters [18–21].

New strategies are required to develop biosensors aiming to increase not only the immobilization efficiency of the probe but also the analytical performance of the transducer [22]. Within this perspective, conjugated polymers (CPs) are interesting materials to consider, since they are well known for their chemical stability, low cost polymerization and ability to be conformed into innumerable structures. In addition, the combination of their transport properties, electrical conductivity or rate of energy migration confers to them the possibility of an amplified sensitivity [23]. In special, the pH-dependent conductivity of polyaniline (PANI) allows this polymer to act as a direct electron mediator for the self-amplification of an electrochemical signal [24–26].

At the same time, metallic nanoparticles are also recognized as outstanding performers on electrochemical biosensor research [51,52]. Gold nanoparticles (AuNps) possess large surface free energy and a large area to volume ratio that provides for an enhanced electrochemically active surface. In fact, the size of the AuNps has a direct implication on their surface area. This intrinsic property of nanoscale materials is essential for obtaining biodevices with higher analytical performances [44–46]. Furthermore, AuNps can be used to promote the immobilization of biomolecules, while preserving their biological activity and directing the charge transfer between the biorecognition layer and the electrode surface [27–29].

In this manner, the use of organic-inorganic hybrid materials is emerging as an innovative alternative in biological sensor systems because of their unique synergetic characteristics [26,30–32]. For this reason, we propose that the association between AuNps and PANI can present promising features in the construction of selective and robust bio sensitive platforms [26,32].

Herein, we describe the development of a label-free genosensor based on an AuNpsPANI hybrid composite for the electrochemical detection of the BRC/ABL fusion gene. The ssDNA used as capture probe was attached on the gold electrode modified with AuNpsPANI composite through electrostatic interactions. Cyclic voltammetry (CV), electrochemical impedance spectroscopy (EIS) and atomic force microscopy (AFM) were used to characterize the manufacturing process and to assess the performance of the biosensor.

2. Materials and methods

2.1. Materials

Tetrachloroauric acid ($HAuCl_4$) and 3-mercaptopropyl-trimethoxysilane (MPTMS) were purchased from Sigma Chemical (St. Louis, MO, USA). Aniline, potassium ferri- and ferrocyanide were obtained from VETEC (SP, Brazil). For the construction of the biosensor, the primer ALL (9;22) 5′-CGGTTGTCGTGTCCGAGG-3′ was used as bio recognition probe. The chimeric transcript was obtained after the amplification of the BCR/ABL oncogene by using both the primer ALL and the primer CML (9;22) 5′-AGCTTCTCCCTGACATCCGTG-3′. Subsequently, the chimerical DNA fragment was subcloned in a pTA vector. The recombinant plasmid sequencing was performed using primers complementary to the plasmid backbone to confirm the subcloning of the chimeric BCR/ABL transcript (Supplementary information Fig. S1). The cDNA samples of patients with leukemia were obtained from the biorepository of the IMIP's Pediatric Oncology Service and kindly provided by Doctor Francisco Pedrosa. cDNA is obtained from the total RNA of patients using a random primer [54,55]. Therefore, the samples are free of contaminants. The gold standard for the molecular monitoring of minimal residual disease in hematologic malignancies is the polymerase chain reaction that also requires genomic pre-amplification. The proposed molecular assay is performed in a lower number of steps for detection of the BCR/ABL fusion gene as compared to polymerase chain reaction (PCR). In addition, the proposed biosensor showed an exceptionally low detection limit and could become a very important tool for leukemia diagnosis and the monitoring of the minimal residual disease level.

2.2. Synthesis of AuNpsPANI hybrid composites

According to our early work [31], aniline (0.03 mol L^{-1}), MPTMS (6.46×10^{-2} mol L^{-1}), and $HAuCl_4$ (0.81 mmol L^{-1}) were used to prepare the AuNpsPANI hybrid composite in ethanol solution under magnetic agitation (1100 rpm) at room temperature for 48 h [31]. After polymerization, the large agglomerates were removed from the sample by centrifugation at 12,000 RPM during 10 min. Finally, the pH of the medium was adjusted with an acidic solution (0.1 M HCl) to promote PANI protonation and MPTMS hydrolysis [32,33]. The strategies for obtaining the sensor device and its biospecific recognition are schematically shown in Fig. 1. The initial step of the synthesis of the AuNpsPANI nanocomposite is based on the release of the ion H^+ from $HAuCl_4$ to the formation of anilinium cations ($PhNH_3^+$). The $[AuCl_4]^-$ acts as an oxidizing agent, promoting the oxidation of the $PhNH_3^+$ and giving rise to polyaniline. During the polymerization process occurs the release of electrons that reduce the $[AuCl_4]^-$ to form gold nanoparticles (AuNps). These AuNps are encapsulated by the polymer matrix. In addition, the 3-mercaptopropyl-trimethoxysilane (MPTMS) is used as a stabilizing agent to prevent the aggregation of the AuNps [31–33]. With this last step, the sulfhydryl groups from MPTMS become ready to serve as a kind of molecular adhesive between the nanocomposite and the surface of the gold electrode.

2.3. Preparation of the biosensor and exposure to target DNA

Initially, the bare gold electrode (BGE, $\phi = 2$ mm) was carefully polished with 0.05 μm α-Al_2O_3 paste and rigorously rinsed and sonicated in ultrapure water for 10 min. Subsequently, the electrode was electrochemically pretreated by CV scanning between 0.7 and −0.2 V in $K_4[Fe(CN)_6]/K_3[Fe(CN)_6]$, until a typical clean gold CV curve was obtained. Next, BGE was dip coated into the 500 μL of AuNpsPANI solution diluted in ethanol in a 1:750 (v/v) ratio for 2 min at room temperature and rinsed with water to remove non-bonded nanocomposite particles. Subsequently, 2 μL of a at 25 pmol μL^{-1} ALL biorecognition probe was dropped on the AuNpsPANI-modified electrode, which was incubated for 10 min. The selectivity and specificity of the genosensor were evaluated by using a recombinant plasmid containing the BCR/ABL fusion gene and a (nonspecific) plasmid with a non-complementary DNA sequence. We tested 0.0694, 0.694, 6.94, 69.4, 694 fM concentrations of recombinant plasmid containing the BCR/ABL fusion gene (positive control), while the concentration of the nonspecific plasmid used as negative control was 6.94 pM. Furthermore, the genosensor was tested with cDNA samples obtained from leukemia positive patients from IMIP. All diagnoses of chromosome translocation (in plasmidial and patient samples) were performed

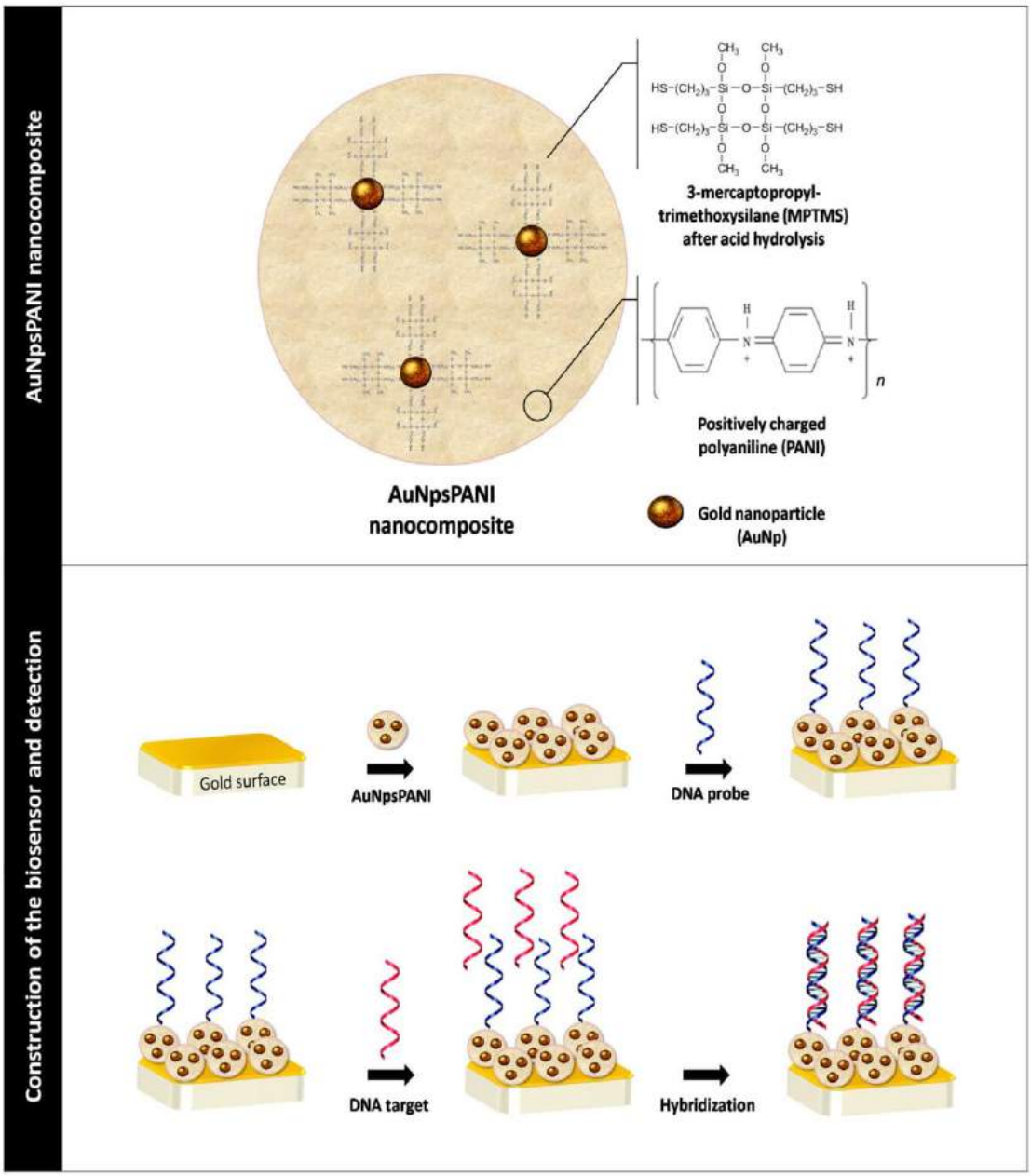

Fig. 1. Schematic representation of the AuNpsPANI nanocomposite and construction of the biosensor.

by dropping 2 μL of each sample solution that was kept on the genosensor surface for 15 min.

2.4. Electrochemical measurements

Electrochemical characterization was carried out on a Autolab PGSTAT 128N potentiostat/galvanostat interfaced with NOVA 1.8 software (Metrohm Autolab Inc., Netherlands). All measurements were performed on a three-electrode electrochemical cell configuration using a solution containing 10 mM $K_4[Fe(CN)_6]/K_3[Fe(CN)_6]$ (1:1) in PBS (10 mM, pH 7.4) as redox probe. The potential of CV measurements was swept between +0.7 V and −0.2 V at 50 mV s^{-1} scan rate. Impedance measurements were performed in the 100 mHz to 100 kHz frequency range under a +10 mV sine wave potential. The fabricated genosensor was used as working electrode, while platinum and Ag/AgCl electrodes (in 3 M KCl) were used as counter and reference electrodes, respectively. All electrochemical measurements were repeated three times at room temperature inside a Faraday cage.

2.5. Atomic force microscopy measurements

The morphological characterization of the sensor before and after its interactions with the BCR/ABL fusion gene was performed using an atomic force microscope (SPM-9500J2; Shimadzu, Tokyo, Japan). Cantilevers with a silicon AFM probe (Multi 75AL, NCHR, 75 kHz resonant frequency, 3 N m^{-1} force constant) were used for the noncontact mode AFM in air at room temperature (approximately 25 °C). Lateral resolution was set to 512 × 512 pixels in a scan area of 5 × 5 μm. At least three areas in each sample were macroscopically separated for analysis. The AFM Gwyddion software was used to analyze the images (Necas et al.).

3. Results

3.1. Morphological analyses

In Fig. 2 we show the changes in the morphology of the electrode surface as evaluated during the stepwise biosensor fabrication process. After evaporation of the solvent, AuNpsPANI nanocomposite particles arrange themselves into agglomerates with a height of 34.3 nm (Fig. 2A). However, the formation of a self-assembled monolayer (SAM) over the surface is favored due to the terminal thiol groups from MPTMS on AuNpsPANI nanocomposite. In Fig. 2B, we show that after the immobilization of the ALL primer the surface becomes uniform with an average height of 51 nm. In Fig. 2C, the morphology of the genosensor after exposure to cDNA sample extracted from whole blood of a positive leukemia patient is shown. As expected, a drastic change in the morphology of the sensor surface was observed, with the presence of peaks up to 82 nm. This result demonstrates the occurrence of specific interaction between the DNA probe and the BCR/ABL fusion gene present in patient sample with CML. On the other hand, non-significant changes in the morphology of the genosensor were observed after its exposure to a patient sample without CML (average height of 59 nm) (Fig. 2D). The height difference for non-complementary samples as compared to the AuNpsPANI-DNA probe can be attributed to a non-specific adsorption on the sensor surface [53].

3.2. Electrochemical characterization

The impedimetric responses shown in Fig. 3A were modelled according to a Randle's equivalent circuit (see inset of Fig. 3A) by use of the NOVA 1.8 software. The corresponding circuit includes (i) Rs, the ohmic resistance of the electrolyte solution, (ii) W_o, the Warburg impedance caused by the diffusion of ions from the bulk electrolyte to the electrode interface, (iii) C_{dl}, the double layer capacitance, and (iv) the charge transfer resistance R_{CT}, which is related to the microscopic processes occurring close to the electrode surface. It is known that both distinct segments are associated to mass diffusion processes that predominantly control electron transfer. We found a smaller R_{CT} value (0.22 kΩ) for BGE, in an indication that the charge transfer process is limited by electron diffusion. Compared to the initial BGE electrode, our results (a corresponding R_{CT} of 2.51 kΩ) indicate that the immobilization of the AuNpsPANI composite induces an increase in the interfacial resistivity of the electrode. This variation, which must be caused by a partial blockage of the charge transfer in the electrical double layer, suggests the formation of an AuNpsPANI monolayer. In addition, after the immobilization of the DNA probe on the AuNpsPANI-modified electrode, we noticed a significant increase (4.71 kΩ) in the R_{CT}. This result indicates that the negative charges of the tethered DNA probes effectively repel the redox agent, thus resulting in an additional increase in the R_{CT} value. Next, when the genosensor was exposed to a leukemia positive sample (be it plasmidial or patient cDNA) to promote hybridization, the increment on the number of negative charges causes the redox probe to be less prone to come nearby the genosensor surface, thus decreasing the overall electron transfer rate and consequently damping the intensity of the sensing signal. Nonetheless, the corresponding results can be still discussed in terms of the positive potential employed in the measurements. In this context, the applied DC potential attracts DNA strands to the surface of the electrode. However, the attractive forces are likely to be more effective over flexible ssDNA than over the stiffer double-stranded DNA (dsDNA) chains. Consequently, the physical barrier to the electrode surface will be more effective in the case when the hybridized complementary strand is substantially lengthier than the probe. Following this reasoning, when the genosensor is exposed to a sample (Section 3.4) containing the whole genome of the patient, the observed increase in the R_{CT} value will not be necessarily caused solely by the amount of BCR/ABL fusion gene copies found in the sample, since the length of the hybridized strand can also contribute to this result.

The electrochemical behavior of electrode was monitored at each step along the genosensor fabrication and the corresponding results are presented in Fig. 3B. The signal of the gold electrode shows a reversible voltammogram in the case of the redox probe. This behavior reveals that the electron transfer reaction is mainly a diffusion-controlled process. After the adsorption of the AuNpsPANI composite on the BGE surface, we noticed a decrease in the amperometric response. This was an expected behavior, since accordingly to the impedimetric results the immobilized nanocomposite should hinder the penetration of the redox probe through the freshly formed SAM. When compared to a BGE voltammogram, the electrode modified with AuNpsPANI and DNA probe exhibits a quasi-reversible behavior, with a considerable decrease in the oxidation/reduction signals and an increase in the separation of the peaks. Most likely, this low transfer rate of the redox couple in the sensor layer should depend on the degree of surface coating, an effect that we will study in more details in a following section.

Furthermore, DNA interaction can result in conformational alterations and changes in the electronic state (redox state) of the conductive polymer, as a planarization of the backbone and displacement of electrons [47,48]. Consequently, the electrochemical properties of the polymer, such as electron transfer rate and its conductivity, can be altered. These events are triggered by the onset of electrostatic interactions, van der Waals forces and H-bonds between the DNA and polymeric chains [48]. Recent reports have suggested that the DNA can control the redox functions of PANI chains, generating a supra-molecular structure of two oppositely charged polyelectrolytes [49,50]. These changes, which would occur predominantly in the outer layers of the polymer in contact with the biomolecule, cause perturbations in the electrical double layer (such as changes in capacitance, conductance, resistance and impedance) that can be monitored by conventional electrochemical techniques [49].

3.3. Selectivity and sensitivity assays

In Fig. 4A we compare the cyclic voltammograms that were obtained when the genosensor was exposed to different concentrations of plasmidial DNA containing the BCR/ABL fusion gene (target DNA – 0.0694, 0.694, 6.94, 69.4, 694 fM) and non-complementary plasmidial DNA (6.94 pM). After the biospecific interaction process, we observed a decrease in the redox peak currents and a reduction in the voltammetric areas. Our results are in accordance to earlier reports [34] that indicate that the hybridization process leads to a gradual reduction of the amperometric response. In this sense, a decrease on the electrochemical response is associated to a reduction on the electron flow rate through the biorecognition layer.

We can define the biodetection degree of the genosensor as the percentage of relative deviation of the anodic current variation (ΔI) between tested samples, which corresponds to

$$\Delta I\,(\%) = \frac{I_b - I_a}{I_a} \times 100, \tag{1}$$

where I_b and I_a correspond to the anodic peak current before and after the hybridization process, respectively. In Table S1, we present the results of ΔI (%) for the AuNpsPANI-DNA probe genosensor, before and after exposure to different concentrations of the target DNA. We take notice of the fact that the gradual increase in the ΔI value correlates well with the rise on the target DNA concentration. After exposing the genosensor to the negative control, we observed a subtle change in the anodic peak current (ΔI = 6.85%).

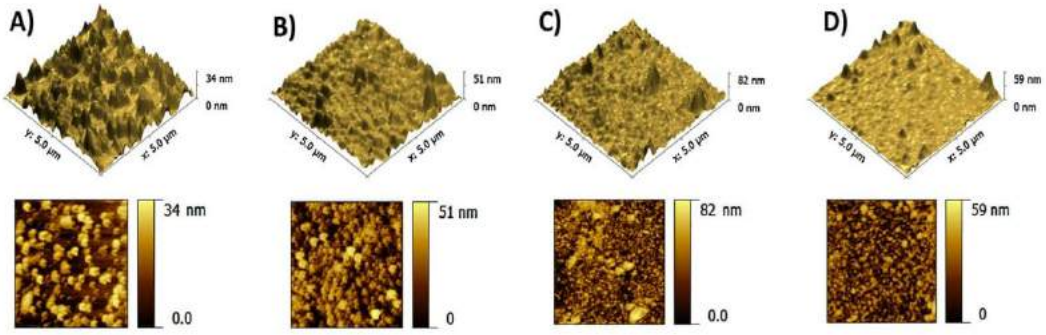

Fig. 2. 3D and 2D AFM images of AuNpsPANI nanocomposite (A), AuNpsPANI-DNA probe (B), AuNpsPANI-DNA probe-CML positive patient sample (C) and AuNpsPANI-DNA probe-CML negative patient sample (D), with the corresponding cross section. Scan area of 5 μm × 5 μm.

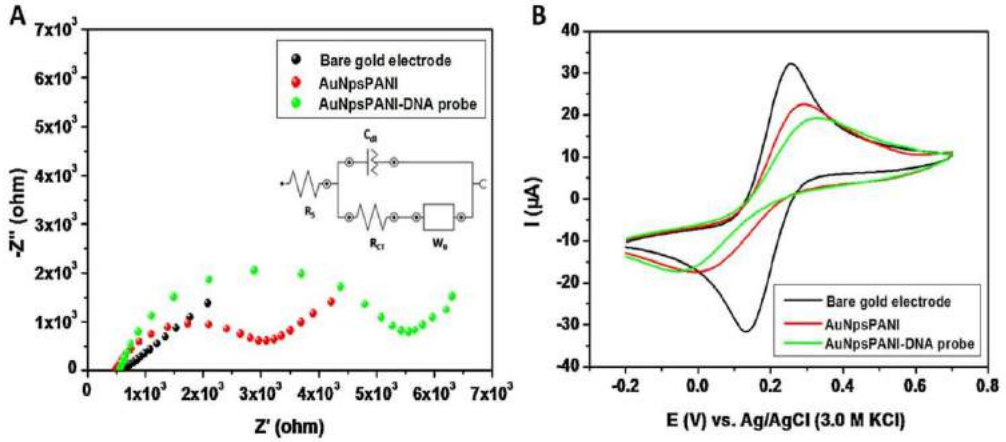

Fig. 3. Nyquist plots (A) and cyclic voltammograms (B) for each step in the assembling of the genosensor. Inset: Equivalent circuit used to fit the impedance results.

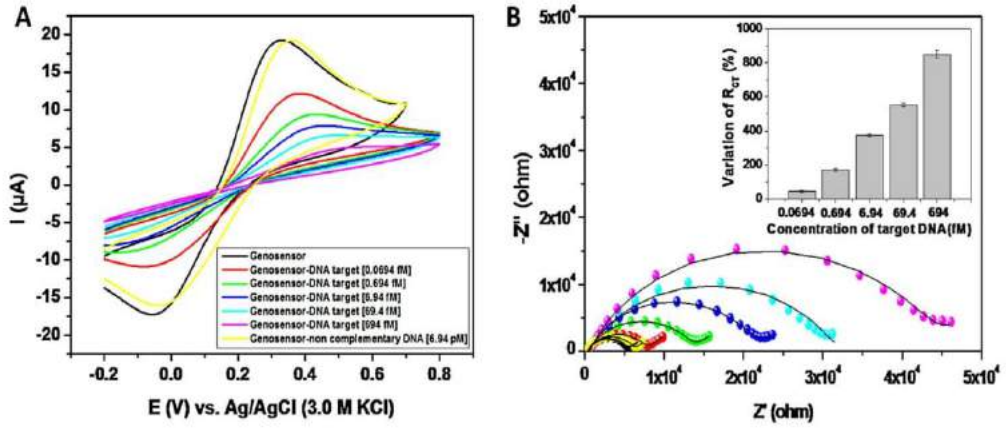

Fig. 4. Cyclic voltammograms (A) and Nyquist plots (B) of the genosensor exposed to different concentrations of recombinant plasmid containing the BCR/ABL fusion gene (DNA target – 0.0694, 0.694, 6.94, 69.4, 694 fM) and nonspecific plasmid (negative control). Inset: ΔR_{CT} (%) of the genosensor after exposure to different concentrations of target DNA. Three replicates for each experimental condition were used. Experimental values are reported as the mean values ± their half-deviation (less than 3%).

Although insignificant when compared to the result obtained for even the lower concentration of recombinant plasmid containing the BCR/ABL fusion gene (ΔI = 60.10%), this result indicates that highly concentrated negative samples might produce a low but non-negligible response, probably as a consequence of the unspecific physical trapping of non-complementary strands.

In Fig. 4B we present the impedimetric behavior of the genosensor after its exposure to plasmidial DNA containing the BCR/ABL fusion gene and to non-complementary plasmidial DNA. We can observe that the EIS results are in agreement with the results obtained by CV.

The results obtained by modelling the data with basis on a Randle's circuit are shown in Table S2. It is convenient to evaluate the performance of the genosensor in terms of the relative variation of the R_{CT} (ΔR_{CT} (%)), which is defined as

$$\Delta R_{CT}\,(\%) = \frac{R_{CT(Genosensor-targetDNA)} - R_{CT(Genosensor)}}{R_{CT(Genosensor)}} \times 100, \qquad (2)$$

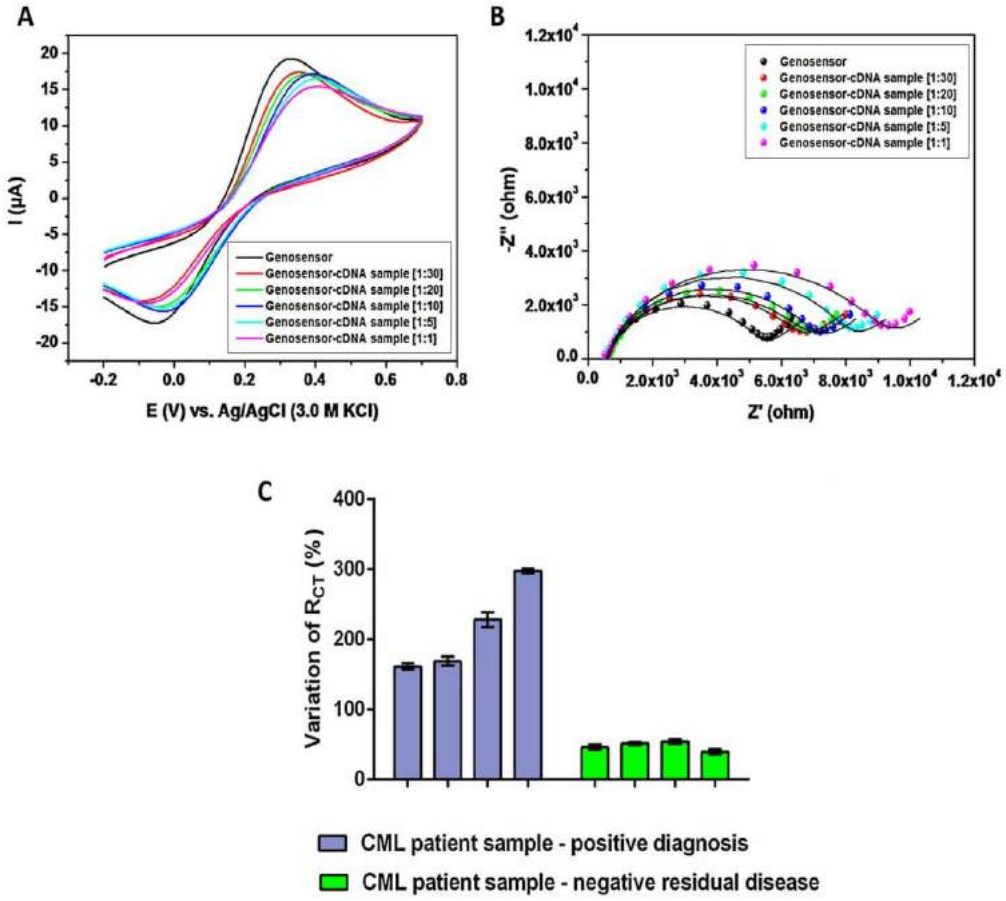

Fig. 5. Cyclic voltammograms (A) and Nyquist plots (B) of the genosensor exposed to cDNA samples of leukemia patients at different dilutions (1:1, 1:5, 1:10, 1:20 and 1:30). Histogram showing the ΔR_{CT} (%) of the genosensor after exposure to CML positive and negative patient samples (C). Three replicates for each experimental condition were used. Experimental values are reported as the mean values ± their half-deviation (less than 3%).

where $R_{CT(Genosensor\text{-}targetDNA)}$ is the measured value after the target DNA has hybridized with the probe, and $R_{CT(Genosensor)}$ corresponds to the initial response of the AuNpsPANI-DNA probe genosensor. In the inset of Fig. 4B, one can see that a linear relationship exists between ΔR_{CT} and the target DNA concentration, with perceptible changes in the ΔR_{CT} values being observed at the different values of the latter. From the impedance analysis, we estimated the lowest detection limit as 69.4 aM (41 DNA copies per μL), a more stringent threshold relative to the sensibility range (10^{-8}–10^{-15} mol L^{-1}) found in earlier reports on methods for detecting the BCR/ABL fusion gene [5,6,35,36]. The detection limit of the genosensor corresponds to lower concentration of the plasmidial sample containing the BCR/ABL fusion gene. The concentrations of 0.0694, 0.694, 6.94, 69.4, 694 fM were evaluated. The detection limit of the genosensor is 69.4 aM (or 0.0694 fM). In addition, in a demonstration of its robust specificity, a low ΔR_{CT} was obtained during the interaction of the genosensor with a non-complementary plasmid.

3.4. Detection of the BRC/ABL fusion gene in patient samples

We treated the patient samples, which were obtained after informed consent, randomly and anonymously during the analysis. All samples were previously diagnosed by conventional PCR and ethidium bromide stained agarose gel electrophoresis (Fig. S2 in the Supplementary information). In this manner, we can ensure the reliability of the results obtained from the proposed sensor system. In Fig. S2 we present the results of the electrophoresis for the PCR products. The positive control for the BCR/ABL fusion gene (CTR+) shows a light band in the gel at about 435 bp. However, no bands were observed for the negative control (CTR-) samples. The A1 and B1 patient samples (cDNA), which correspond to CML positive diagnosis, show sharp bands in the gel, a fact coherent with the finding of the band in the positive control. The A2 sample, from a patient with negative residual disease, does not present any band related to the BCR/ABL fusion gene. Also, the B2 patient sample, which comes from a weakly positive residual disease case, exhibits a very low intensity brand, indicating a low expression of the BCR/ABL fusion gene. The glyceraldehyde-3-phosphate dehydrogenase (GAPDH) was used as an internal control for sample loading and in addition have allowed us to verify that the sample processing was efficient, discarding the possibility of its degradation. This constitutive gene is expressed at high levels in most tissues and cells independently of the adopted experimental conditions.

In Fig. 5A, we present the voltammetric response of the genosensor after exposure to cDNA samples of leukemia patients at different dilutions (1:1, 1:5, 1:10, 1:20 and 1:30). We noticed a decrease in the peak current values that were obtained after the AuNpsPANI-DNA probe genosensor interact with the cDNA samples. The sensitivity of the genosensor to detect the BCR/ABL fusion gene in patient samples was monitored by measuring the variation of the anodic peak current (Table S1). In addition, we have verified that the ΔI (%) values decrease as the samples are progressively diluted (Supplementary information Fig. S3).

Table 1
Comparison of the analytical performance of the AuNpsPANI biosensor with other electrochemical DNA biosensors developed to detect BCR/ABL fusion gene.

References	Sensor platform	Detection technique	Platform construction time	Electrochemical detection time	Detection limit
This Work	Gold surface/AuNpsPANI/DNA probe	CV and EIS	12 min	15 min	69.4×10^{-18} M
[5]	Glassy carbon surface/DNA probe with terminal amino group	DPV	–	35 min	5.9×10^{-8} M
[38]	Gold surface/DNA probe (thiolated hairpin locked nucleic acids)	CV, EIS and DPV	3 h	~1 h	1.2×10^{-10} M
[6]	Glassy carbon surface/graphene sheets/chitosan/PANI/AuNps/DNA probe	CV, EIS and DPV	~19 h	~2.5 h	2.1×10^{-12} M
[13]	ITO coated glass substrate/nanostructured composite of chitosan and cadmium-telluride quantum dots/DNA probe with terminal amino group	CV and DPV	~16.5 h	1 min	2.6×10^{-12} M
[36]	Glassy carbon surface/DNA probe	CV, EIS and DPV	–	35 min	3.0×10^{-12} M
[35]	Glassy carbon surface/chitosan/cerium dioxide/multiwalled carbon nanotubes/AuNps/thiolate DNA probe	CV and DPV	~1.5 h	55 min	5.0×10^{-13} M
[12]	Glassy carbon surface/sulfonic-terminated aminobenzenesulfonic acid/DNA probe (18-mer locked nucleic acids)	CV, EIS and DPV	~30 min	~35 min	9.4×10^{-13} M
[41]	Gold surface/thiolate DNA probe (CdSeTe/CdS quantum dots tagging)	ASV	~13 h	~18.5 h	2.0×10^{-15} M
[40]	Carbon paste surface/FePt nanoparti-cles/electrochemically reduced graphene oxide/DNA probe	EIS	–	–	2.6×10^{-15} M
[42]	Gold surface/thiolate DNA probe	CV and EIS	3 h	1 h	10.0×10^{-15} M
[43]	Indium-tin oxide (ITO) coated glass substrate/tri-*n*-octylphosphine oxide-capped cadmium selenide quantum dots/thiolate DNA probe	DPV	~30 min	2 min	10.0×10^{-15} M

In Fig. 5B we present the EIS responses in the form of Nyquist plots. The incubation of the genosensor with patient cDNA samples resulted in an increase of the R_{CT} at the electrode/electrolyte interface, in a confirmation that the BCR/ABL fusion gene is present. In Table S2, we show the information obtained through the theoretical modelling of the EIS results. In addition, we present the degree of surface coating (θ), a parameter used to evaluate the bioactivity of the sensor, which was calculated as

$$\theta = 1 - \frac{R_{CT(Genosensor)}}{R_{CT(Genosensor-cDNAsample)}}. \quad (3)$$

In this equation, $R_{CT(Genosensor)}$ is the charge transfer resistance of the AuNpsPANI-DNA probe genosensor and $R_{CT(Genosensor-cDNAsample)}$ is the corresponding value for the sensor after exposure to each sample. Knowledge of the θ values allows the quantification of the percent coverage of the sensor surface after the biospecific recognition [16]. Naturally, these values are correlated to the number of hybridized DNA strands at the sensor surface. Hence, the study of θ provides additional and complementary information about the biodetection process. In Fig. S4 we show the percentage of surface coverage after the interaction of the genosensor with the samples. These results confirmed the filling of the recognition sites by the BRC/ABL fusion gene, as a result of their hybridization with the cDNA samples.

From the bioanalytical studies previously presented it was possible to estimate the optimal dilution factor for performing the detection in clinical samples. It is probable that the less diluted samples (1:1 e 1:5) cause a nonspecific adsorption of the oligonucleotides on the sensor surface. As demonstrated in Fig. S4, there was an exponential increase in the θ values for the dilutions 1:1 and 1:5. For this reason, the dilution 1:10 was chosen as the most adequate for the implementation of electrochemical tests using actual leukemia patient samples.

In Fig. 5C we show the bioactivity of the genosensor after incubation with eight samples coming from different patients. According to the corresponding ΔR_{CT} values, we identify two groups of samples. The first (columns in blue) is composed of CML positive samples, obtained in the diagnosis of cancer, while the group of columns in green is composed of CML negative samples, which were obtained from patients in the final stage of their treatment

(i.e., with negative residual disease). As it can be verified, there is a large variation in the ΔR_{CT} values (from 161.14% to 297.73%) for the genosensor exposed to positive samples and an insignificant change for the case of negative samples (39.84% to 46.07%). Also, the electrochemical responses for the CML negative samples are very similar. This response profile can be attributed to the biorecognition of the ABL and BCR constitutive genes that can bind with the probe. In summary, the AuNpsPANI-DNA probe genosensor has shown an excellent specificity and the ability to discriminate between CML positive and negative samples. In addition, it has also demonstrated high sensitivity for the diagnosis of leukemia and monitoring of the level of minimal residual disease.

4. Discussion

We believe that the above results confirm that these AuNpsPANI based biosensors exhibit the necessary bioactivity, sensibility and specificity to be used as sensing platforms for actual leukemia patient samples. In addition, when compared to other BCR/ABL fusion gene sensors described in the literature [12,37], our genosensor demands a shorter preparation time while achieving an outstanding detection limit (Table 1).

The proposed nanostructured platform presents chemical stability and high surface area. The microenvironment created by the AuNpsPANI hybrid composite ensures a stable immobilization of DNA probes, with the maintenance of their conformational structure. In association with the electrochemical kinetics of the platform, these properties are valuable for the detection capability of a low concentration of the BCR/ABL fusion gene. To the best of our knowledge the detection limit of the proposed genosensor (69.4 aM) is the lowest concentration at which the BCR/ABL fusion gene was detected. Moreover, the detection process is fast, label-free and requires a small sample volume.

In fact, only 12 min are required to modify and immobilize the probe, and the label-free biodetection can be implemented within a total time of 15 min. These values should be compared to the estimated time involved in the construction of other sensor platforms, which varies from 30 min to 19 h [5,6,12,35,36,38–40]. Then, the construction time of our platform appears as the lowest reported in the literature. We attribute this difference to the chemisorption strategy adopted to structure our sensor platform. The principle of construction is based on the strong affinity between sulfur atoms of MPTMS (molecule present in the nanocomposite) and gold atoms of the electrode. Subsequently, DNA probe is electrostatically immobilized on the modified electrode for obtaining AuNpsPANI-DNA probe genosensor.

We emphasize that not all platforms consider the covalent immobilization of the DNA probe. At the same time, when used as active transducing elements in genosensors, materials such as carbon nanotubes, cerium dioxide nanoparticles, chitosan [35], iron-platinum nanoparticles [40] and graphene sheets [6] usually demand the presence of a secondary signal amplifier or reporter.

In addition, while all biosensors must have as a minimal requirement a good detection capability, other properties should be considered for their clinical and commercial applicability, such as construction simplicity, fast response time and low cost. The molecular assay here described is performed in a lower number of steps for detection of the BCR/ABL fusion gene as compared to polymerase chain reaction (PCR), the gold standard method for the molecular monitoring of minimal residual disease in hematologic malignancies [56]. In addition, the proposed biosensor showed an exceptional detection limit and could become a very important tool for leukemia diagnosis and monitoring of the level of minimal residual disease.

5. Conclusions

We constructed an electrochemical DNA biosensor based on AuNpsPANI hybrid composite that exhibits high specificity and selectivity to detect the presence of the BCR/ABL fusion gene in leukemia patient samples. The voltammetric and impedimetric analyses were used not only to follow the process of preparation of these sensor systems, but also to test their biospecific recognition capability. These biosensors displayed a detection limit of 69.4 aM in the diagnosis of the presence of the BCR/ABL fusion gene in patient samples. In fact, we have showed that due to their sensitivity and analytical performance these AuNpsPANI-DNA probe systems can be used in an efficient for the diagnosis of leukemia and monitoring of minimal residual disease. Also, this label-free biodetection system can be built in a short time and at low cost. Therefore, we suggest that the biosensor here described appears as a promising alternative tool for clinical research of the BCR/ABL chimeric oncogene, by allowing the diagnosis of early-stage cancer.

Acknowledgements

The authors are grateful for the support provided by the Brazilian National Council for Scientific and Technological Development (CNPq), Rede ELINOR de Nanobiotecnologia/CAPES, MCT/FINEP, PROPESQ/UFPE and FACEPE-PPSUS-APQ-0040-4.00/13. The authors are also grateful to Doctor Francisco Pedrosa for providing the cDNA samples stored in the biorepository of the Pediatric Oncology Service at the IMIP and Nucleus of Technology Platforms of the Research Center Aggeu Magalhães, Fiocruz-PE, Brazil, by the sequencing of recombinant transcripts.

Appendix A. Supplementary data

Supplementary data associated with this article can be found, in the online version, at http://dx.doi.org/10.1016/j.colsurfb.2016.09.029.

References

[1] C. Cobaleda, N. Gutiérrez-Cianca, J. Pérez-Losada, T. Flores, R. García-Sanz, M. González, et al., A primitive hematopoietic cell is the target for the leukemic transformation in human Philadelphia-positive acute lymphoblastic leukemia, Blood 95 (2000) 1007–1013.
[2] C.J. Harrison, Acute lymphoblastic leukaemia, Best Pract. Res. Clin. Haematol. 14 (2001) 593–607.
[3] C.G. Mullighan, C.B. Miller, I. Radtke, L.A. Phillips, J. Dalton, J. Ma, et al., BCR-ABL1 lymphoblastic leukaemia is characterized by the deletion of Ikaros, Nature 453 (2008) 110–114.
[4] A.S. Advani, A.M. Pendergast, Bcr–Abl variants: biological and clinical aspects, Leuk. Res. 26 (2002) 713–720.
[5] X.-H. Lin, P. Wu, W. Chen, Y.-F. Zhang, X.-H. Xia, Electrochemical DNA biosensor for the detection of short DNA species of chronic myelogenous leukemia by using methylene blue, Talanta 72 (2007) 468–471.
[6] L. Wang, E. Hua, M. Liang, C. Ma, Z. Liu, S. Sheng, et al., Graphene sheets, polyaniline and AuNPs based DNA sensor for electrochemical determination of BCR/ABL fusion gene with functional hairpin probe, Biosens. Bioelectron. 51 (2014) 201–207.
[7] H. Parry, S. Damery, N. Mudondo, P. Hazlewood, T. McSkeane, S. Aung, et al., Primary care management of early stage chronic lymphocytic leukaemia is safe and effective, QJM 08 (2015) 789–794.
[8] S. Soverini, A. Hochhaus, F.E. Nicolini, F. Gruber, T. Lange, G. Saglio, et al., BCR-ABL kinase domain mutation analysis in chronic myeloid leukemia patients treated with tyrosine kinase inhibitors: recommendations from an expert panel on behalf of European LeukemiaNet, Blood 118 (2011) 1208–1215.
[9] A.S. Corbin, A. Agarwal, M. Loriaux, J. Cortes, M.W. Deininger, B.J. Druker, Human chronic myeloid leukemia stem cells are insensitive to imatinib despite inhibition of BCR-ABL activity, J. Clin. Invest. 121 (2011) 396–409.
[10] F. D'Alessio, P. Mirabelli, E. Mariotti, M. Raia, R. Di Noto, G. Fortunato, et al., Miniaturized flow cytometry-based BCR-ABL immunoassay in detecting leptomeningeal disease, Leuk. Res. 35 (2011) 1290–1293.
[11] A. Bennour, I. Ouahchi, M. Moez, M. Elloumi, A. Khelif, A. Saad, et al., Comprehensive analysis of BCR/ABL variants in chronic myeloid leukemia patients using multiplex RT-PCR, Clin. Lab. 58 (2011) 433–439.

[12] J. Chen, J. Zhang, K. Wang, X. Lin, L. Huang, G. Chen, Electrochemical biosensor for detection of BCR/ABL fusion gene using locked nucleic acids on 4-aminobenzenesulfonic acid-modified glassy carbon electrode, Anal. Chem. 80 (2008) 8028–8034.

[13] A. Sharma, C.M. Pandey, G. Sumana, U. Soni, S. Sapra, A.K. Srivastava, et al., Chitosan encapsulated quantum dots platform for leukemia detection, Biosens. Bioelectron. 38 (2012) 107–113.

[14] C. Jianrong, M. Yuqing, H. Nongyue, W. Xiaohua, L. Sijiao, Nanotechnology and biosensors, Biotechnol. Adv. 22 (2004) 505–518.

[15] L. Sun, L. Yu, W. Shen, DNA nanotechnology and its applications in biomedical research, J. Biomed. Nanotechnol. 10 (2014) 2350–2370.

[16] D.M.N. Luna, K.Y.P.S. Avelino, M.T. Cordeiro, C.A.S. Andrade, M.D.L. Oliveira, Electrochemical immunosensor for dengue virus serotypes based on 4-mercaptobenzoic acid modified gold nanoparticles on self-assembled cysteine monolayers, Sens. Actuators B 220 (2015) 565–572.

[17] A. Sassolas, B.D. Leca-Bouvier, L.J. Blum, DNA biosensors and microarrays, Chem. Rev. 108 (2008) 109–139.

[18] S. Jampasa, W. Wonsawat, N. Rodthongkum, W. Siangproh, P. Yanatatsaneejit, T. Vilaivan, et al., Electrochemical detection of human papillomavirus DNA type 16 using a pyrrolidinyl peptide nucleic acid probe immobilized on screen-printed carbon electrodes, Biosens. Bioelectron. 54 (2014) 428–434.

[19] L. Civit, A. Fragoso, C.K. O'Sullivan, Electrochemical biosensor for the multiplexed detection of human papillomavirus genes, Biosens. Bioelectron. 26 (2010) 1684–1687.

[20] N. Nasirizadeh, H.R. Zare, M.H. Pournaghi-Azar, M.S. Hejazi, Introduction of hematoxylin as an electroactive label for DNA biosensors and its employment in detection of target DNA sequence and single-base mismatch in human papilloma virus corresponding to oligonucleotide, Biosens. Bioelectron. 26 (2011) 2638–2644.

[21] S.X. Wang, G. Li, Advances in giant magnetoresistance biosensors with magnetic nanoparticle tags: review and outlook, IEEE Trans. Magn. 44 (2008) 1687–1702.

[22] S. Sagadevan, M. Periasamy, Recent trends in nanobiosensors and their applications—a review, Rev. Adv. Mater. Sci. 36 (2014) 62–69.

[23] D.T. McQuade, A.E. Pullen, T.M. Swager, Conjugated polymer-based chemical sensors, Chem. Rev. 100 (2000) 2537–2574.

[24] Y. Cao, P. Smith, A.J. Heeger, Counter-ion induced processibility of conducting polyaniline and of conducting polyblends of polyaniline in bulk polymers, Synth. Met. 48 (1992) 91–97.

[25] R.Y. Suckeveriene, E. Zelikman, G. Mechrez, M. Narkis, Literature review: conducting carbon nanotube/polyaniline nanocomposites, Rev. Chem. Eng. 27 (2011) 15–21.

[26] C. Liu, D. Jiang, G. Xiang, L. Liu, F. Liu, X. Pu, An electrochemical DNA biosensor for the detection of Mycobacterium tuberculosis, based on signal amplification of graphene and a gold nanoparticle-polyaniline nanocomposite, Analyst 139 (2014) 5460–5465.

[27] S. Liu, D. Leech, H. Ju, Application of colloidal gold in protein immobilization, electron transfer, and biosensing, Anal. Lett. 36 (2003) 1–19.

[28] P. Yáñez-Sedeño, J.M. Pingarrón, Gold nanoparticle-based electrochemical biosensors, Anal. Bioanal. Chem. 382 (2005) 884–886.

[29] J.M. Pingarrón, P. Yáñez-Sedeño, A. González-Cortés, Gold nanoparticle-based electrochemical biosensors, Electrochim. Acta 53 (2008) 5848–5866.

[30] C. Sanchez, B. Julian, P. Belleville, M. Popall, Applications of hybrid organic-inorganic nanocomposites, J. Mater. Chem. 15 (2005) 3559–3592.

[31] R.S. Santos, C.S. Andrade, C. dos Santos, C. de Melo, Visible luminescence in polyaniline/(gold nanoparticle) composites, J. Nanopart. Res. 15 (2013) 1–11.

[32] K.Y.P.S. Avelino, C.A.S. Andrade, C.P. de Melo, M.L. Nogueira, M.T.S. Correia, L.C.B.B. Coelho, et al., Biosensor based on hybrid nanocomposite and CramoLL lectin for detection of dengue glycoproteins in real samples, Synth. Met. 194 (2014) 102–108.

[33] H.P.O. Nascimento, M.D.L. Oliveira, C.P. de Melo, G.J.L. Silva, M.T. Cordeiro, C.A.S. Andrade, An impedimetric biosensor for detection of dengue serotype at picomolar concentration based on gold nanoparticles-polyaniline hybrid composites, Colloids Surf. B: Biointerfaces 86 (2011) 414–419.

[34] M.P. Costa, C.A.S. Andrade, R.A. Montenegro, F.L. Melo, M.D.L. Oliveira, Self-assembled monolayers of mercaptobenzoic acid and magnetite nanoparticles as an efficient support for development of tuberculosis genosensor, J. Colloid Interface Sci. 433 (2014) 141–148.

[35] S. Li, L. Wang, Y. Li, X. Zhu, L. Zhong, L. Lu, et al., Electrochemical determination of BCR/ABL fusion gene based on in situ synthesized gold nanoparticles and cerium dioxide nanoparticles, Colloids Surf. B:

[36] G.-X. Zhong, J.-X. Ye, F.-Q. Bai, F.-H. Fu, W. Chen, A.-L. Liu, et al., Electrochemical biosensor for detection of BCR/ABL fusion gene based on isorhamnetin as hybridization indicator, Sens. Actuators B 204 (2014) 326–332.

[37] A.A. Ensafi, M. Taei, H.R. Rahmani, T. Khayamian, Sensitive DNA impedance biosensor for detection of cancer, chronic lymphocytic leukemia, based on gold nanoparticles/gold modified electrode, Electrochim. Acta 56 (2011) 8176–8183.

[38] L. Lin, X. Lin, J. Chen, W. Chen, M. He, Y. Chen, Electrochemical biosensor for detection of BCR/ABL fusion gene based on hairpin locked nucleic acids probe, Electrochem. Commun. 11 (2009) 1650–1653.

[39] F. Wang, S. Hu, Electrochemical sensors based on metal and semiconductor nanoparticles, Microchim. Acta. 165 (2009) 1–22.

[40] J. Yang, W. Zhang, Indicator-free impedimetric detection of BCR/ABL fusion gene based on ordered FePt nanoparticle-decorated electrochemically reduced graphene oxide, J. Solid State Electrochem. 18 (2014) 2863–2868.

[41] L. Hu, T. Tan, G. Chen, K. Zhang, J.-J. Zhu, Ultrasensitive electrochemical detection of BCR/ABL fusion gene fragment based on polymerase assisted multiplication coupling with quantum dot tagging, Electrochem. Commun. 35 (2013) 104–107.

[42] K. Wang, J. Chen, J. Chen, A. Liu, G. Li, H. Luo, et al., A sandwich-type electrochemical biosensor for detection of BCR/ABL fusion gene using locked nucleic acids on gold electrode, Electroanalysis 21 (2009) 1159–1166.

[43] A. Sharma, C.M. Pandey, Z. Matharu, U. Soni, S. Sapra, G. Sumana, et al., Nanopatterned cadmium selenide Langmuir–Blodgett platform for leukemia detection, Anal. Chem. 84 (2012) 3082–3089.

[44] A. Bonanni, M. Pumera, Y. Miyahara, Influence of gold nanoparticle size (2–50 nm) upon its electrochemical behavior: an electrochemical impedance spectroscopic and voltammetric study, Phys. Chem. Chem. Phys. 13 (2011) 4980–4986.

[45] S. Chen, R.S. Ingram, M.J. Hostetler, J.J. Pietron, R.W. Murray, T.G. Schaaff, J.T. Khoury, M.M. Alvarez, R.L. Whetten, Gold nanoelectrodes of varied size: transition to molecule-like charging, Science 280 (1998) 2098–2101.

[46] N. Nath, A. Chilkoti, Label-free biosensing by surface plasmon resonance of nanoparticles on glass: optimization of nanoparticle size, Anal. Chem. 76 (2004) 5370–5378.

[47] U. Lange, N.V. Roznyatovskaya, V.M. Mirsky, Conducting polymers in chemical sensors and arrays, Anal. Chim. Acta 614 (2008) 1–26.

[48] T. Ohtake, H. Tanaka, Redox-induced actuation in macromolecular and self-assembled systems, Polym. J. (2015).

[49] K. Arora, N. Prabhakar, S. Chand, B.D. Malhotra, Ultrasensitive DNA hybridization biosensor based on polyaniline, Biosens. Bioelectron. 23 (2007) 613–620.

[50] Y. Xiao, A.B. Kharitonov, F. Patolsky, Y. Weizmann, I. Willner, Electrocatalytic intercalator-induced winding of double-stranded DNA with polyaniline, Chem. Commun. 13 (2003) 1540–1541.

[51] X. Luo, A. Morrin, A.J. Killard, M.R. Smyth, Application of nanoparticles in electrochemical sensors and biosensors, Electroanalysis 18 (2006) 319–326.

[52] P.D. Howes, R. Chandrawati, M.M. Stevens, Colloidal nanoparticles as advanced biological sensors, Science 346 (2014) 1247390.

[53] J. Wang, G. Rivas, J.R. Fernandes, J.L.L. Paz, M. Jiang, R. Waymire, Indicator-free electrochemical DNA hybridization biosensor, Anal. Chim. Acta 375 (1998) 197–203.

[54] E. Beillard, N. Pallisgaard, V.H.J. Van der Velden, W. Bi, R. Dee, E. van der Schoot, E. Delabesse, E. Macintyre, E. Gottardi, G. Saglio, F. Watzinger, T. Lion, J.J.M. van Dongen, P. Hokland, J. Gabert, Evaluation of candidate control genes for diagnosis and residual disease detection in leukemic patients using 'real-time'quantitative reverse-transcriptase polymerase chain reaction (RQ-PCR)—a Europe against cancer program, Leukemia 17 (2003) 2474–2486.

[55] J. Gabert, E. Beillard, V.H.J. Van der Velden, W. Bi, D. Grimwade, N. Pallisgaard, G. Barbany, G. Cazzaniga, J.M. Cayuela, H. Cave, F. Pane, J.L.E. Aerts, D. De Micheli, X. Thirion, V. Pradel, M. González, S. Viehmann, M. Malec, G. Saglio, J.J.M. van Dongen, Standardization and quality control studies of 'real-time'quantitative reverse transcriptase polymerase chain reaction of fusion gene transcripts for residual disease detection in leukemia—a Europe against cancer program, Leukemia 17 (2003) 2318–2357.

[56] R. Mir, I. Ahmad, J. Javid, M. Zuberi, P. Yadav, R. Shazia, M. Masroor, S. Guru, P.C. Ray, N. Gupta, A. Saxena, Simple multiplex RT-PCR for identifying common fusion BCR-ABL transcript types and evaluation of molecular response of the a2b2 and a2b3 transcripts to Imatinib resistance in north Indian chronic myeloid leukemia patients, Indian J. Cancer 52 (2015) 314–318.

CAPÍTULO 6

6 ARTIGO 2

Artigo a ser submetido à revista *Sensors and Actuators B: Chemical*

Fabrication of a novel nanostructured platform based on aminopropyltriethoxysilane-functionalized zinc oxide nanoparticles and carbon nanotubes for impedimetric monitoring of the BCR/ABL fusion gene

FABRICATION OF A NOVEL NANOSTRUCTURED PLATFORM BASED ON AMINOPROPYLTRIETHOXYSILANE-FUNCTIONALIZED ZINC OXIDE NANOPARTICLES AND CARBON NANOTUBES FOR IMPEDIMETRIC MONITORING OF THE BCR/ABL FUSION GENE

Karen Y.P.S. Avelino[1], Isaac Aaron Morales[2], Norma Lucena-Silva[3,4], César A.S. Andrade[1,2], Maria D.L. Oliveira[1,2]*

[1]Programa de Pós-Graduação em Bioquímica e Fisiologia, Universidade Federal de Pernambuco, 50670-901 Recife, PE, Brasil.

[2]Programa de Pós-Graduação em Inovação Terapêutica, Universidade Federal de Pernambuco, 50670-901 Recife, PE, Brasil.

[3]Centro de Pesquisas Aggeu Magalhães, Fundação Oswaldo Cruz (Fiocruz), 50670-420 Recife, PE, Brasil.

[4]Laboratório de Biologia Molecular, Departamento de Oncologia Pediátrica, Instituto de Medicina Integral Professor Fernando Figueira (IMIP), 50070-550 Recife, PE, Brasil.

*To whom correspondence should be addressed.

Maria D.L. Oliveira, Departamento de Bioquímica, UFPE, 50670-901, Recife, PE, Brazil

Phone: +55-81-2126.8450; Fax: +55-81-2126.8547

E-mail: m_danielly@yahoo.com.br

Abstract

BCR/ABL fusion gene is one of the main biomarkers for leukemia, found in over 90 % of the patients with chronic myeloid leukemia (CML). In this study, we report a new electrochemical DNA biosensor based on cysteine (Cys), carboxylated multiwalled carbon nanotubes (cMWCNTs) and aminopropyltriethoxysilane functionalized zinc oxide nanoparticles (ZnONps/NH_2) for label-free detection of the BCR/ABL fusion gene. The nanostructured platform was assembled on a gold surface via specific chemical coupling between the functional groups of the biomolecules and of the nanomaterials. The surface morphology and the electrochemical properties of the steps of biosensor construction and its bioactivity were investigated by atomic force microscopy (AFM), cyclic voltammetry (CV) and electrochemical impedance spectroscopy (EIS), respectively. AFM images showed changes in the topographic profile of the biosensor after exposure to positive samples, evidencing the hybridization process. We verified that the proposed platform has excellent electron transfer properties, ability to self-amplify the electrochemical signal and high surface area for immobilization of the DNA probe. When evaluating the analytical performance of the biosensor with cDNA samples of leukemia patients, were observed significant changes in the amperometric currents and in the resistance to charge transfer (R_{CT}) values. The biosensor displayed reproducibility, selectivity, fast response time and a limit of detection (LOD) as low as 6.94 aM. Hence, the proposed biodevice allows BCR/ABL fusion gene analysis in clinical samples, enabling the early-stage diagnosis of the cancer and the monitoring of minimum levels of residual disease.

Keywords: BCR/ABL fusion gene; biosensor; electrochemistry; leukemia; carbon nanotubes; zinc oxide nanoparticles.

1. Introduction

The BCR/ABL fusion gene, also known as Philadelphia chromosome, is generated from the reciprocal translocation between chromosomes 9 and 22 t(9;22) (q34; q11). This oncogene is associated with the myeloid and lymphoid neoplasms pathogenesis, such as chronic myeloid leukemia (CML) and acute lymphoid leukemia (ALL) [1]. The identification of the BCR/ABL fusion gene enables an early cancer diagnosis and monitoring of the disease regression during treatment. Moreover, makes possible the detection of residual leukemic cells, especially after bone marrow transplantation [2].

The presence of residual leukemic cells without clinical evidence of cancer is defined as minimal residual disease [3]. The monitoring of minimal residual disease is essential to assess the patient's response to treatment, delineate the risk of recurrence of leukemia and guide therapeutic decisions against cancer [4, 5]. The monitoring of minimal residual disease should be considered by health professionals as a routine clinical practice, since it is one of the main indicators for the prognosis of leukemia [3, 6]. Thus, the methods used in the monitoring should have high precision and sensitivity to detect minimum levels of the disease [6].

The diagnosis of leukemia can be obtained through hematological exams, cytogenetics and molecular assays. Currently, the conventional methods used for diagnosis of the BCR/ABL fusion gene comprise chromosome analysis, fluorescent *in situ* hybridization, flow cytometry, Southern blot analysis and quantitative real-time reverse-transcription polymerase chain reaction [7]. Among the disadvantages of these methods are the limited sensitivity, high investments for the acquisition of complex equipment and time-consuming experimental protocols, that restrict their wide use in laboratory and hospital areas. Therefore, the development of a simple and effective molecular assay for the detection of the BCR/ABL fusion gene is of great interest for improvement of the patients' health with leukemia [8].

In the last years, advances in nanoscience and biotechnology have enabled the development of new electronic devices, as electrochemical genosensors. The functional strategy of these devices is based on the specificity of DNA probes and analytical capacity of the signal transduction methods [9]. The main challenges for the development of electrochemical genosensors are: a) preservation of the conformational structure and bioactivity of the immobilized molecules on transducer surfaces; and, b) improvement of the sensitivity to detect subtle changes in the electrochemical properties of the sensor [10]. In this scenario, the biocompatible nanostructured platforms arise as an innovative alternative to obtaining devices with high analytical performance. Furthermore, nanostructured platforms

can be chemically modified with functional groups ensuring a stable anchoring process through covalent bonds with DNA probes [11]. As described in previous works, the chemical immobilization of DNA sequences on solid substrates reduces the non-specific adsorption and the leaching process of the sensor layer [12, 13].

Carbon nanotubes (CNTs) have become the subject of numerous research since its discovery by Iijima in 1991 [14]. CNTs have applications in different areas due to their strong mechanical strength, high surface-volume ratio, conductivity and unique electronic structure. They are composed by a hexagonal network of carbon atoms in a cylinder shape with sp^2 hybridization. CNTs can be obtained as single-walled carbon nanotubes (SWCNTs) or multiwalled carbon nanotubes (MWCNTs) [15]. In addition, CNTs can be functionalized with chemical groups (e.g. COOH, NH_2, SH) and associated with polymers or metal particles to obtain new materials with improved properties [16]. CNTs have been extensively employed as direct electrons mediators between the electrode and the biomolecule, enabling the self-amplification of the electrochemical signal [17-19]. In addition, CNT-based electrochemical transducers decrease overpotential and present a lower detection limit [20-22].

In particular, we highlight the use of zinc oxide nanoparticles (ZnONps) to obtain biomolecular electronic devices mainly due to their physical characteristic of a semi-conductor material with a low band gap energy (3.37 eV). ZnONps also exhibit high ratio between surface area and volume, high catalytic efficiency, chemical stability, biocompatibility, non-toxicity and unique optical properties [23]. Recently, studies have demonstrated synthesis mechanisms for the chemical functionalization of ZnONps [24, 25]. A great promise for the construction of nanostructured platforms are ZnONps-NH_2. The ZnONps-NH_2 have intrinsic properties of the metallic oxide and chemical characteristics of the aminosilane, being able to increase the immobilization density, stability and reduce the leaching process of biomolecules [24, 26].

Assuming the premise that CNTs and ZnONps are nanomaterials with highly attractive electrochemical properties [23], we developed a new biosensitive platform for label-free diagnosis of the BRC/ABL fusion gene. Through a process of chemical structuring, our platform based on cysteine (Cys), cMWCNTs and ZnONps-NH_2 was obtained. After a detailed study of the modification steps, a DNA probe was covalently immobilized and used as biorecognition element.

2. Materials and methods

2.1. Materials

Cys, cMWCNTs, ZnONps (< 50 nm particle size and purity > 97 %), N-hydroxysulfosuccinimide (NHS), 1-ethyl-3-(3-dimethylaminopropyl)carbodiimide (EDC), aminopropyltriethoxysilane (APTES) and bovine serum albumin (BSA) were purchased from Sigma Chemical (St. Louis, MO, USA). Potassium ferricyanide ($K_3[Fe(CN)_6]$), potassium ferrocyanide ($K_4[Fe(CN)_6]$), nitric acid (HNO_3), glutaraldehyde, methanol, acetone and alumina (α-Al_2O_3) were obtained from VETEC (SP, Brazil). The experiments were performed using the primer ALL (9;22) 5'-amine-CGGTTGTCGTGTCCGAGG-3'. The chimeric transcript was obtained according to the methodology described by Marques et al. (2011) [27]. The BCR/ABL fusion gene was amplified using both the primer ALL and the primer CML (9;22) 5'-AGCTTCTCCCTGACATCCGTG-3'. Posteriorly, a pTA vector was used for subcloning of the chimerical DNA fragment. cDNA samples of patients with leukemia were obtained from the biorepository of the Pediatric Oncology Service at the Professor Fernando Figueira Integral Medicine Institute. A random primer was used to the reverse transcription of the total RNA of the patients to obtain cDNA samples. The plasmid and cDNA samples were prepared in 10 mM phosphate buffer saline (PBS) at pH 7.4 and stored frozen. All aqueous solutions were prepared with deionized water obtained from a Milli-Q plus purification system (Billerica, MA, USA).

2.2. Modification of ZnONps with APTES

The modification of ZnONps with APTES was performed according to Grasset et al. (2003) [26]. 1.5 g of zinc oxide was dispersed into 50 mL of deionized water and, subsequently, the pH was adjusted to 6.5 with the addition of HNO_3 solution (2 M). The suspension was stirred for 1 hour and then 1 mL of APTES was added. Subsequently, the mixture was stirred for a further 24 hours. After the excess APTES was removed by filtration and washing with alcohol and acetone. The obtained powder was dried at 60 °C and stored out at laboratory temperature (22 ± 0.1 °C). Then, APTES-modified ZnONps (1 mg/mL) were suspended in methanol. Prior to use, the suspension was submitted to an ultrasonic bath for 1 hour to obtain a homogeneous mixture [26].

2.3. Preparation of the sensor system

Initially, the bare gold electrode (BGE, ϕ = 2 mm) was polished with 0.05 μm α-Al_2O_3 paste, rinsed with deionized water and sonicated for 10 min. Subsequently, 2 μL of Cys solution in PBS (pH 7.4) was drop coated on the BGE for 30 min to obtain a self-assembled layer [28]. In order to determine the ideal concentration of Cys for preparation of the

biosensor, different concentrations (10, 20, 30, 40, 50 and 60 mM) were evaluated. Subsequently, Cys-modified electrode was rinsed with deionized water to remove non-bonded molecules.

Then, cMWCNTs were dispersed in methanol at a concentration of 4 μg/mL. cMWCNTs suspension was submitted to an ultrasonic bath for 1 h to obtain a homogeneous mixture. EDC and NHS were used as coupling agents allowing the chemical bonding between cMWCNTs and Cys-modified electrode. The addition of EDC (0.4 M) and NHS (0.1 M) in cMWCNTs suspension at a ratio of 1:1:2 (v/v) resulted in the activation of the carboxyl groups of the nanotubes enabling the reaction with Cys amino groups [29]. The activation of the nanotubes was performed during 30 min and thereafter 2 μL of the cMWCNTs/EDC/NHS suspension was dropped on Cys layer. The evaluation of the conjugation time was performed at 15, 20, 25, 30 and 35 min.

Then, 1 μL EDC (0.4 M) was added on the Cys-cMWCNTs modified electrode for 5 min, followed by the addition of 1 μL of NHS (0.1 M) for 5 min. Subsequently, 2 μL of the ZnONps/NH_2 suspension at 1 mg/mL were added and the electrode was rinsed with deionized water to removal of the unbounded particles. The study of the conjugation time of the nanoparticles on the modified electrode was carried out at the times of 10, 20, 30, 40, 50 and 60 minutes.

The probe immobilization on the nanostructured platform was based on covalent bonds between amino groups of the APTES and amine-modified DNA probe using glutaraldehyde as a bifunctional crosslinking agent. 1 μL of glutaraldehyde was added on the modified gold surface for 5 min and, subsequently, 2 μL primer ALL (25 pmol μL^{-1}, used as biorecognition probe) was dropped on the nanostructured platform for 15 min. Finally, the modified electrode was immersed in BSA solution (25 pmol μL^{-1}) to block any nonspecific binding sites. Then, the Cys-cMWCNTs-ZnONps/NH_2-probe-BSA sensor system was obtained (Fig. 1).

2.4. Bioactivity study of the sensor system

Recombinant plasmids containing the BCR/ABL fusion gene and plasmids with non-complementary DNA sequences were used to evaluate the specificity and selectivity of the biosensor, respectively. We also evaluated the bioactivity of the sensor using cDNA samples obtained from leukemia positive patients. Furthermore, we studied the electrochemical behavior of the sensor system after exposure to cDNA samples of non-leukemic patients containing the genome of *Escherichia coli* (*E. coli*), *Candida albicans* (*C. albicans*),

Mycobacterium tuberculosis (*M. tuberculosis*), *Schistosoma mansoni* (*S. mansoni*) and Hepatitis C virus (HCV). In these assays, 2 μL of each sample were dropped on the sensor surface for 15 min aiming the detection of the BCR/ABL fusion gene (in plasmid and patient samples). We emphasize that two different selectivity tests were performed to ensure the legitimacy of the biodetection signal, one with plasmid samples containing non-complementary DNA sequences and another with cDNA samples of leukemia negative patients with the genome of different species. All clinical samples were obtained after informed consent of the patients and the procedures were approved by the local ethics committee.

2.5. Electrochemical measurements

The electrochemical experiments were performed on a PGSTAT 128N potentiostat/galvanostat interfaced with NOVA 1.11 software (Metrohm Autolab Inc., Netherlands). The electrochemical cell was composed by three electrodes immersed in a solution containing 10 mM $K_4[Fe(CN)_6]/K_3[Fe(CN)_6]$ (1:1, v/v) in PBS (10 mM, pH 7.4), used as redox probe. A bare gold electrode was used as working electrode. A platinum wire and Ag/AgCl electrode saturated with KCl were used, respectively, as counter and reference electrodes. CV measurements were carried out at a 50 $mV.s^{-1}$ scan rate in a range of potential between -0.2 V and +0.7 V. The impedance measurements were recorded in a frequency ranging from 100 mHz to 100 kHz under a sine wave potential of +10 mV. The electrochemical experiments were performed in triplicate at room temperature (~ 24 ºC) inside a Faraday cage.

2.6. Atomic force microscopy measurements

The topographic characterization of the sensor system was performed using a SPM-9500 atomic force microscope (Shimadzu, Tokyo, Japan). AFM images were obtained in noncontact mode through cantilevers with a silicon AFM probe (Multi 75AL, NCHR, resonant frequency = 75 kHz, force constant = 3 $N.m^{-1}$) at room temperature. Lateral resolution was set to 512 × 512 pixels in a scan area of 5 × 5 μm. The images were obtained from at least three macroscopically separated areas of each sample for removal of artifacts. AFM Gwyddion software was used to analyze the images.

2.7. Fourier transform infrared (FTIR) spectroscopy measurements

FTIR analysis was performed on a FTIR IRTRACER-100 (Shimadzu Co., USA) spectrophotometer interfaced to Softwarelab Solution IR. The transmittance spectrum was obtained from 400 to 4000 cm^{-1} with resolution of 1 cm^{-1} using KBr pellets.

3. Results and discussion

3.1. FTIR analyses

FTIR spectroscopy was used to evaluate the presence of amine groups in the ZnONps after modification with APTES. Fig. S1 shows the FTIR spectrum for ZnONps/NH_2 samples in the range of 400 to 4000 cm^{-1}. The FTIR spectrum of the ZnONps/NH_2 shows a peak at 434 cm^{-1} due to the vibration of the Zn-O bond [30]. The broad band observed in the range of 3350 to 3500 cm^{-1} corresponds to the stretching mode of the -OH and -NH_2 groups. In addition, -OH and -NH_2 groups are derived from the hydrogen bonds with the adsorbed water molecules and from the functionalization process with APTES, respectively [24, 30]. The bands observed at 1632 cm^{-1} and 1553 cm^{-1} are related to the bending mode of the -OH and -NH_2 groups [30, 31]. The presence of bands in the range of 2845 to 2865 cm^{-1} and 2916 to 2936 cm^{-1} indicates the symmetric and asymmetric stretch of the -CH_2 group, respectively [32]. The vibrations at 1384 cm^{-1} and 2947 cm^{-1} are attributed to the stretching and bending modes of the Si-CH_2 group [33]. Moreover, stretching vibration of the Si-O group is observed at 989 cm^{-1} [34]. The band at 873 cm^{-1} corresponds to Si-O-Zn bond that indicates the effective functionalization of the ZnONps [24]. In contact with large humidity percentages present in the air, the APTES methyl groups are hydrolyzed to carbonyl moieties. These carbonyl moieties are identified in the spectrum from the vibration at 2359 cm^{-1} [30].

3.2. Topographic analyses

3D and 2D AFM images of the modified electrode are shown in Fig. 2. The addition of Cys on solid substrate results in a self-assembled layer with agglomerates of maximum height of 32.7 nm (Fig. 2A). Subsequently, the interaction with cMWCNTs results in changes in the topographic profile. The presence of numerous peaks with similar heights characterizes the tubular morphology of the cMWCNTs (Fig. 2B) [35]. After the conjugation of the ZnONps/NH_2, the surface morphology was modified due to the presence of heterogeneously dispersed nanoparticles (Fig. 2C). The surface roughness for the Cys-cMWCNTs-ZnONps/NH_2 and Cys-cMWCNTs-ZnONps/NH_2-probe-BSA layers were experimentally determined as 134 and 147 nm, respectively. As reported in the literature, the network

structure observed in the Fig. 2D arises due to the attachment of the DNA sequences, indicating the appropriate biofunctionalization of the surface [36, 37]. In sequence, the biosensor was exposed to a cDNA sample of leukemia patient and as expected, we observed a drastic change in the topography of the sensor system with peaks up to 181 nm (Fig. 2E). This phenomenon is due to the hybridization process between the DNA probe and the BCR/ABL fusion gene expressed in patients with CML. In contrast, non-significant differences in the morphology of the biosensor were observed after its contact with a patient sample without CML (maximum height of 151 nm) (Fig. 2F). Therefore, our AFM analyzes suggest the highly organized structuring, specificity and selectivity of the sensing platform.

3.3. Electrochemistry characterization of the biosensor

Fig. 3 evidences the cyclic voltammograms (A) and impedance spectra (B) for each step of assembly of the biosensor. We performed a theoretical simulation of the experimental data through the NOVA 1.11 software. The impedimetric responses were modeled by the Randle's equivalent circuit (see inset of Fig. 3B) constituted of: (i) Rs, ohmic resistance of the electrolyte solution; (ii) Z_W, Warburg impedance related to mass transport resistance of the electroactive species in the bulk solution to the electrode surface; (iii) CPE, constant phase element; and (iv) R_{CT}, charge transfer resistance associated to the thermodynamic processes that occur on the electrode surface and that influence the charge transfer. In the Table S1 are shows the values of the equivalent circuit elements obtained from the fitting of the impedance results.

Fig. 3A shows that the bare gold electrode (BGE) presents a reversible voltammogram in the presence of the electrolytic probe with symmetrical and well defined anodic and cathodic peaks. In addition, was observed that the BGE spectrum is characterized by a small semi-circle and low R_{CT} value (R_{CT} = 0.17 kΩ) (Fig. 3B). This electrochemical behavior is associated to an electron transfer kinetics mainly controlled by mass diffusion in the double electric layer.

After the modification of the BGE with Cys, were verified a reduction of the amperometric current (Fig. 3A) and an increase in the resistive properties (R_{CT} = 3.36 kΩ) (Fig. 3B), indicating the formation of the Cys layer on the solid substrate. When evaluating the impedimetric profile of the Cys layer as a function of its concentration, we found that from the concentration of 10 to 40 mM there is a linear increase in the diameters of the Cole-Cole semi-circles (Fig. S2A) and, consequently, in the R_{CT} values (Fig. S2B). In contrast, was observed that concentrations greater than 40 mM, such as 50 and 60 mM, do not significantly

affect the impedimetric behavior of the modified electrode. This phenomenon may be associated with the saturation of the electroactive surface, which prevents the immobilization of new Cys molecules. Therefore, we considered the concentration of 40 mM as the ideal concentration for the biosensor assembly. Cys molecules have terminal thiol groups (SH-) that interact strongly with the gold atoms of the working electrode by means of covalent bonds. This process, called chemisorption leads to the formation of self-assembled layers with a high degree of molecular organization, an essential feature for the construction of nanostructured sensors [28, 38].

The addition of cMWCNTs on the Cys layer causes higher oxidation and reduction peaks (Fig. 3A) and an increase in the system conductance (R_{CT} = 0.02 kΩ) (Fig. 3B). The study about the influence of the incubation time of the cMWCNTs on the Cys-modified electrode is presented in Fig. S3. We noticed that between the times of 10 and 20 minutes there was an increase in the voltammetric signals (Fig. S3A). In reason of the Ipa values follow a sigmoidal curve model with plateau starting at 20 minutes, the system current becomes constant in the times of 25, 30 and 35 minutes (Fig. S3B). This behavior may be related to steric hindrance and to unavailability of free amino groups of the Cys molecules for the anchoring of new cMWCNTs [39, 40]. Considering the obtained results, we conclude that 20 minutes is the ideal time for the conjugation of the cMWCNTs, since long periods do not affect the redox behavior of the Cys-cMWCNTs layer.

Following the biosensor construction stages, addition of the ZnONps/NH_2 on the electrode modified with Cys and cMWCNTs resulted in a decrease in the amperometric response (Fig. 3A) and an increase in the resistance to electron passage (R_{CT} = 2.54 kΩ) (Fig. 3B). Despite the semi-conductive characteristic of the metallic oxide, the functionalized nanoparticle partially reduces the current generated in the system. The evaluation of the incubation time of the nanoparticles is presented in Fig. S4. We observed that between 10 and 30 minutes there is a gradual decrease of the voltammetric areas (Fig. S4A) and an increase in the EIE measurements (Fig. S4B). However, from the time of 30 minutes occurs a significant change in the electrochemical profile of the system. Taking into account the results obtained, we believe that incubation times greater than 30 minutes cause a relatively higher conjugation of ZnONps/NH_2. This fact can lead to agglomeration of the nanoparticles and to irreversible blocking of the redox process on the electrode surface. Thus, 30 minutes was considered the best time for incubation of the ZnONps/NH_2 on the substrate modified with Cys-cMWCNTs.

After obtaining the Cys-cMWCNTs-ZnONps/NH_2 nanostructured platform, the biorecognition probe was immobilized. We noticed a significant decrease in the

oxidation/reduction signals (Fig. 3A) and an increase in the R_{CT} value (R_{CT} = 3.32 kΩ) (Fig. 3B). These results indicate the low penetration of the redox probe in the sensor system. One of the factors that contribute to this event is the electrostatic repulsion between the phosphate groups of the DNA probe and the negatively charged polyelectrolytes [41]. In addition, was found that the exposure of the sensor system to BSA solution causes the blockage of the non-specific sites. This result is demonstrated through the current reduction (Fig. 3A) and increase in the impedimetric response (R_{CT} = 5.08 kΩ) (Fig. 3B). Therefore, from the electrochemical analyzes was possible to characterize each construction step of the biosensor (Cys-cMWCNTs-ZnONps/NH_2-probe-BSA).

3.4. Sensitivity and selectivity assays

The analytical performance of the biosensor was evaluated through specific hybridization with the BCR/ABL fusion gene present in recombinant plasmids. Fig. 4A shows the cyclic voltammograms for the biosensor after its exposure to different concentrations of complementary target DNA (6.94, 694, 6940, 69400 and 694000 aM). These concentrations were tested in triplicates in order to determine the detection interval of the bioelectrode. After the biodetection process, was verified a reduction in the voltammetric responses and a decrease in the oxidation and reduction currents. According to previous studies, the phenomenon mentioned reveals the formation of double-stranded DNA (dsDNA) on the biosensor surface, which acts as an additional barrier to the passage of the redox probe ions [42, 43]. In this way, we verified that the biorecognition process leads to a proportional decrease in the CV measurements.

The bioactivity of the sensor system with plasmidial samples can be represented by the percentage of relative deviation of the anodic current variation (ΔI) [44],

$$\Delta I(\%) = \frac{I_b - I_a}{I_b} \times 100 \quad (1)$$

where I_b and I_a correspond to the anodic peak current before and after the hybridization process, respectively. In Table S2, we showed the amperometric anodic shift for the biosensor after its interaction with different concentrations of the chimeric oncogene. It can be observed that the ΔI values are related to the concentrations tested through a linear increase, which demonstrates the sensitivity of the biosensor. The selectivity was evaluated using recombinant plasmids with non-complementary DNA sequences at a concentration of 694000 aM. We reported an insignificant change in the ΔI after the interaction of the biosensor with the

negative control (ΔI = 2.46 %). This value was much lower than the result obtained for the lowest concentration of the recombinant plasmid containing the BCR/ABL fusion gene (ΔI = 21.89 %). Thus, we revealed the selectivity of the system.

The Nyquist diagrams obtained after exposure of the biosensor to the chimeric transcript in variable concentrations were shown in Fig. 4B. Initially, can be seen that the interaction of the biosensor with the plasmid samples results in an increase in the diameters of the Cole-Cole semicircles (Fig. 4B). This analysis shows that the detection of the BCR/ABL fusion gene causes an impediment to the charge transfer on the electrode surface. Thus, we verified that the specific hybridization process causes an intensification of the impedimetric response.

The above informations clearly show that the biosensor is able to recognize the BCR/ABL fusion gene in plasmid samples, as can be observed by the increase in the R_{CT} (Table S1). Since that the DNA complexes formed in the sensing layer have non-conductive properties, the R_{CT} resistive component is suitable to monitor the bioactivity of the system. For these reasons, the relative variation of the R_{CT} (ΔR_{CT}) was used to characterize the analytical performance of the biosensor. ΔR_{CT} is calculated as follows [45]:

$$\Delta R_{CT}\ (\%) = \frac{R_{CT(Biosensor-target\ DNA)} - R_{CT(Biosensor)}}{R_{CT(Biosensor)}} \times 100 \quad (2)$$

where $R_{CT(Biosensor\text{-}target\ DNA)}$ is the measured value after the target DNA recognition and $R_{CT(Biosensor)}$ corresponds to the initial response of the biosensor (Cys-cMWCNTs-ZnONps/NH_2-probe-BSA).

The Table S1 shows the ΔR_{CT} values versus the plasmid concentrations. We evidenced a percentage variation from 12.93 % to 192.62 %. From the calibration test (see inset of Fig. 4B) was obtained linear regression equation expressed as follows: y = 16.14 ln(x) - 17.87 with a correlation coefficient (R^2) of 0.99. Where y corresponds to the ΔR_{CT} and x the concentration of target DNA (aM). The linearization of the x-axis was performed by taking the logarithmic scale of the concentration. This ΔR_{CT} response indicates the linear sensitivity of the biosensor to variable oncogene concentrations.

The selectivity was also investigated in terms of ΔR_{CT}, where we obtained a value of 2.75 %. Thus, was found that the interaction of the biosensor with a non-complementary DNA sequence does not lead to a significant impedimetric response. This result also demonstrates the low capacity of the biosensor for unspecific adsorption. From the electrochemical analyzes, we show that the biosensor is able to detect the BCR/ABL fusion gene at a

concentration as low as 6.94 aM. Recently, we described the construction of a hybrid composite-based biosensor for the diagnosis of this same oncogene with a LOD of 69.4 aM [44]. Therefore, through a new nanostructure platform was possible to improve the analytical performance of the bioelectrode in ten times. This high sensitivity is crucial for the monitoring of minimal residual disease with an impact on the prognosis of leukemia.

The analytical comparison between the biosensor presented in this work and the other DNA biosensors reported in the literature for the electrochemical detection of the BCR/ABL fusion gene is shown in Table S3. We found that the LOD of 6.94 aM corresponds to the lowest concentration at which the chimeric oncogene can be identified. Furthermore, was observed that our sensing platform requires a short time to detect the molecular target (15 minutes). In relation to the other electrochemical biosensors, we seen that they demand a long detection time of up to 18.5 hours (Table S3). Considering the sensitivity, selectivity and fast response time, the developed nanodevice can be considered a promising tool for the impedimetric determination of the BCR/ABL fusion gene in cDNA samples of leukemia patients.

3.5. Detection of the BRC/ABL fusion gene in patient samples

A detailed analysis of the biodetection performance of the sensor is shown in Fig. S5, after its exposure to cDNA samples at different dilutions. As can be seen, the assays with cDNA samples of leukemia patients cause a decrease of the voltammetric areas (Fig. S5A). This result is due to the formation of the hybridized DNA strands on the biosensor surface, which maintain unfavorable electrostatic interactions with the redox pair [46]. The sensitivity also was monitored by ΔI (%) measurements (Table S2). We noticed a linear decrease in the ΔI (%) values to the extent that the samples are diluted (1: 1, 1: 5, 1:10, 1:20 and 1:30). In this study, the nanobioelectrode shown to be sensitive to detect the BCR/ABL fusion gene in cDNA samples containing entire genome of the patient.

Fig. S5B reveals that after the incubation of the biosensor with leukemia samples at different dilutions there is a change in the impedance spectra. As expected, the biorecognition process leads to an increase in the interfacial resistance. We also found that the ΔR_{CT} values decrease as a function of the more dilute samples (Table S1). The electrochemical results made explicit the capture of the BCR/ABL fusion gene on the biosensor surface. This event interrupts the electron transport between the solution and the electrode, resulting in an increased impedance.

In order to quantify the percent coverage of the biosensor after its exposure to cDNA samples, we calculated the degree of surface coating (θ) according to equation 3 [28].

$$\theta = 1 - \frac{R_{CT(Biosensor)}}{R_{CT(Biosensor-cDNA\ sample)}} \quad (3)$$

Where, $R_{CT(Biosensor)}$ is the R_{CT} value of the biosensor (Cys-cMWCNTs-ZnONps/NH_2-probe-BSA) and $R_{CT(Biosensor\text{-}cDNA\ sample)}$ is the corresponding value for the biosensor after exposure to each sample. The θ serves as an additional parameter to evaluate the bioactivity of the proposed system. Was observed that the θ values increase proportionally to the extent that the samples become more concentrated (Fig. S5C). Evidently, these results may be correlated with the amount of oligonucleotides detected, since they remain trapped on the recognition sites of the biosensor.

Based on the previously presented studies, we estimated an ideal dilution factor for the biodetection assays with cDNA samples. Although our biosensor does not present evidence for the non-specific adsorption process, it is known that very concentrated samples favor this physical phenomenon [44]. For this reason, the 1:10 dilution was chosen as the most suitable and used in our experimental protocol for the diagnosis of the BCR/ABL fusion gene in clinical samples.

As shown in Fig. 5A, a biodetection study was carried with ten cDNA samples of different patients. The biosensor presented two profiles of electrochemical response characterized by ΔR_{CT}. For the first group (columns in grey) we obtained expressive impedimetric responses with ΔR_{CT} values varying from 118.50 to 201.18 %. As expected, patients samples diagnosed with CML were included in this group. In opposition, for the second group (columns in yellow) we measured low ΔR_{CT} values ranging from 6.69 to 22.24 %. In this group, were included the patients samples after the anti-leukemia therapy. Despite being low, these impedimetric responses are significant, since the BCR and ABL constitutive genes can bind to the biorecognition probe. In view of the results presented, we highlight the potential of our biosensor to discriminate between positive and negative leucemia samples.

To assess the authenticity of the biodetection signal, we decided to evaluate the bioactivity of the sensor system with cDNA samples of non-leukemic patients containing the genome of HCV, *C. albicans*, *M. tuberculosis*, *S. mansoni* and *E. coli*. The Fig. 5B shows that the responses of the biosensor before and after the biodetection assay are similar. In relation to the ΔR_{CT}, were obtained values ranging from 2.75 to 16.92 % (inset in the Fig. 5B). Thus, we note that the genome of different species do not interfere in the analytical performance of

the biosensor. In addition, the biosensor shown to be highly specific and selective for the BCR/ABL fusion gene.

4. Conclusions

In summary, we developed a new electrochemical DNA biosensor for the ultrasensitive and label-free detection of the BCR/ABL fusion gene in leukemia patient samples. Through a series of covalent linkages, the nanostructured platform based on Cys, cMWCNTs and ZnONps/NH_2 was constructed on a gold surface and showed unique properties for the sensing interface. We highlight the highly organized molecular structure, high surface area in relation to the volume, presence of free chemical groups for the anchoring of biomolecules and other nanomaterials, self-amplification of the electrochemical signal and, mainly, maintenance of the conformational structure and hybridization capacity of the immobilized DNA probes. Through the electrochemical characterization, was verified that the proposed sensor system is able to detect the BCR/ABL fusion gene in minimum concentrations (LOD = 6.94 aM, which to our knowledge corresponds to the lowest value described in the literature) with short detection time, response reproducibility, high specificity and selectivity. Therefore, our biosensor is a valuable tool for the clinical research of the BCR/ABL fusion gene, contributing to the early diagnosis of cancer and to the monitoring of residual disease, especially after the transplantation of bone marrow.

Acknowledgements

The authors are grateful for the support of the Brazilian National Council for Scientific and Technological Development/CNPq (grant 302885/2015-3 and 302930/2015-9), MCT/FINEP, PROPESQ/UFPE and FACEPE-PPSUS-APQ-0040-4.00/13.

Formatting of funding sources

This research did not receive any specific grant from funding agencies in the public, commercial, or not-for-profit sectors.

Competing interests

The authors declare that there is no competing interests for publication of this paper.

Figure Captions

Figure 1. Schematic representation of the APTES functionalized ZnO nanoparticle (A) and fabrication process of the biosensor (B).

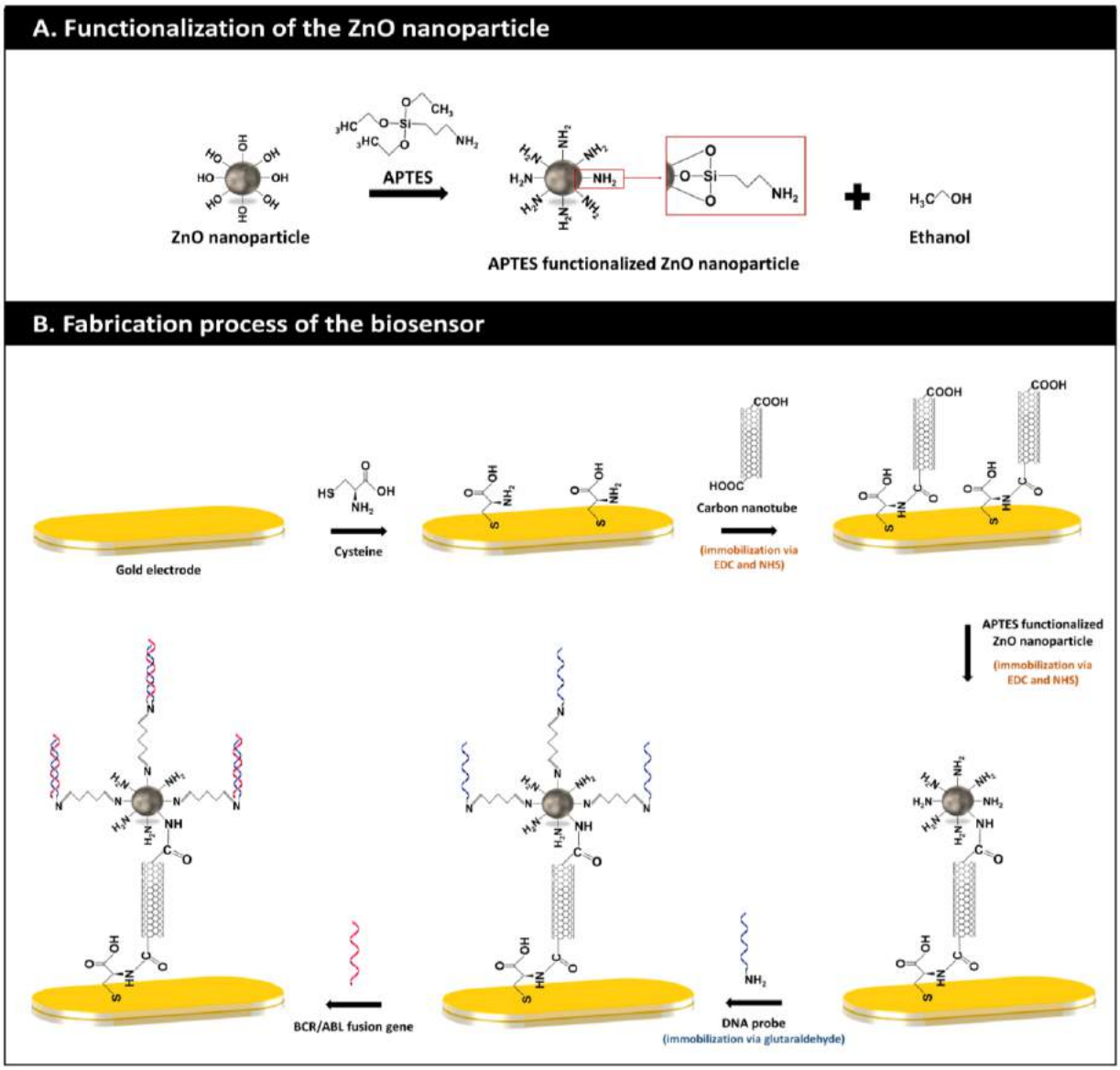

Figure 2. 3D e 2D AFM images for the electrode modified with Cys (A), Cys-cMWCNTs (B), Cys-cMWCNTs-ZnONps/NH_2 (C), Cys-cMWCNTs-ZnONps/NH_2-probe-BSA (D), Cys-cMWCNTs-ZnONps/NH_2-probe-BSA-CML positive sample (E) and Cys-cMWCNTs-ZnONps/NH_2-probe-BSA-CML negative sample (F). Scan area of 5 µm × 5 µm.

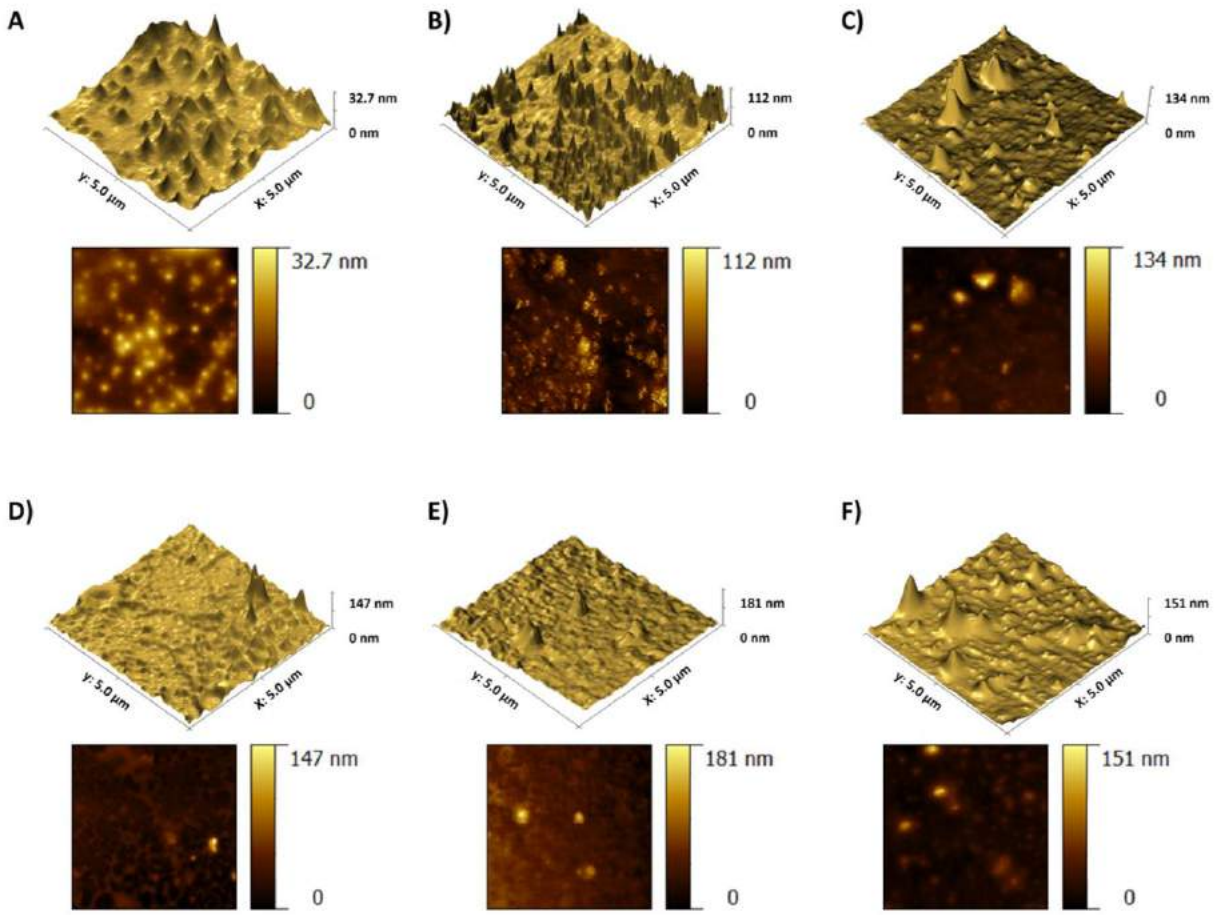

Figure 3. Cyclic voltammograms (A) and impedance spectra (B) for each step of assembly of the biosensor. Inset: Equivalent circuit used to fit the impedance measurements.

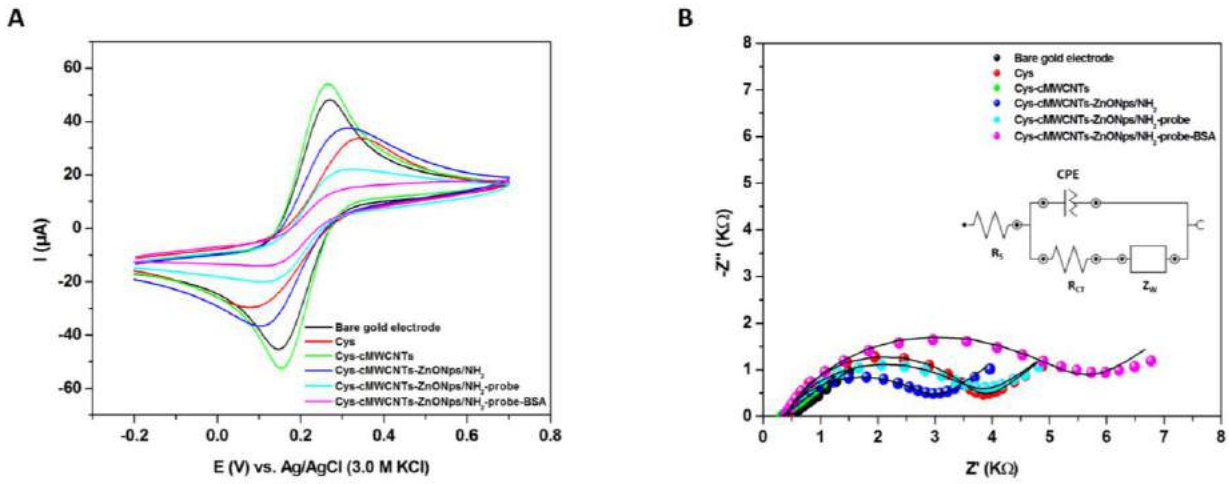

Figure 4. Cyclic voltammograms (A) and impedance spectra (B) for the biosensor exposed to different concentrations of recombinant plasmids containing the BCR/ABL fusion gene (DNA target – 6.94, 694, 6940, 69400 and 694000 aM). Inset: Calibration curve of the biosensor.

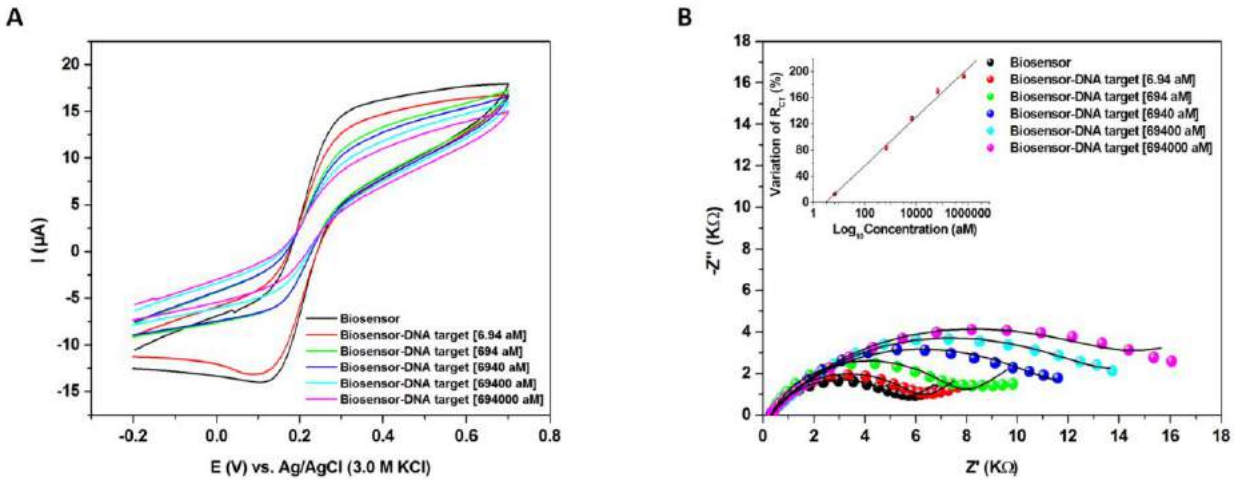

Figure 5. ΔR_{CT} values for the biodetection assay with cDNA samples of different leucemia patients (A). Impedimetric response for the study with cDNA sample of leukemia patient and cDNA samples of non-leukemic patients containing the genome of HCV, *C. albicans*, *M. tuberculosis*, *S. mansoni* and *E. coli* (B). Inset: ΔR_{CT} (%) values obtained from the assays with positive leukemia sample and negative leukemia samples containing the genome of different species. Three replicates for each experimental condition were used; experimental values are described as the mean values ± their half-deviation.

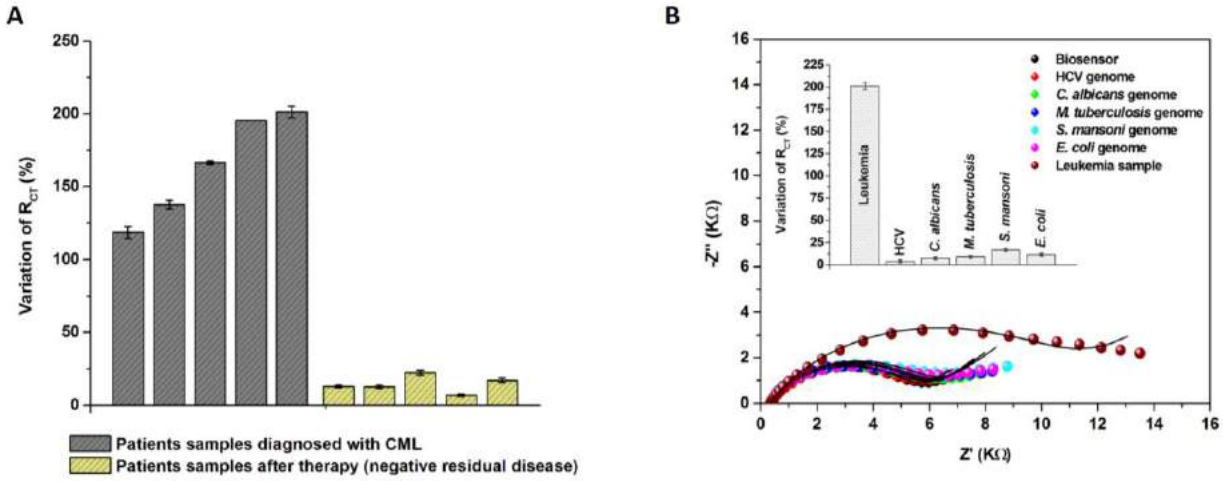

References

[1] K.M. Badger-Brown, L.C. Gillis, M.L. Bailey, J.M. Penninger, D.L. Barber, CBL-B is required for leukemogenesis mediated by BCR-ABL through negative regulation of bone marrow homing, Leukemia, 27(2013) 1146-54.
[2] L. Wang, E. Hua, M. Liang, C. Ma, Z. Liu, S. Sheng, et al., Graphene sheets, polyaniline and AuNPs based DNA sensor for electrochemical determination of BCR/ABL fusion gene with functional hairpin probe, Biosensors and Bioelectronics, 51(2014) 201-7.
[3] M.I. Del Principe, F. Buccisano, L. Maurillo, G. Sconocchia, M. Cefalo, M.I. Consalvo, et al., Minimal Residual Disease in Acute Myeloid Leukemia of Adults: Determination, Prognostic Impact and Clinical Applications, Mediterranean Journal of Hematology and Infectious Diseases, 8(2016) e2016052.
[4] T. Szczepanski, Why and how to quantify minimal residual disease in acute lymphoblastic leukemia?, Leukemia, 21(2007) 622-6.
[5] P.J. Sung, S.M. Luger, Minimal Residual Disease in Acute Myeloid Leukemia, Current Treatment Options in Oncology, 18(2017) 1.
[6] J.J.M. van Dongen, V.H.J. van der Velden, M. Brüggemann, A. Orfao, Minimal residual disease diagnostics in acute lymphoblastic leukemia: need for sensitive, fast, and standardized technologies, Blood, 125(2015) 3996-4009.
[7] A. Bennour, A. Saad, H. Sennana, Chronic myeloid leukemia: Relevance of cytogenetic and molecular assays, Critical Reviews in Oncology/Hematology, 97(2016) 263-74.
[8] A. Sharma, C.M. Pandey, G. Sumana, U. Soni, S. Sapra, A.K. Srivastava, et al., Chitosan encapsulated quantum dots platform for leukemia detection, Biosensors and Bioelectronics, 38(2012) 107-13.
[9] I.A.M. Frias, K.Y.P.S. Avelino, R.R. Silva, C.A.S. Andrade, M.D.L. Oliveira, Trends in Biosensors for HPV: Identification and Diagnosis, Journal of Sensors, 2015(2015) 16.
[10] M.I. Pividori, A. Merkoçi, S. Alegret, Electrochemical genosensor design: immobilisation of oligonucleotides onto transducer surfaces and detection methods, Biosensors and Bioelectronics, 15(2000) 291-303.
[11] M.K. Patel, M.A. Ali, M. Zafaryab, V.V. Agrawal, M.M.A. Rizvi, Z.A. Ansari, et al., Biocompatible nanostructured magnesium oxide-chitosan platform for genosensing application, Biosensors and Bioelectronics, 45(2013) 181-8.
[12] F. Lucarelli, S. Tombelli, M. Minunni, G. Marrazza, M. Mascini, Electrochemical and piezoelectric DNA biosensors for hybridisation detection, Analytica Chimica Acta, 609(2008) 139-59.
[13] A. Liu, K. Wang, S. Weng, Y. Lei, L. Lin, W. Chen, et al., Development of electrochemical DNA biosensors, TrAC Trends in Analytical Chemistry, 37(2012) 101-11.
[14] S. Iijima, Helical Microtubules of Graphitic Carbon, Nature, 354(1991) 56.
[15] W. Yang, K.R. Ratinac, S.P. Ringer, P. Thordarson, J.J. Gooding, F. Braet, Carbon Nanomaterials in Biosensors: Should You Use Nanotubes or Graphene?, Angewandte Chemie International Edition, 49(2010) 2114-38.
[16] K. Balasubramanian, M. Burghard, Chemically Functionalized Carbon Nanotubes, Small, 1(2005) 180-92.
[17] C.A.S. Andrade, J.M. Nascimento, I.S. Oliveira, C.V.J. de Oliveira, C.P. de Melo, O.L. Franco, et al., Nanostructured sensor based on carbon nanotubes and clavanin A for bacterial detection, Colloids and Surfaces B: Biointerfaces, 135(2015) 833-9.
[18] N. Hernández-Ibáñez, L. García-Cruz, V. Montiel, C.W. Foster, C.E. Banks, J. Iniesta, Electrochemical lactate biosensor based upon chitosan/carbon nanotubes modified screen-printed graphite electrodes for the determination of lactate in embryonic cell cultures, Biosensors and Bioelectronics, 77(2016) 1168-74.
[19] H.S. Magar, M.E. Ghica, M.N. Abbas, C.M.A. Brett, A novel sensitive amperometric choline biosensor based on multiwalled carbon nanotubes and gold nanoparticles, Talanta, 167(2017) 462-9.

[20] C.B. Jacobs, M.J. Peairs, B.J. Venton, Review: Carbon nanotube based electrochemical sensors for biomolecules, Analytica Chimica Acta, 662(2010) 105-27.
[21] C.-M. Tîlmaciu, M.C. Morris, Carbon nanotube biosensors, Frontiers in Chemistry, 3(2015) 59.
[22] Z. Zhu, L. Garcia-Gancedo, A.J. Flewitt, H. Xie, F. Moussy, W.I. Milne, A Critical Review of Glucose Biosensors Based on Carbon Nanomaterials: Carbon Nanotubes and Graphene, Sensors (Basel, Switzerland), 12(2012) 5996-6022.
[23] S. Kumar, W. Ahlawat, R. Kumar, N. Dilbaghi, Graphene, carbon nanotubes, zinc oxide and gold as elite nanomaterials for fabrication of biosensors for healthcare, Biosensors and Bioelectronics, 70(2015) 498-503.
[24] T.T.X. Hang, N.T. Dung, T.A. Truc, N.T. Duong, B. Van Truoc, P.G. Vu, et al., Effect of silane modified nano ZnO on UV degradation of polyurethane coatings, Progress in Organic Coatings, 79(2015) 68-74.
[25] N. Rabin Nurun, J. Morshed, H. Akhter, S. Islam Md, A. Hossain Md, M. Elias, et al., Surface Modification of the ZnO Nanoparticles with γ-Aminopropyltriethoxysilane and Study of Their Photocatalytic Activity, Optical Properties and Antibacterial Activities, International Journal of Chemical Reactor Engineering2016, p. 785.
[26] F. Grasset, N. Saito, D. Li, D. Park, I. Sakaguchi, N. Ohashi, et al., Surface modification of zinc oxide nanoparticles by aminopropyltriethoxysilane, Journal of Alloys and Compounds, 360(2003) 298-311.
[27] E.A.L.V. Marques, L. Neves, T.C. Fonseca, M.M. Lins, F. Pedrosa, N. Lucena-Silva, Molecular Findings in Childhood Leukemia in Brazil: High Frequency of MLL-ENL Fusion/t(11;19) in Infant Leukemia, Journal of Pediatric Hematology/Oncology, 33(2011) 470-4.
[28] D.M.N. Luna, K.Y.P.S. Avelino, M.T. Cordeiro, C.A.S. Andrade, M.D.L. Oliveira, Electrochemical immunosensor for dengue virus serotypes based on 4-mercaptobenzoic acid modified gold nanoparticles on self-assembled cysteine monolayers, Sensors and Actuators B: Chemical, 220(2015) 565-72.
[29] Y. Wan, W. Deng, Y. Su, X. Zhu, C. Peng, H. Hu, et al., Carbon nanotube-based ultrasensitive multiplexing electrochemical immunosensor for cancer biomarkers, Biosensors and Bioelectronics, 30(2011) 93-9.
[30] A. Umar, M.M. Rahman, M. Vaseem, Y.-B. Hahn, Ultra-sensitive cholesterol biosensor based on low-temperature grown ZnO nanoparticles, Electrochemistry Communications, 11(2009) 118-21.
[31] J. Breczko, E. Regulska, A. Basa, M. Baran, K. Winkler, M.E. Plonska-Brzezinska, Three-Component EC-SPR Biosensor Based on Graphene Oxide, SiO2 and Gold Nanoparticles in NADH Determination, ECS Journal of Solid State Science and Technology, 5(2016) M3018-M25.
[32] B.M. Keyes, L.M. Gedvilas, X. Li, T.J. Coutts, Infrared spectroscopy of polycrystalline ZnO and ZnO:N thin films, Journal of Crystal Growth, 281(2005) 297-302.
[33] I.A. Rahman, M. Jafarzadeh, C.S. Sipaut, Synthesis of organo-functionalized nanosilica via a co-condensation modification using γ-aminopropyltriethoxysilane (APTES), Ceramics International, 35(2009) 1883-8.
[34] S. Chandra, S. Mehta, S. Nigam, D. Bahadur, Dendritic magnetite nanocarriers for drug delivery applications, New Journal of Chemistry, 34(2010) 648-55.
[35] C.Y. Yang, S.-M. Chen, S. Palanisamy, Simultaneous Electrochemical Determination of Dopamine, Uric acid, Tryptophan on Electropolymerized Aminothiazole and Gold nanoparticles Modified Carbon nanotubes Modified Electrode, International Journal of Electrochemical Science, 11(2016) 11.
[36] K. Arora, A. Chaubey, R. Singhal, R.P. Singh, M.K. Pandey, S.B. Samanta, et al., Application of electrochemically prepared polypyrrole–polyvinyl sulphonate films to DNA biosensor, Biosensors and Bioelectronics, 21(2006) 1777-83.
[37] A.M. Oliveira Brett, A.-M. Chiorcea, Atomic Force Microscopy of DNA Immobilized onto a Highly Oriented Pyrolytic Graphite Electrode Surface, Langmuir, 19(2003) 3830-9.
[38] A. Sassolas, B.D. Leca-Bouvier, L.J. Blum, DNA Biosensors and Microarrays, Chemical Reviews, 108(2008) 109-39.

[39] T. Wink, S. J. van Zuilen, A. Bult, W. P. van Bennekom, Self-assembled Monolayers for Biosensors, Analyst, 122(1997) 43R-50R.
[40] H.-P. Wu, C.-C. Huang, T.-L. Cheng, W.-L. Tseng, Sodium hydroxide as pretreatment and fluorosurfactant-capped gold nanoparticles as sensor for the highly selective detection of cysteine, Talanta, 76(2008) 347-52.
[41] E.E. Ferapontova, Hybridization Biosensors Relying on Electrical Properties of Nucleic Acids, Electroanalysis, 29(2017) 6-13.
[42] A. Benvidi, A. Dehghani Firouzabadi, M. Dehghan Tezerjani, S.M. Moshtaghiun, M. Mazloum-Ardakani, A. Ansarin, A highly sensitive and selective electrochemical DNA biosensor to diagnose breast cancer, Journal of Electroanalytical Chemistry, 750(2015) 57-64.
[43] Y. Ye, J. Gao, H. Zhuang, H. Zheng, H. Sun, Y. Ye, et al., Electrochemical gene sensor based on a glassy carbon electrode modified with hemin-functionalized reduced graphene oxide and gold nanoparticle-immobilized probe DNA, Microchimica Acta, 184(2017) 245-52.
[44] K.Y.P.S. Avelino, I.A.M. Frias, N. Lucena-Silva, R.G. Gomes, C.P. de Melo, M.D.L. Oliveira, et al., Attomolar electrochemical detection of the BCR/ABL fusion gene based on an amplifying self-signal metal nanoparticle-conducting polymer hybrid composite, Colloids and Surfaces B: Biointerfaces, 148(2016) 576-84.
[45] G.S. Santos, C.A.S. Andrade, I.S. Bruscky, L.B. Wanderley, F.L. Melo, M.D.L. Oliveira, Impedimetric nanostructured genosensor for detection of schistosomiasis in cerebrospinal fluid and serum samples, Journal of Pharmaceutical and Biomedical Analysis, 137(2017) 163-9.
[46] A. Gutiérrez, E.N. Primo, M. Eguílaz, C. Parrado, M.D. Rubianes, G.A. Rivas, Quantification of neurotransmitters and metabolically related compounds at glassy carbon electrodes modified with bamboo-like carbon nanotubes dispersed in double stranded DNA, Microchemical Journal, 130(2017) 40-6.

CAPÍTULO 7

7 CONCLUSÕES

- Dois biossensores eletroquímicos baseados em a) AuNpsPANI e b) Cys-cMWCNT-ZnONp/NH_2 foram construídos com sucesso para a detecção ultrassensível do oncogene quimérico BCR/ABL.
- As medidas obtidas a partir da VC e EIE, utilizando o par redox $Fe(CN)^{-3/-4}$ como sonda eletroquímica, possibilitaram a caracterização e compreensão dos processos físico-químicos relacionados à cada etapa de montagem dos biossensores.
- O compósito híbrido AuNpsPANI apresentou excelentes propriedades para a construção de plataformas nanoestruturadas biossensíveis. Através do processo de quimissorção, uma camada automontada de AuNpsPANI foi facilmente obtida sobre uma superfície de ouro. Enquanto as nanopartículas aumentaram a área eletroquimicamente ativa e mediaram a transferência de elétrons entre a interface eletrodo/solução, o polímero conjugado possibilitou a adsorção física das sondas de DNA por meio de interações eletrostáticas. Em adição, destaca-se que o biossensor baseado em AuNpsPANI foi construído de forma simples, reprodutível e em um curto período de tempo (12 minutos).
- A nova plataforma de interfaceamento baseada em Cys-cMWCNT-ZnONp/NH_2 foi elaborada de maneira efetiva através de uma série de ligações covalentes sobre um substrato de ouro. Esta apresentou propriedades únicas para a construção de sistemas de biodetecção. Ressalta-se a presença de grupos químicos livres para a ancoragem de biomoléculas e a capacidade de amplificar o sinal eletroquímico.
- Através de ensaios de bioatividade com amostras plasmidiais, foi constatado que os dois biossensores desenvolvidos apresentam a capacidade de reconhecimento bioespecífico com elevada sensibilidade e seletividade. Estes biodispositivos identificaram o oncogene quimérico BCR/ABL em concentrações mínimas na ordem de atomolar. No nosso conhecimento, os limites de detecção estimados foram os menores valores descritos na literatura até o momento para o diagnóstico do oncogene quimérico BCR/ABL. Além disso, as respostas analíticas foram obtidas rapidamente, em um intervalo de 15 minutos e sem marcadores adicionais.
- Os biossensores também demonstraram habilidade para o diagnóstico do oncogene quimérico BCR/ABL em amostras clínicas de pacientes com leucemia (amostras de

cDNA). Além disso, foram capazes de diferenciar as amostras positivas e negativas para LMC.

- Apesar de ambos os biossensores apresentarem elevada reprodutibilidade, seletividade, especificidade e rápido tempo de resposta para a identificação do oncogene quimérico BCR/ABL, é importante ressaltar que o biossensor baseado em Cys-cMWCNT-ZnONp/NH_2 demonstrou sensibilidade superior com um limite de detecção de 6,94 aM.
- Portanto, os biossensores descritos nesta dissertação podem ser considerados ferramentas promissoras para a pesquisa clínica e laboratorial do oncogene quimérico BCR/ABL, contribuindo para o diagnóstico precoce do câncer e para o monitoramento de níveis mínimos da doença, especialmente, após o transplante de medula óssea.

CAPÍTULO 8

8 PERSPECTIVAS

Após a construção e caracterização eletroquímica dos biossensores constituídos por a) AuNpsPANI e b) Cys-cMWCNT-ZnONp/NH_2, pode-se destacar como perspectivas a realização de ensaios de validação analítica. Estes poderão contemplar os estudos de estabilidade de armazenamento, reusabilidade e a ação de interferentes sobre a resposta eletroquímica. Ao comprovar a capacidade de reconhecimento bioespecífico frente à amostras plasmidiais e amostras de cDNA, novos protocolos experimentais poderão ser desenvolvidos para a realização de testes de biodetecção em amostras clínicas sem amplificação prévia por PCR. Sabe-se que, um dos desafios para o diagnóstico do oncogene quimérico BCR/ABL neste tipo de amostra é o baixo número de cópias de DNA em relação, por exemplo, a grande quantidade de moléculas de RNA transcritas para a tradução proteica. No entanto, este obstáculo é superado ao considerar os baixos limites de detecção dos biossensores desenvolvidos. Por fim, as plataformas nanoestruturadas propostas nesta dissertação poderão ser utilizadas no desenvolvimento de outros biossensores com aplicações distintas, como a identificação de microrganismos e o diagnóstico de outras neoplasias malignas, doenças crônico-degenerativas, negligenciadas ou cardiovasculares.

CAPÍTULO 9

9 APÊNDICES

9.1 Apêndice A – Material suplementar referente ao artigo 1

Artigo publicado na revista *Colloids and Surfaces B: Biointerfaces*

Attomolar electrochemical detection of the BCR/ABL fusion genebased on an amplifying self-signal metal nanoparticle-conductingpolymer hybrid composite

Supplementary material

ELECTROCHEMICAL DETECTION IN ATOMOLAR OF THE BCR/ABL FUSION GENE BASED ON A SELF-SIGNAL AMPLIFYING METAL NANOPARTICLE-CONDUCTING POLYMER HYBRID COMPOSITE

Karen Y.P.S. Avelino[1], Isaac Aaron Morales[2], Norma Lucena-Silva[3,4], Renan Garcia Gomes[3,4], Celso P. de Melo[5], Maria D.L. Oliveira[1,2], César A.S. Andrade[1,2*]

[1]Programa de Pós-Graduação em Bioquímica e Fisiologia, Universidade Federal de Pernambuco, 50670-901 Recife, PE, Brasil.

[2]Programa de Pós-Graduação em Inovação Terapêutica, Universidade Federal de Pernambuco, 50670-901 Recife, PE, Brasil.

[3]Centro de Pesquisas Aggeu Magalhães, Fundação Osvaldo Cruz (Fiocruz), 50670-420 Recife, PE, Brasil.

[4]Laboratório de Biologia Molecular, Departamento de Oncologia Pediátrica, Instituto de Medicina Integral Professor Fernando Figueira (IMIP), 50070-550 Recife, PE, Brasil.

[5]Departamento de Física, Universidade Federal de Pernambuco, 50670-901 Recife, PE, Brasil.

*To whom correspondence should be addressed.

C.A.S. Andrade, Departamento de Bioquímica, UFPE, 50670-901, Recife, PE, Brazil

Phone: +55-81-2126.8450; Fax: +55-81-2126.8547

E-mail: csrandrade@gmail.com

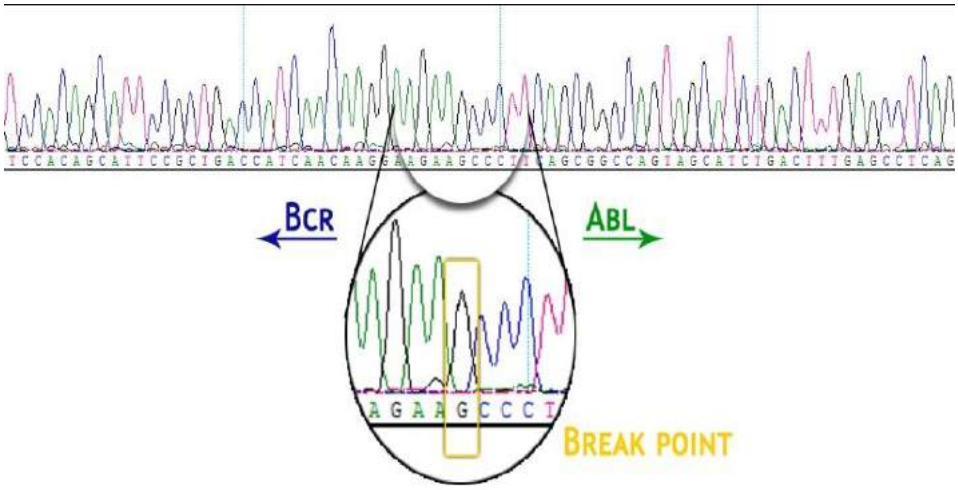

Figure S1. Electropherogram showing the sequencing of the BCR/ABL oncogene and fusion point (break point).

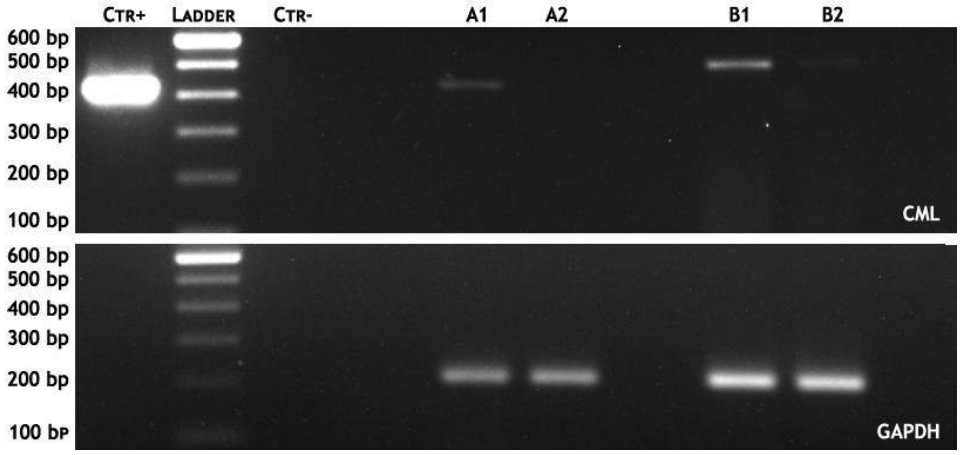

Figure S2. Polyacrylamide gel electrophoresis of PCR products (cDNA). The lanes from left to right represent: positive control for the BCR/ABL fusion gene (CTR+); DNA marker (the brands from up to down: 600, 500, 400, 300, 200 and 100 bp); negative control for the BCR/ABL fusion gene (CTR-); A1 patient sample with CML positive diagnosis; A2 patient sample with negative residual disease; B1 patient sample with CML positive diagnosis; B2 patient sample with weakly positive residual disease. The glyceraldehyde-3-phosphate dehydrogenase (GAPDH) was used as a loading control.

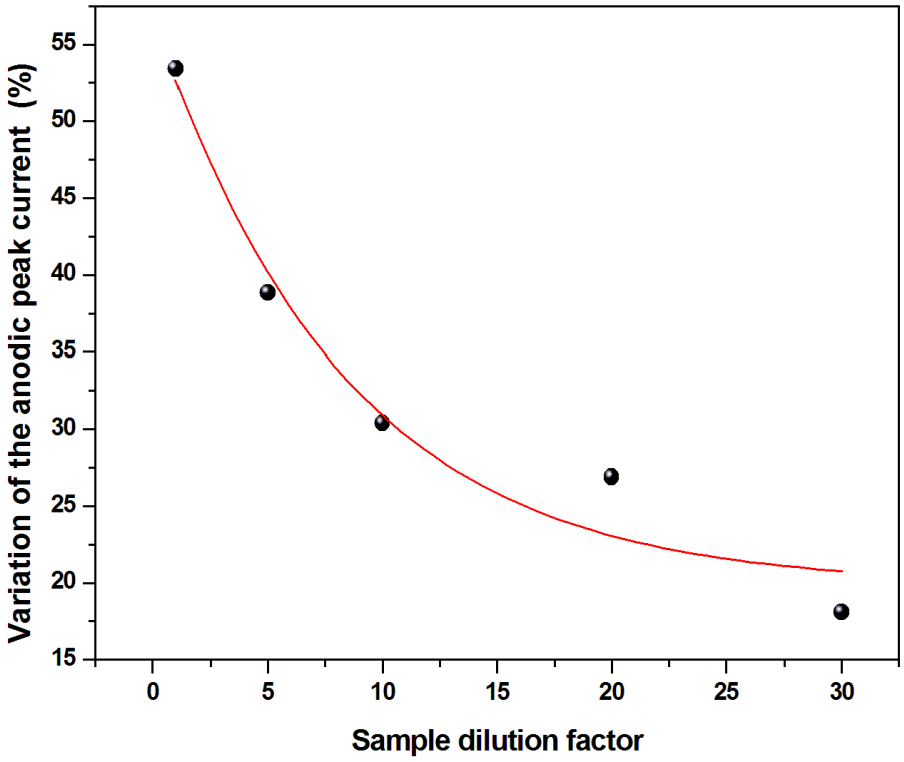

Figure S3. ΔI (%) of the genosensor after exposure to different dilutions of cDNA samples.

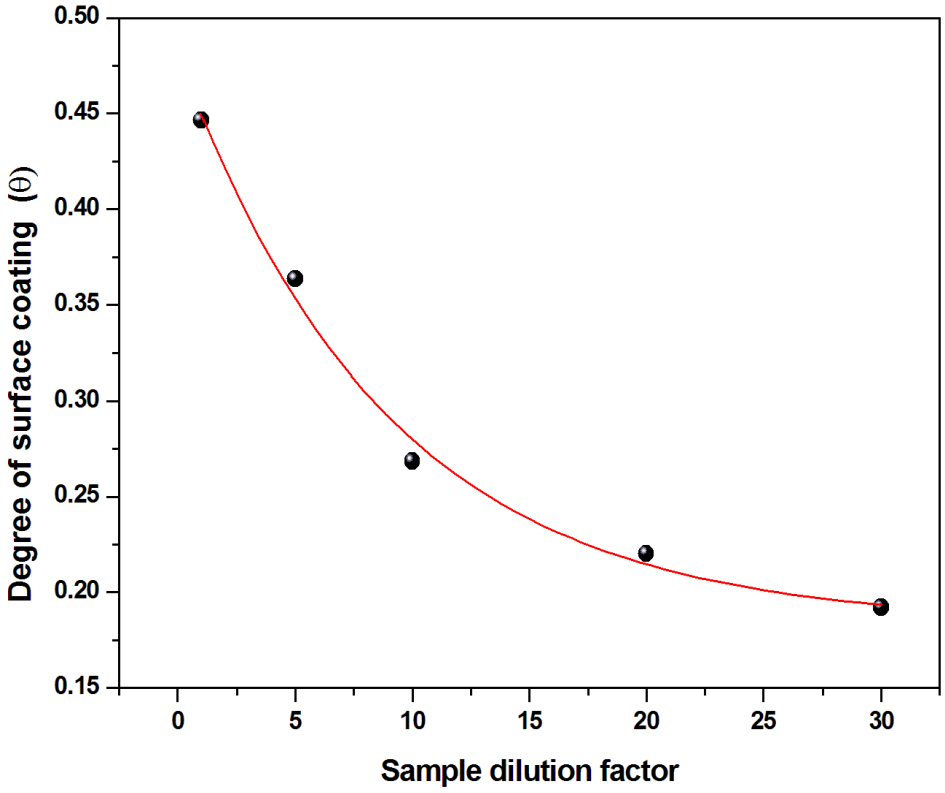

Figure S4. Θ values as a function of the different dilutions of cDNA sample.

Table S1. Amperometric anodic shift for the genosensor before and after the hybridization with DNA target, non-complementary DNA sequence and cDNA sample of leukemia patient.

Modified electrode	DNA target (fM)	Before ($1/I_b$ μA^{-1})	After ($1/I_a$ μA^{-1})	ΔI (%)
Genosensor	-	0.0569	-	-
Genosensor-DNA target	0.0694	-	0.0911	60.10
Genosensor-DNA target	0.694	-	0.1334	134.44
Genosensor-DNA target	6.94	-	0.1790	214.58
Genosensor-DNA target	69.4	-	0.2444	329.52
Genosensor-DNA target	694	-	1.5410	2608.26
Genosensor-Non complementary DNA	6.94×10^3	-	0.0608	6.85
	Sample dilution factor			
Genosensor	-	0.0569	-	-
Genosensor-cDNAsample	1:1	-	0.0873	53.43
Genosensor-cDNAsample	1:5	-	0.0790	38.84
Genosensor-cDNAsample	1:10	-	0.0742	30.40
Genosensor-cDNAsample	1:20	-	0.0722	26.89
Genosensor-cDNAsample	1:30	-	0.0672	18.10

Genosensor = AuNpsPANI-DNA probe

Table S2. Values of the equivalent circuit elements obtained from the fitting of the impedance results derived from the biodetection in plasmid samples and cDNA samples. Three replicates for each experimental condition were used; experimental values are reported as the mean values ± their half-deviation.

Modified electrode	DNA target (fM)	R_S (Ω)	C_{dl}(μF)	R_{CT} (kΩ)	W	N
Baregoldelectrode	-	514.66 ± 25.42	115.66 ± 14.29	0.22 ± 0.01	517.33 ± 29.50	0.47 ± 0.02
AuNpsPANI	-	498.66 ± 2.30	5.34 ± 1.36	2.51 ± 0.10	600.33 ± 86.17	0.75 ± 0.06
AuNpsPANI-DNA probe	-	565 ± 2.62	2.20 ± 0.05	4.71 ± 0.11	643 ± 2.10	0.870 ± 0.04
Genosensor-DNA target	0.0694	528.66 ± 0.57	1.25 ± 0.01	6.82 ± 0.35	412.66 ± 2.30	0.775 ± 0
Genosensor-DNA target	0.694	496.66 ± 0.57	1.34 ± 0	12.83 ± 0.35	410 ± 3.60	0.752 ± 0.0005
Genosensor-DNA target	6.94	477 ± 5.29	1.45 ± 0.02	22.36 ± 0.30	606.33 ± 0.57	0.727 ± 0.001
Genosensor-DNA target	69.4	423.66 ± 6.02	1.52 ± 0.02	30.73 ± 0.45	2.09 ± 0.17	0.711 ± 0.002
Genosensor-DNA target	694	616.33 ± 0.57	1.09 ± 0	44.66 ± 1.006	367 ± 14.42	0.764 ± 0
Genosensor-Non complementary DNA	6.94×10^3	392 ± 0.58	1.99 ± 0.03	5.78 ± 0.18	706 ± 0.62	0.829 ± 0.001
	Sample dilution factor					
Genosensor-cDNAsample	1:1	563 ± 0.46	3.04 ± 0.01	8.51 ± 0.32	671 ± 3.1	0.83 ± 0.001
Genosensor-cDNAsample	1:5	573 ± 0.56	2.77 ± 0.02	7.40 ± 0.26	666 ± 4.2	0.866 ± 0.002
Genosensor-cDNAsample	1:10	566 ± 0.57	2.90 ± 0.01	6.44 ± 0.20	646 ± 5.5	0.85 ± 0.001
Genosensor-cDNAsample	1:20	626 ± 0.54	3.74 ± 0.03	6.04 ± 0.16	633 ± 5.1	0.839 ± 0.001
Genosensor-cDNAsample	1:30	584 ± 0.57	2.98 ± 0.01	5.83 ± 0.18	551 ± 4.3	0.849 ± 0.002

Genosensor = AuNpsPANI-DNA probe

9.2 Apêndice B – Material suplementar referente ao artigo 2

Artigo a ser submetido à revista *Sensors and Actuators B: Chemical*

Fabrication of a novel nanostructured platform based on aminopropyltriethoxysilane-functionalized zinc oxide nanoparticles and carbon nanotubes for impedimetric monitoring of the BCR/ABL fusion gene

Supplementary material

FABRICATION OF A NOVEL NANOSTRUCTURED PLATFORM BASED ON AMINOPROPYLTRIETHOXYSILANE-FUNCTIONALIZED ZINC OXIDE NANOPARTICLES AND CARBON NANOTUBES FOR IMPEDIMETRIC MONITORING OF THE BCR/ABL FUSION GENE

Karen Y.P.S. Avelino[1], Isaac Aaron Morales[2], Norma Lucena-Silva[3,4], César A.S. Andrade[1,2], Maria D.L. Oliveira[1,2]*

[1]Programa de Pós-Graduação em Bioquímica e Fisiologia, Universidade Federal de Pernambuco, 50670-901 Recife, PE, Brasil.

[2]Programa de Pós-Graduação em Inovação Terapêutica, Universidade Federal de Pernambuco, 50670-901 Recife, PE, Brasil.

[3]Centro de Pesquisas Aggeu Magalhães, Fundação Osvaldo Cruz (Fiocruz), 50670-420 Recife, PE, Brasil.

[4]Laboratório de Biologia Molecular, Departamento de Oncologia Pediátrica, Instituto de Medicina Integral Professor Fernando Figueira (IMIP), 50070-550 Recife, PE, Brasil.

*To whom correspondence should be addressed.

Maria D.L. Oliveira, Departamento de Bioquímica, UFPE, 50670-901, Recife, PE, Brazil

Phone: +55-81-2126.8450; Fax: +55-81-2126.8547

E-mail: m_danielly@yahoo.com.br

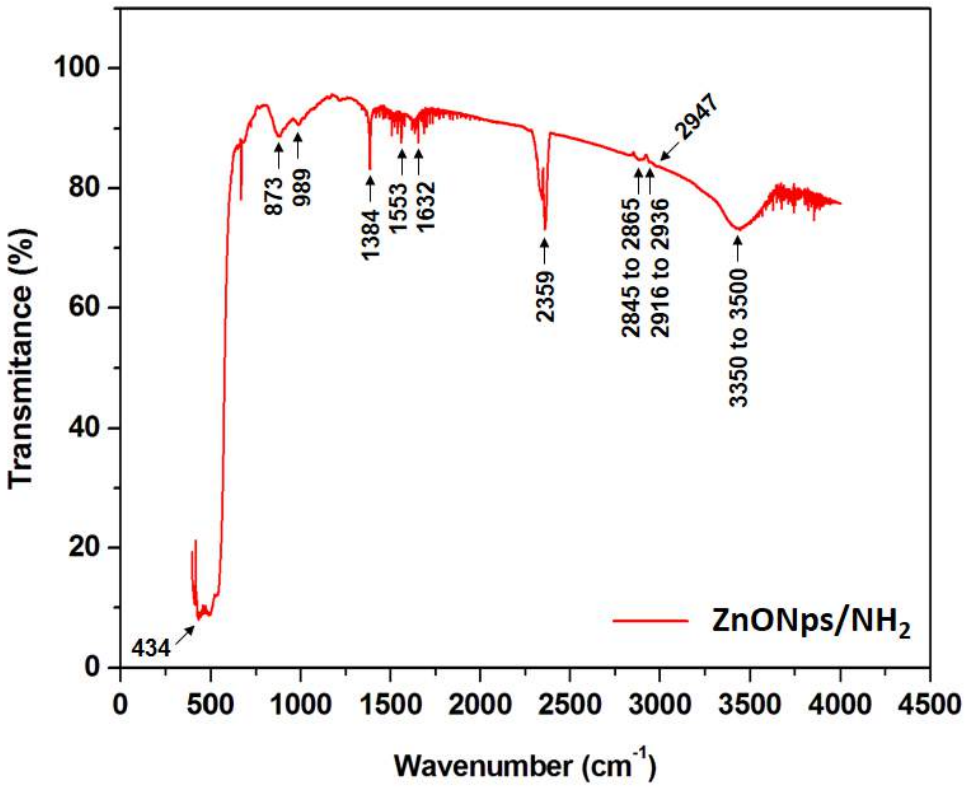

Figure S1. FTIR spectrum recorded for the ZnONps functionalized with APTES (ZnONps/NH_2) in the range of 400 to 4000 cm^{-1}.

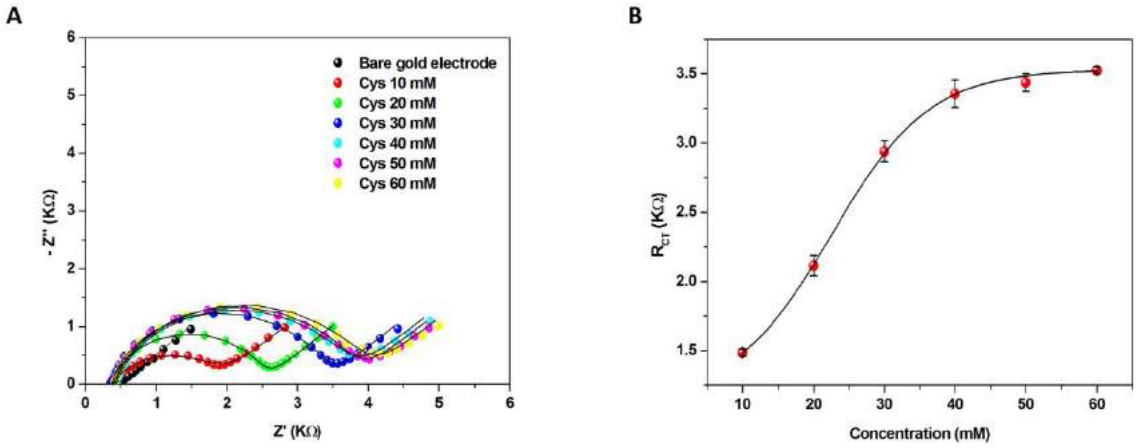

Figure S2. Impedance spectra (A) and R_{CT} values (B) for the self-assembled Cys layers at different concentrations (10, 20, 30, 40, 50 e 60 mM). Three replicates for each experimental condition were used; experimental values are described as the mean values ± their half-deviation.

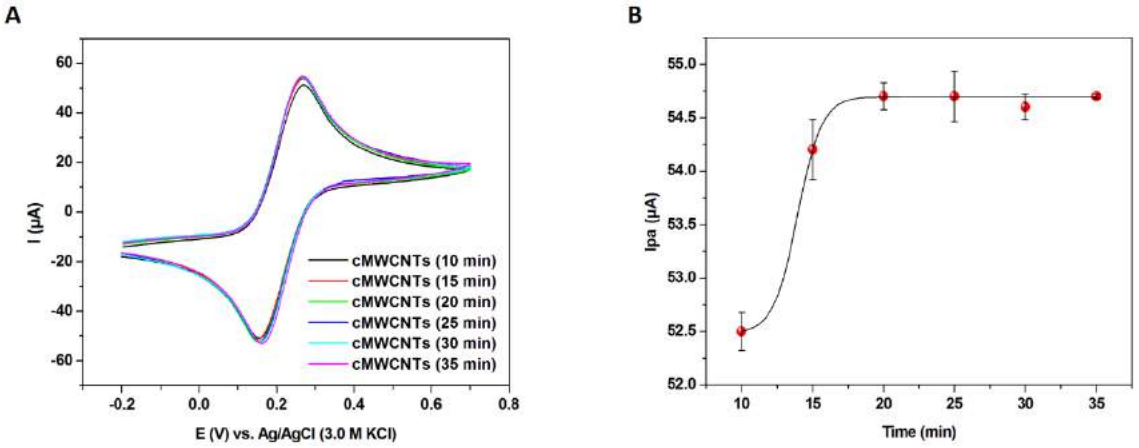

Figure S3. Cyclic voltammograms (A) and anodic peak currents (Ipa) (B) for different incubation times of the cMWCNTs (10, 15, 20, 25, 30 and 35 minutes). Three replicates for each experimental condition were used; experimental values are described as the mean values ± their half-deviation.

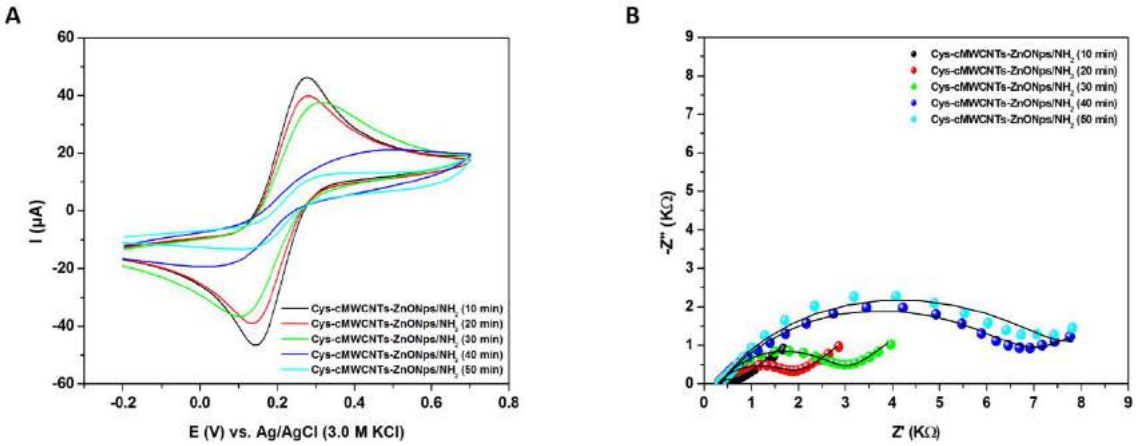

Figure S4. Cyclic voltammograms (A) and impedance spectra (B) for different incubation times of the ZnONps/NH_2.

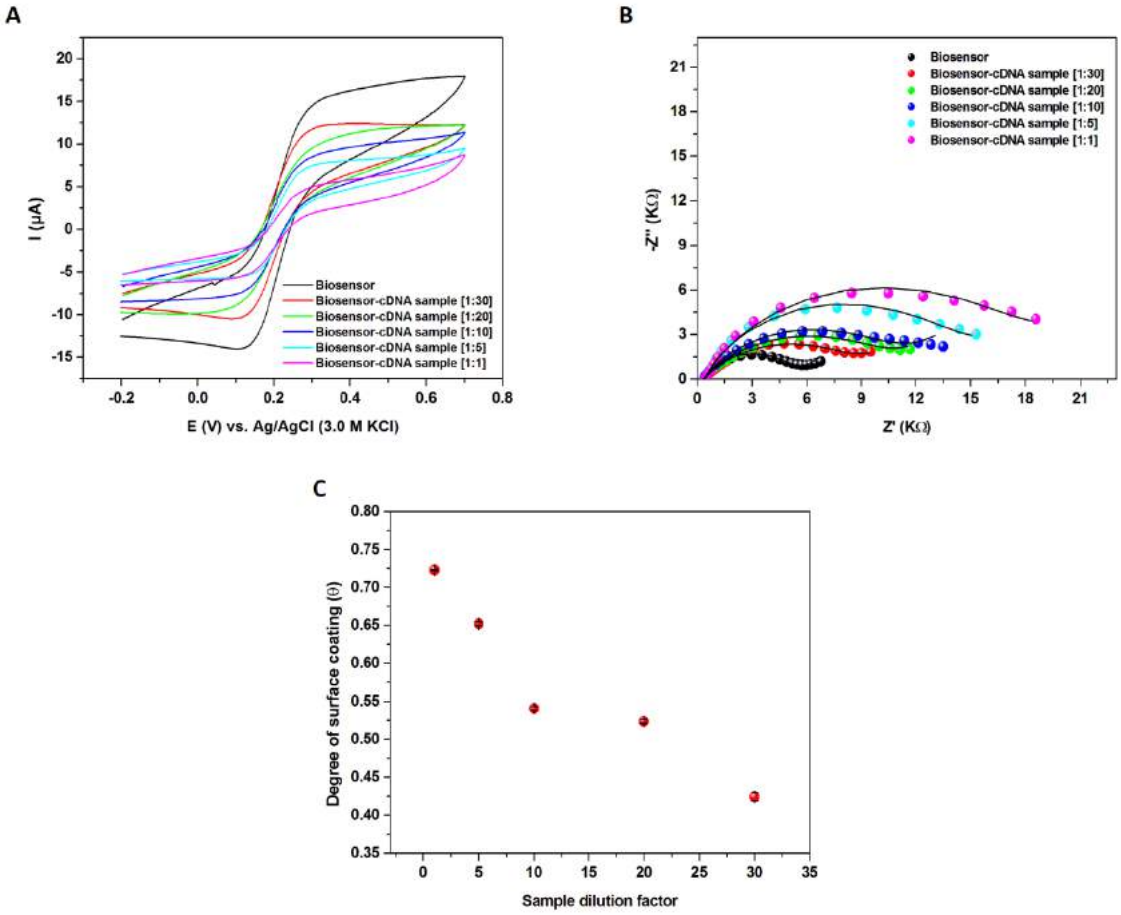

Figure S5. Cyclic voltammograms (A), impedance spectra (B) and Θ values (C) for the biosensor after exposure to different dilutions of cDNA samples of leukemia patient (sample dilution factors – 1:1, 1:5, 1:10, 1:20 and 1:30). Three replicates for each experimental condition were used; experimental values are described as the mean values ± their half-deviation.

Table S1. Values of the equivalent circuit elements obtained from the fitting of the impedance results derived the hybridization with DNA target (BCR/ABL fusion gene), non-complementary DNA sequence and cDNA samples of leukemia patient. Three replicates for each experimental condition were used; experimental values are described as the mean values ± their half-deviation.

Modified electrode	**DNA target (aM)**	**CPE (μF)**	**n**	**R_{CT} (KΩ)**	**ΔR_{CT} (%)**
Bare gold electrode	-	72.77 ± 84.46	0.59 ± 0.15	0.17 ± 0.04	-
Cys	-	2.61 ± 0.07	0.84 ± 0.03	3.36 ± 0.10	-
Cys-cMWCNTs	-	167.67 ± 6.43	0.41 ± 0.02	0.02 ± 0.01	-
Cys-cMWCNTs-ZnONps/NH_2	-	6.99 ± 0.03	0.73 ± 0.05	2.54 ± 0.01	-
Cys-cMWCNTs-ZnONps/NH_2-probe	-	6.06 ± 0.04	0.74 ± 0	3.32 ± 0.02	-
Cys-cMWCNTs-ZnONps/NH_2-probe-BSA	-	5.49 ± 0.05	0.74 ± 0.06	5.08 ± 0.21	-
Biosensor-DNA target	6.94	4.24 ± 0.05	0.76 ± 0.05	5.74 ± 0.03	12.93 ± 0.63
Biosensor-DNA target	694	2.77 ± 0.03	0.78 ± 0.01	7.22 ± 0.06	83.66 ± 3.94
Biosensor-DNA target	6 940	13.55 ± 0.07	0.63 ± 0.07	11.60 ± 0.14	128.35 ± 2.78
Biosensor-DNA target	69400	11.77 ± 0.06	0.63 ± 0	13.70 ± 0.20	169.80 ± 3.94
Biosensor-DNA target	694000	9.33 ± 0.06	0.63 ± 0	14.87 ± 0.15	192.65 ± 3.01
Biosensor-non complementary DNA	694000	7.47 ± 0.08	0.71 ± 0	5.22 ± 0.01	2.75 ± 0.20
	Sample dilution factor				
Biosensor-leukemia cDNA sample	1:1	11.83 ± 0.06	0.73 ± 0.01	18.33 ± 0.06	260.89 ± 1.14
Biosensor-leukemia cDNA sample	1:5	11.70 ±	0.76 ±	14.60 ±	187.40 ±

		0.10	0.06	0.10	1.97
Biosensor-leukemia cDNA sample	1:10	7.12 ± 0.03	0.66 ± 0	11.07 ± 0.06	117.85 ± 1.14
Biosensor-leukemia cDNA sample	1:20	11.77 ± 0.06	0.61 ± 0.06	10.67 ± 0.06	109.97 ± 1.14
Biosensor-leukemia cDNA sample	1:30	15.43 ± 0.06	0.60 ± 0.06	8.82 ± 0.08	73.69 ± 1.50
	Sample dilution factor				
Biosensor-cDNA sample (*E. coli*)	1:10	4.34 ± 0.52	0.70 ± 0.01	5.66 ± 0.08	11.42 ± 1.57
Biosensor-cDNA sample (*C. albicans*)	1:10	3.71 ± 0.47	0.71 ± 0.03	5.45 ± 0.08	7.22 ± 1.53
Biosensor-cDNA sample (*M. tuberculosis*)	1:10	3.40 ± 0.08	0.71 ± 0.03	5.53 ± 0.08	8.86 ± 1.61
Biosensor-cDNA sample (*S. mansoni*)	1:10	3.78 ± 0.13	0.71 ± 0.03	5.94 ± 0.08	16.93 ± 1.61
Biosensor-cDNA sample (HCV)	1:10	7.86 ± 0.14	0.68 ± 0.01	5.27 ± 0.08	3.67 ± 1.53

Biosensor = Cys-cMWCNTs-ZnONps/NH_2-probe-BSA

Table S2. Amperometric anodic shift for the biosensor after the hybridization with DNA target (BCR/ABL fusion gene), non-complementary DNA sequence and cDNA samples of leukemia patient.

Modified electrode	**DNA target (aM)**	**Before (I_b µA)**	**After (I_a µA)**	**ΔI (%)**
Biosensor	-	11.89	-	-
Biosensor-DNA target	6.94	-	9.75	21.89
Biosensor-DNA target	694	-	6.68	78.01
Biosensor-DNA target	6 940	-	5.62	111.26
Biosensor-DNA target	69400	-	4.97	138.94
Biosensor-DNA target	694000		4.53	162.54
Biosensor-non complementary DNA	694000	-	11.60	2.46
	Sample dilution factor			
Biosensor	-	11.89	-	-
Biosensor-cDNAsample	1:1	-	2.76	330.71
Biosensor-cDNAsample	1:5	-	4.06	192.85
Biosensor-cDNAsample	1:10	-	4.91	142.21
Biosensor-cDNAsample	1:20	-	6.45	84.11
Biosensor-cDNAsample	1:30	-	8.66	37.26

Biosensor = Cys-cMWCNTs-ZnONps/NH_2-probe-BSA

Table S3. Analytical comparison between the biosensor presented in this work and the other DNA biosensors reported in the literature for the electrochemical detection of the BCR/ABL fusion gene.

Biosensitive nanostructured platform	Analytical technique	Detection time	Detection limit (M)	Reference
Gold surface – Cys – cMWCNTs – ZnONps/NH_2 – aminated DNA probe	CV and EIS	15 min	6.94×10^{-18}	This work
Gold surface – hybrid composite of gold nanoparticles (AuNps) and polyaniline (PANI) – DNA probe	CV and EIS	15 min	69.40×10^{-18}	[1]
Gold surface – thiolated DNA probe (were used amplification probes and CdSeTe/CdS quantum dots tagging)	ASV	~ 18.5 hours	2×10^{-15}	[2]
Carbon paste surface – FePt nanoparticle-decorated electrochemically reduced graphene oxide – DNA probe	EIS	-	2.60×10^{-15}	[3]
ITO coated glass substrate – tri-n-octylphosphine oxide-capped cadmium selenide quantum dots – thiolated DNA probe	DPV	2 min	10×10^{-15}	[4]
Gold surface – thiolated DNA probe (reporter probe labeled biotin)	CV and EIS	60 min	10×10^{-15}	[5]
Glassy carbon surface – poly-eriochrome black T film – AuNps – DNA probe (thiolated hairpin locked nucleic acids)	CV, EIS and DPV	~ 60 min	1×10^{-13}	[6]
Glassy carbon surface – chitosan – cerium dioxide nanoparticles – MWCNT – AuNps – thiolated DNA probe	CV and DPV	55 min	5×10^{-13}	[7]
Glassy carbon surface – aminobenzenesulfonic acid –	CV, EIS and DPV	~ 35 min	9.40×10^{-13}	[8]

aminated DNA probe (18-mer locked nucleic acids)				
ITO surface – silane – cadmium/telluride quantum dots – aminated DNA probe	CV and DPV	-	1×10^{-12}	[9]
Glassy carbon electrode – graphene sheets – PANI – AuNps – thiolated DNA probe	CV, EIS and DPV	~ 90 min	1.05×10^{-12}	[10]
Glassy carbon surface – graphene sheets – chitosan – PANI – AuNps – functionalized hairpin DNA probe (5'-SH and 3'-biotin)	CV, EIS and DPV	~ 2.5 hours	2.11×10^{-12}	[11]
ITO coated glass substrate – nanostructured composite of chitosan and cadmium/telluride quantum dots – aminated DNA probe	CV and DPV	1 min	2.56×10^{-12}	[12]
Glassy carbon surface – aminated DNA probe	CV, EIS and DPV	35 min	3×10^{-12}	[13]
Gold surface – AuNps – DNA probe (thiolated hairpin locked nucleic acids)	CV, EIS and DPV	~ 60 min	1×10^{-10}	[14]
Gold surface – DNA probe (thiolated hairpin locked nucleic acids)	CV, EIS and DPV	~ 60 min	1.20×10^{-10}	[15]
Glassy carbon surface – aminated DNA probe (sodium tanshinone IIA sulfonate used as electrochemical indicator)	CV and DPV	30 min	6.70×10^{-9}	[16]
Glassy carbon surface – aminated DNA probe (2-nitroacridone used as electrochemical indicator)	CV and DPV	30 min	6.70×10^{-9}	[17]
Glassy carbon surface – aminated DNA probe	DPV	35 min	5.90×10^{-8}	[18]

ASV – anodic stripping voltammetry; CV – cyclic voltammetry; DPV – differential pulse voltammetry; EIS – electrochemical impedance spectroscopy.

References

[1] K.Y.P.S. Avelino, I.A.M. Frias, N. Lucena-Silva, R.G. Gomes, C.P. de Melo, M.D.L. Oliveira, et al., Attomolar electrochemical detection of the BCR/ABL fusion gene based on an amplifying self-signal metal nanoparticle-conducting polymer hybrid composite, Colloids and Surfaces B: Biointerfaces, 148(2016) 576-84.
[2] L. Hu, T. Tan, G. Chen, K. Zhang, J.-J. Zhu, Ultrasensitive electrochemical detection of BCR/ABL fusion gene fragment based on polymerase assisted multiplication coupling with quantum dot tagging, Electrochemistry Communications, 35(2013) 104-7.
[3] J. Yang, W. Zhang, Indicator-free impedimetric detection of BCR/ABL fusion gene based on ordered FePt nanoparticle-decorated electrochemically reduced graphene oxide, Journal of Solid State Electrochemistry, 18(2014) 2863-8.
[4] A. Sharma, C.M. Pandey, Z. Matharu, U. Soni, S. Sapra, G. Sumana, et al., Nanopatterned Cadmium Selenide Langmuir–Blodgett Platform for Leukemia Detection, Analytical Chemistry, 84(2012) 3082-9.
[5] K. Wang, J. Chen, J. Chen, A. Liu, G. Li, H. Luo, et al., A Sandwich-Type Electrochemical Biosensor for Detection of BCR/ABL Fusion Gene Using Locked Nucleic Acids on Gold Electrode, Electroanalysis, 21(2009) 1159-66.
[6] L. Lin, J. Chen, Q. Lin, W. Chen, J. Chen, H. Yao, et al., Electrochemical biosensor based on nanogold-modified poly-eriochrome black T film for BCR/ABL fusion gene assay by using hairpin LNA probe, Talanta, 80(2010) 2113-9.
[7] S. Li, L. Wang, Y. Li, X. Zhu, L. Zhong, L. Lu, et al., Electrochemical determination of BCR/ABL fusion gene based on in situ synthesized gold nanoparticles and cerium dioxide nanoparticles, Colloids and Surfaces B: Biointerfaces, 112(2013) 344-9.
[8] J. Chen, J. Zhang, K. Wang, X. Lin, L. Huang, G. Chen, Electrochemical Biosensor for Detection of BCR/ABL Fusion Gene Using Locked Nucleic Acids on 4-Aminobenzenesulfonic Acid-Modified Glassy Carbon Electrode, Analytical Chemistry, 80(2008) 8028-34.
[9] A. Sharma, G. Sumana, S. Sapra, B.D. Malhotra, Quantum Dots Self Assembly Based Interface for Blood Cancer Detection, Langmuir, 29(2013) 8753-62.
[10] X. Chen, L. Wang, S. Sheng, T. Wang, J. Yang, G. Xie, et al., Coupling a universal DNA circuit with graphene sheets/polyaniline/AuNPs nanocomposites for the detection of BCR/ABL fusion gene, Analytica Chimica Acta, 889(2015) 90-7.
[11] L. Wang, E. Hua, M. Liang, C. Ma, Z. Liu, S. Sheng, et al., Graphene sheets, polyaniline and AuNPs based DNA sensor for electrochemical determination of BCR/ABL fusion gene with functional hairpin probe, Biosensors and Bioelectronics, 51(2014) 201-7.
[12] A. Sharma, C.M. Pandey, G. Sumana, U. Soni, S. Sapra, A.K. Srivastava, et al., Chitosan encapsulated quantum dots platform for leukemia detection, Biosensors and Bioelectronics, 38(2012) 107-13.
[13] G.-X. Zhong, J.-X. Ye, F.-Q. Bai, F.-H. Fu, W. Chen, A.-L. Liu, et al., Electrochemical biosensor for detection of BCR/ABL fusion gene based on isorhamnetin as hybridization indicator, Sensors and Actuators B: Chemical, 204(2014) 326-32.
[14] L. Lin, J. Kang, S. Weng, J. Chen, A. Liu, X. Lin, et al., Locked nucleic acids biosensor for detection of BCR/ABL fusion gene using benzoate binuclear copper (II) complex as hybridization indicator, Sensors and Actuators B: Chemical, 155(2011) 1-7.
[15] L. Lin, X. Lin, J. Chen, W. Chen, M. He, Y. Chen, Electrochemical biosensor for detection of BCR/ABL fusion gene based on hairpin locked nucleic acids probe, Electrochemistry Communications, 11(2009) 1650-3.
[16] J. Chen, J. Zhang, Q. Zhuang, J. Chen, X. Lin, Hybridization biosensor using sodium tanshinone IIA sulfonate as electrochemical indicator for detection of short DNA species of chronic myelogenous leukemia, Electrochimica Acta, 53(2008) 2716-23.

[17] J. Chen, J. Zhang, L. Huang, X. Lin, G. Chen, Hybridization biosensor using 2-nitroacridone as electrochemical indicator for detection of short DNA species of Chronic Myelogenous Leukemia, Biosensors and Bioelectronics, 24(2008) 349-55.
[18] X.-H. Lin, P. Wu, W. Chen, Y.-F. Zhang, X.-H. Xia, Electrochemical DNA biosensor for the detection of short DNA species of Chronic Myelogenous Leukemia by using methylene blue, Talanta, 72(2007) 468-71.

CAPÍTULO 10

10 ANEXOS

10.1 Anexo A – Diretrizes da revista *Sensors and Actuators B: Chemical*

SENSORS AND ACTUATORS B: CHEMICAL

An international journal devoted to research and development of chemical transducers

ELSEVIER

AUTHOR INFORMATION PACK

TABLE OF CONTENTS

ISSN: 0925-4005

DESCRIPTION

Sensors & Actuators, B: Chemical is an interdisciplinary journal dedicated to covering research and development in the field of **chemical sensors**, **actuators** and **microsystems**.

The scope of the journal encompasses, but is not restricted to, the following areas:
- Sensing principles and mechanisms
- New materials development (transducers and sensitive/recognition components)
- Fabrication technology
- Actuators
- Optical devices
- Electrochemical devices
- Mass-sensitive devices
- Gas sensors
- Biosensors
- Analytical microsystems
- Environmental, process control and biomedical applications
- Signal processing
- Sensor and sensor-array chemometrics

μTAS - Micro Total Analysis Systems: Microsystems for the generation, handling and analysis of (bio)chemical information

The special section of *Sensors & Actuators, B: Chemical* on **micro TAS** is dedicated to contributions concerning miniaturised systems for (bio)chemical synthesis and analysis, also comprising work on Bio-MEMS, Lab-on-a-chip, biochips and microfluidics.

Topics covered by the micro TAS section include:
- Physics and chemistry of microfluidics
- Microfabrication technology for micro TAS
- Analytical chemical aspects
- Detectors, sensors, arrays for micro TAS
- Micro TAS applications
- DNA analysis
- Microinstrumentation
- Microsystems for combinatorial chemistry.

AUDIENCE

Academic and Industrial Researchers in Analytical Chemistry and Instrument Development

IMPACT FACTOR

2015: 4.758 © Thomson Reuters Journal Citation Reports 2016

ABSTRACTING AND INDEXING

Analytical Abstracts
Cambridge Scientific Abstracts
Chemical Abstracts
Compendex
Computer and Control Abstracts
Current Contents
Metals Abstracts
EIC/Intelligence
Electrical and Electronics Abstracts
Engineered Materials Abstracts
Engineering Index
FIZ Karlsruhe
PASCAL/CNRS
Physics Abstracts
Science Citation Index
Scopus

EDITORIAL BOARD

Fluorescence spectroscopy, Time-resolved fluorescence; Oxygen sensors; Sensor material chemistry.
G. Rivas, Universidad Nacional de Córdoba, Córdoba, Argentina
Electrochemical devices; Electrochemical (bio)sensors; Enzymatic biosensors; Affinity biosensors; Biocatalytic sensors; DNA biosensors; Hybridization and DNA-damage biosensors; Immunosensors; Aptasensors, Glycobiosensors. (Bio)Sensing principles. Nanobiotechnology and Nanobiomedicine: (bio)sensors based on nanomaterials (carbon nanotubes, graphene and related materials, nanoparticles). Neurotransmitters sensors. Biomarkers Sensors. Modified electrodes. Surface plasmon resonance biosensors. Biomedical and Environmental applications
Y. Shimizu, Nagasaki University, Nagasaki, Japan
Semiconductor gas sensors including metal oxide-based and polymer-based gas sensors, humidity sensors based on any principles, Sensing principles and mechanisms of semiconductor gas sensors, Nanstructured materials and carbon-based materials for gas sensor applications.
M. Tokeshi, Hokkaido University, Sapporo, Japan
Microfluidics, Biosensors.
U. Weimar, Eberhard-Karls-Universität Tübingen, Tübingen, Germany
Chemical sensor systems, data processing of chemical sensor systems, related pattern recognition and multi-component analysis, electronic noses, application of chemical sensor systems. Metal-oxide chemical gas sensors, polymer based chemical gas sensors, innovative gas sensor solutions, sensing principles and mechanisms.

Editorial Board

GUIDE FOR AUTHORS

Your Paper Your Way

We now differentiate between the requirements for new and revised submissions. You may choose to submit your manuscript as a single Word or PDF file to be used in the refereeing process. Only when your paper is at the revision stage, will you be requested to put your paper in to a 'correct format' for acceptance and provide the items required for the publication of your article.
To find out more, please visit the Preparation section below.

Aims and Scope

Sensors & Actuators, B: Chemical is an interdisciplinary journal dedicated to covering research and development in the field of chemical sensors, actuators, micro- and nanosystems.
The scope of the journal encompasses, but is not restricted to, the following areas:

- Sensing principles and mechanisms
- New materials development (transducers and sensitive/recognition components)
- Fabrication technology including nanotechnology
- Actuators
- Optical devices
- Electrochemical devices
- Mass-sensitive devices
- Gas sensors
- Biosensors
- Bio-MEMS
- Analytical microsystems
- Environmental
- Process control
- Biomedical applications
- Signal processing
- Sensor and sensor-array chemometrics

μTAS - Micro Total Analysis Systems *Microsystems for the generation, handling and analysis of (bio)chemical information*. The special section of Sensors & Actuators, B: Chemical on μTAS is dedicated to contributions concerning miniaturised systems for (bio)chemical synthesis and analysis, also comprising work on Bio-MEMS, Lab-on-a-chip, biochips and *microfluidics*.

Topics covered by the μTAS section include:

- Lab-on-a-chip
- Physics and chemistry of microfluidics
- Microfabrication technology for μTAS
- Analytical chemical aspects
- Detectors, sensors, arrays for μTAS
- μTAS applications
- DNA analysis
- Microinstrumentation
- Microsystems for combinatorial chemistry

Types of paper

Sensors and Actuators B: Chemical, welcomes full length research papers and review articles, and short communications. Full length papers should in general not exceed 5000 words or about 12 printed pages including tables and diagrams. Short communications should not exceed 2000 words or 4 printed pages. For all contributions the acceptance criteria are quality, originality, and scientific and technological relevance to the field. An adequate referencing to the state-of-the-art is essential.

Submission checklist

You can use this list to carry out a final check of your submission before you send it to the journal for review. Please check the relevant section in this Guide for Authors for more details.

Ensure that the following items are present:

One author has been designated as the corresponding author with contact details:

- E-mail address

• Full postal address

All necessary files have been uploaded:
Manuscript:
• Include keywords
• All figures (include relevant captions)
• All tables (including titles, description, footnotes)
• Ensure all figure and table citations in the text match the files provided
• Indicate clearly if color should be used for any figures in print
Graphical Abstracts / Highlights files (where applicable)
Supplemental files (where applicable)

Further considerations
• Manuscript has been 'spell checked' and 'grammar checked'
• All references mentioned in the Reference List are cited in the text, and vice versa
• Permission has been obtained for use of copyrighted material from other sources (including the Internet)
• Relevant declarations of interest have been made
• Journal policies detailed in this guide have been reviewed
• Referee suggestions and contact details provided, based on journal requirements

For further information, visit our Support Center.

BEFORE YOU BEGIN

Ethics in publishing

Please see our information pages on Ethics in publishing and Ethical guidelines for journal publication.

Declaration of interest

All authors are requested to disclose any actual or potential conflict of interest including any financial, personal or other relationships with other people or organizations within three years of beginning the submitted work that could inappropriately influence, or be perceived to influence, their work. More information.

Submission declaration and verification

Submission of an article implies that the work described has not been published previously (except in the form of an abstract or as part of a published lecture or academic thesis or as an electronic preprint, see 'Multiple, redundant or concurrent publication' section of our ethics policy for more information), that it is not under consideration for publication elsewhere, that its publication is approved by all authors and tacitly or explicitly by the responsible authorities where the work was carried out, and that, if accepted, it will not be published elsewhere in the same form, in English or in any other language, including electronically without the written consent of the copyright-holder. To verify originality, your article may be checked by the originality detection service CrossCheck.

Changes to authorship

Authors are expected to consider carefully the list and order of authors **before** submitting their manuscript and provide the definitive list of authors at the time of the original submission. Any addition, deletion or rearrangement of author names in the authorship list should be made only **before** the manuscript has been accepted and only if approved by the journal Editor. To request such a change, the Editor must receive the following from the **corresponding author**: (a) the reason for the change in author list and (b) written confirmation (e-mail, letter) from all authors that they agree with the addition, removal or rearrangement. In the case of addition or removal of authors, this includes confirmation from the author being added or removed.
Only in exceptional circumstances will the Editor consider the addition, deletion or rearrangement of authors **after** the manuscript has been accepted. While the Editor considers the request, publication of the manuscript will be suspended. If the manuscript has already been published in an online issue, any requests approved by the Editor will result in a corrigendum.

Article transfer service
This journal is part of our Article Transfer Service. This means that if the Editor feels your article is more suitable in one of our other participating journals, then you may be asked to consider transferring the article to one of those. If you agree, your article will be transferred automatically on your behalf with no need to reformat. Please note that your article will be reviewed again by the new journal. More information.

Copyright

Upon acceptance of an article, authors will be asked to complete a 'Journal Publishing Agreement' (see more information on this). An e-mail will be sent to the corresponding author confirming receipt of the manuscript together with a 'Journal Publishing Agreement' form or a link to the online version of this agreement.

Subscribers may reproduce tables of contents or prepare lists of articles including abstracts for internal circulation within their institutions. Permission of the Publisher is required for resale or distribution outside the institution and for all other derivative works, including compilations and translations. If excerpts from other copyrighted works are included, the author(s) must obtain written permission from the copyright owners and credit the source(s) in the article. Elsevier has preprinted forms for use by authors in these cases.

For open access articles: Upon acceptance of an article, authors will be asked to complete an 'Exclusive License Agreement' (more information). Permitted third party reuse of open access articles is determined by the author's choice of user license.

Author rights
As an author you (or your employer or institution) have certain rights to reuse your work. More information.

Elsevier supports responsible sharing
Find out how you can share your research published in Elsevier journals.

Role of the funding source

You are requested to identify who provided financial support for the conduct of the research and/or preparation of the article and to briefly describe the role of the sponsor(s), if any, in study design; in the collection, analysis and interpretation of data; in the writing of the report; and in the decision to submit the article for publication. If the funding source(s) had no such involvement then this should be stated.

Funding body agreements and policies
Elsevier has established a number of agreements with funding bodies which allow authors to comply with their funder's open access policies. Some funding bodies will reimburse the author for the Open Access Publication Fee. Details of existing agreements are available online.

Open access

This journal offers authors a choice in publishing their research:

Open access
- Articles are freely available to both subscribers and the wider public with permitted reuse.
- An open access publication fee is payable by authors or on their behalf, e.g. by their research funder or institution.

Subscription
- Articles are made available to subscribers as well as developing countries and patient groups through our universal access programs.
- No open access publication fee payable by authors.

Regardless of how you choose to publish your article, the journal will apply the same peer review criteria and acceptance standards.

For open access articles, permitted third party (re)use is defined by the following Creative Commons user licenses:

Creative Commons Attribution (CC BY)
Lets others distribute and copy the article, create extracts, abstracts, and other revised versions, adaptations or derivative works of or from an article (such as a translation), include in a collective work (such as an anthology), text or data mine the article, even for commercial purposes, as long as they credit the author(s), do not represent the author as endorsing their adaptation of the article, and do not modify the article in such a way as to damage the author's honor or reputation.

Creative Commons Attribution-NonCommercial-NoDerivs (CC BY-NC-ND)
For non-commercial purposes, lets others distribute and copy the article, and to include in a collective work (such as an anthology), as long as they credit the author(s) and provided they do not alter or modify the article.

The open access publication fee for this journal is **USD 3100**, excluding taxes. Learn more about Elsevier's pricing policy: https://www.elsevier.com/openaccesspricing.

Green open access
Authors can share their research in a variety of different ways and Elsevier has a number of green open access options available. We recommend authors see our green open access page for further information. Authors can also self-archive their manuscripts immediately and enable public access from their institution's repository after an embargo period. This is the version that has been accepted for publication and which typically includes author-incorporated changes suggested during submission, peer review and in editor-author communications. Embargo period: For subscription articles, an appropriate amount of time is needed for journals to deliver value to subscribing customers before an article becomes freely available to the public. This is the embargo period and it begins from the date the article is formally published online in its final and fully citable form. Find out more.

This journal has an embargo period of 24 months.

Elsevier Publishing Campus
The Elsevier Publishing Campus (www.publishingcampus.com) is an online platform offering free lectures, interactive training and professional advice to support you in publishing your research. The College of Skills training offers modules on how to prepare, write and structure your article and explains how editors will look at your paper when it is submitted for publication. Use these resources, and more, to ensure that your submission will be the best that you can make it.

Language (usage and editing services)
Please write your text in good English (American or British usage is accepted, but not a mixture of these). Authors who feel their English language manuscript may require editing to eliminate possible grammatical or spelling errors and to conform to correct scientific English may wish to use the English Language Editing service available from Elsevier's WebShop.

Submission

Our online submission system guides you stepwise through the process of entering your article details and uploading your files. The system converts your article files to a single PDF file used in the peer-review process. Editable files (e.g., Word, LaTeX) are required to typeset your article for final publication. All correspondence, including notification of the Editor's decision and requests for revision, is sent by e-mail.

Please sunmit your article via http://www.elsevier.com/locate/snb

Referees
Authors are required to submit the names, addresses and e-mail addresses of five potential reviewers who could objectively review their manuscripts if asked to do so by the journal editors. The editor retains the sole right to decide whether or not the suggested reviewers are used. Please note that if no reviewer names are submitted, publication of your manuscript may be delayed.

PREPARATION

Use of word processing software
It is important that the file be saved in the native format of the word processor used. The text should be in single-column format. Keep the layout of the text as simple as possible. Most formatting codes will be removed and replaced on processing the article. In particular, do not use the word processor's options to justify text or to hyphenate words. However, do use bold face, italics, subscripts, superscripts etc. When preparing tables, if you are using a table grid, use only one grid for each individual table and not a grid for each row. If no grid is used, use tabs, not spaces, to align columns. The electronic text should be prepared in a way very similar to that of conventional manuscripts (see

also the Guide to Publishing with Elsevier). Note that source files of figures, tables and text graphics will be required whether or not you embed your figures in the text. See also the section on Electronic artwork.
To avoid unnecessary errors you are strongly advised to use the 'spell-check' and 'grammar-check' functions of your word processor.

Article structure

Subdivision - numbered sections
Divide your article into clearly defined and numbered sections. Subsections should be numbered 1.1 (then 1.1.1, 1.1.2, ...), 1.2, etc. (the abstract is not included in section numbering). Use this numbering also for internal cross-referencing: do not just refer to 'the text'. Any subsection may be given a brief heading. Each heading should appear on its own separate line.

Introduction
State the objectives of the work and provide an adequate background, avoiding a detailed literature survey or a summary of the results.

Material and methods
Provide sufficient detail to allow the work to be reproduced. Methods already published should be indicated by a reference: only relevant modifications should be described.

Results
Results should be clear and concise.

Discussion
This should explore the significance of the results of the work, not repeat them. A combined Results and Discussion section is often appropriate. Avoid extensive citations and discussion of published literature.

Conclusions
The main conclusions of the study may be presented in a short Conclusions section, which may stand alone or form a subsection of a Discussion or Results and Discussion section.

Appendices
If there is more than one appendix, they should be identified as A, B, etc. Formulae and equations in appendices should be given separate numbering: Eq. (A.1), Eq. (A.2), etc.; in a subsequent appendix, Eq. (B.1) and so on. Similarly for tables and figures: Table A.1; Fig. A.1, etc.

Essential title page information

• ***Title.*** Concise and informative. Titles are often used in information-retrieval systems. Avoid abbreviations and formulae where possible.
• ***Author names and affiliations.*** Please clearly indicate the given name(s) and family name(s) of each author and check that all names are accurately spelled. Present the authors' affiliation addresses (where the actual work was done) below the names. Indicate all affiliations with a lower-case superscript letter immediately after the author's name and in front of the appropriate address. Provide the full postal address of each affiliation, including the country name and, if available, the e-mail address of each author.
• ***Corresponding author.*** Clearly indicate who will handle correspondence at all stages of refereeing and publication, also post-publication. **Ensure that the e-mail address is given and that contact details are kept up to date by the corresponding author.**
• ***Present/permanent address.*** If an author has moved since the work described in the article was done, or was visiting at the time, a 'Present address' (or 'Permanent address') may be indicated as a footnote to that author's name. The address at which the author actually did the work must be retained as the main, affiliation address. Superscript Arabic numerals are used for such footnotes.

Abstract

A concise and factual abstract is required. The abstract should state briefly the purpose of the research, the principal results and major conclusions. An abstract is often presented separately from the article, so it must be able to stand alone. For this reason, References should be avoided, but if essential, then cite the author(s) and year(s). Also, non-standard or uncommon abbreviations should be avoided, but if essential they must be defined at their first mention in the abstract itself.

Highlights
Highlights are mandatory for this journal. They consist of a short collection of bullet points that convey the core findings of the article and should be submitted in a separate editable file in the online submission system. Please use 'Highlights' in the file name and include 3 to 5 bullet points (maximum 85 characters, including spaces, per bullet point). You can view example Highlights on our information site.

Keywords

Immediately after the abstract, provide a maximum of 6 keywords, using American spelling and avoiding general and plural terms and multiple concepts (avoid, for example, 'and', 'of'). Be sparing with abbreviations: only abbreviations firmly established in the field may be eligible. These keywords will be used for indexing purposes.

Abbreviations
Define abbreviations that are not standard in this field in a footnote to be placed on the first page of the article. Such abbreviations that are unavoidable in the abstract must be defined at their first mention there, as well as in the footnote. Ensure consistency of abbreviations throughout the article.

Acknowledgements
Collate acknowledgements in a separate section at the end of the article before the references and do not, therefore, include them on the title page, as a footnote to the title or otherwise. List here those individuals who provided help during the research (e.g., providing language help, writing assistance or proof reading the article, etc.).

Formatting of funding sources
List funding sources in this standard way to facilitate compliance to funder's requirements:

Funding: This work was supported by the National Institutes of Health [grant numbers xxxx, yyyy]; the Bill & Melinda Gates Foundation, Seattle, WA [grant number zzzz]; and the United States Institutes of Peace [grant number aaaa].

It is not necessary to include detailed descriptions on the program or type of grants and awards. When funding is from a block grant or other resources available to a university, college, or other research institution, submit the name of the institute or organization that provided the funding.

If no funding has been provided for the research, please include the following sentence:

This research did not receive any specific grant from funding agencies in the public, commercial, or not-for-profit sectors.

Math formulae
Please submit math equations as editable text and not as images. Present simple formulae in line with normal text where possible and use the solidus (/) instead of a horizontal line for small fractional terms, e.g., X/Y. In principle, variables are to be presented in italics. Powers of e are often more conveniently denoted by exp. Number consecutively any equations that have to be displayed separately from the text (if referred to explicitly in the text).

Footnotes
Footnotes should be used sparingly. Number them consecutively throughout the article. Many word processors can build footnotes into the text, and this feature may be used. Otherwise, please indicate the position of footnotes in the text and list the footnotes themselves separately at the end of the article. Do not include footnotes in the Reference list.

Artwork

Electronic artwork
General points
- Make sure you use uniform lettering and sizing of your original artwork.
- Embed the used fonts if the application provides that option.
- Aim to use the following fonts in your illustrations: Arial, Courier, Times New Roman, Symbol, or use fonts that look similar.
- Number the illustrations according to their sequence in the text.
- Use a logical naming convention for your artwork files.
- Provide captions to illustrations separately.
- Size the illustrations close to the desired dimensions of the published version.

• Submit each illustration as a separate file.
A detailed guide on electronic artwork is available.
You are urged to visit this site; some excerpts from the detailed information are given here.
Formats
If your electronic artwork is created in a Microsoft Office application (Word, PowerPoint, Excel) then please supply 'as is' in the native document format.
Regardless of the application used other than Microsoft Office, when your electronic artwork is finalized, please 'Save as' or convert the images to one of the following formats (note the resolution requirements for line drawings, halftones, and line/halftone combinations given below):
EPS (or PDF): Vector drawings, embed all used fonts.
TIFF (or JPEG): Color or grayscale photographs (halftones), keep to a minimum of 300 dpi.
TIFF (or JPEG): Bitmapped (pure black & white pixels) line drawings, keep to a minimum of 1000 dpi.
TIFF (or JPEG): Combinations bitmapped line/half-tone (color or grayscale), keep to a minimum of 500 dpi.
Please do not:
• Supply files that are optimized for screen use (e.g., GIF, BMP, PICT, WPG); these typically have a low number of pixels and limited set of colors;
• Supply files that are too low in resolution;
• Submit graphics that are disproportionately large for the content.

Color artwork
Please make sure that artwork files are in an acceptable format (TIFF (or JPEG), EPS (or PDF), or MS Office files) and with the correct resolution. If, together with your accepted article, you submit usable color figures then Elsevier will ensure, at no additional charge, that these figures will appear in color online (e.g., ScienceDirect and other sites) regardless of whether or not these illustrations are reproduced in color in the printed version. **For color reproduction in print, you will receive information regarding the costs from Elsevier after receipt of your accepted article**. Please indicate your preference for color: in print or online only. Further information on the preparation of electronic artwork.

Figure captions
Ensure that each illustration has a caption. Supply captions separately, not attached to the figure. A caption should comprise a brief title (**not** on the figure itself) and a description of the illustration. Keep text in the illustrations themselves to a minimum but explain all symbols and abbreviations used.

Tables

Please submit tables as editable text and not as images. Tables can be placed either next to the relevant text in the article, or on separate page(s) at the end. Number tables consecutively in accordance with their appearance in the text and place any table notes below the table body. Be sparing in the use of tables and ensure that the data presented in them do not duplicate results described elsewhere in the article. Please avoid using vertical rules and shading in table cells.

References

Citation in text
Please ensure that every reference cited in the text is also present in the reference list (and vice versa). Any references cited in the abstract must be given in full. Unpublished results and personal communications are not recommended in the reference list, but may be mentioned in the text. If these references are included in the reference list they should follow the standard reference style of the journal and should include a substitution of the publication date with either 'Unpublished results' or 'Personal communication'. Citation of a reference as 'in press' implies that the item has been accepted for publication.

Reference links
Increased discoverability of research and high quality peer review are ensured by online links to the sources cited. In order to allow us to create links to abstracting and indexing services, such as Scopus, CrossRef and PubMed, please ensure that data provided in the references are correct. Please note that incorrect surnames, journal/book titles, publication year and pagination may prevent link creation. When copying references, please be careful as they may already contain errors. Use of the DOI is encouraged.

A DOI can be used to cite and link to electronic articles where an article is in-press and full citation details are not yet known, but the article is available online. A DOI is guaranteed never to change, so you can use it as a permanent link to any electronic article. An example of a citation using DOI

for an article not yet in an issue is: VanDecar J.C., Russo R.M., James D.E., Ambeh W.B., Franke M. (2003). Aseismic continuation of the Lesser Antilles slab beneath northeastern Venezuela. Journal of Geophysical Research, http://dx.doi.org/10.1029/2001JB000884i. Please note the format of such citations should be in the same style as all other references in the paper.

Web references
As a minimum, the full URL should be given and the date when the reference was last accessed. Any further information, if known (DOI, author names, dates, reference to a source publication, etc.), should also be given. Web references can be listed separately (e.g., after the reference list) under a different heading if desired, or can be included in the reference list.

Data references
This journal encourages you to cite underlying or relevant datasets in your manuscript by citing them in your text and including a data reference in your Reference List. Data references should include the following elements: author name(s), dataset title, data repository, version (where available), year, and global persistent identifier. Add [dataset] immediately before the reference so we can properly identify it as a data reference. The [dataset] identifier will not appear in your published article.

References in a special issue
Please ensure that the words 'this issue' are added to any references in the list (and any citations in the text) to other articles in the same Special Issue.

Reference management software
Most Elsevier journals have their reference template available in many of the most popular reference management software products. These include all products that support Citation Style Language styles, such as Mendeley and Zotero, as well as EndNote. Using the word processor plug-ins from these products, authors only need to select the appropriate journal template when preparing their article, after which citations and bibliographies will be automatically formatted in the journal's style. If no template is yet available for this journal, please follow the format of the sample references and citations as shown in this Guide.

Users of Mendeley Desktop can easily install the reference style for this journal by clicking the following link:
http://open.mendeley.com/use-citation-style/sensors-and-actuators-b-chemical
When preparing your manuscript, you will then be able to select this style using the Mendeley plug-ins for Microsoft Word or LibreOffice.

Reference formatting
There are no strict requirements on reference formatting at submission. References can be in any style or format as long as the style is consistent. Where applicable, author(s) name(s), journal title/book title, chapter title/article title, year of publication, volume number/book chapter and the pagination must be present. Use of DOI is highly encouraged. The reference style used by the journal will be applied to the accepted article by Elsevier at the proof stage. Note that missing data will be highlighted at proof stage for the author to correct. If you do wish to format the references yourself they should be arranged according to the following examples:

Reference style
Text: Indicate references by number(s) in square brackets in line with the text. The actual authors can be referred to, but the reference number(s) must always be given.
Example: '..... as demonstrated [3,6]. Barnaby and Jones [8] obtained a different result ....'
List: Number the references (numbers in square brackets) in the list in the order in which they appear in the text.
Examples:
Reference to a journal publication:
[1] J. van der Geer, J.A.J. Hanraads, R.A. Lupton, The art of writing a scientific article, J. Sci. Commun. 163 (2010) 51–59.
Reference to a book:
[2] W. Strunk Jr., E.B. White, The Elements of Style, fourth ed., Longman, New York, 2000.
Reference to a chapter in an edited book:
[3] G.R. Mettam, L.B. Adams, How to prepare an electronic version of your article, in: B.S. Jones, R.Z. Smith (Eds.), Introduction to the Electronic Age, E-Publishing Inc., New York, 2009, pp. 281–304.
Reference to a website:
[4] Cancer Research UK, Cancer statistics reports for the UK. http://www.cancerresearchuk.org/aboutcancer/statistics/cancerstatsreport/, 2003 (accessed 13.03.03).

Reference to a dataset:
[dataset] [5] M. Oguro, S. Imahiro, S. Saito, T. Nakashizuka, Mortality data for Japanese oak wilt disease and surrounding forest compositions, Mendeley Data, v1, 2015. http://dx.doi.org/10.17632/xwj98nb39r.1.

Journal abbreviations source
Journal names should be abbreviated according to the List of Title Word Abbreviations.

Video
Elsevier accepts video material and animation sequences to support and enhance your scientific research. Authors who have video or animation files that they wish to submit with their article are strongly encouraged to include links to these within the body of the article. This can be done in the same way as a figure or table by referring to the video or animation content and noting in the body text where it should be placed. All submitted files should be properly labeled so that they directly relate to the video file's content. In order to ensure that your video or animation material is directly usable, please provide the files in one of our recommended file formats with a preferred maximum size of 150 MB. Video and animation files supplied will be published online in the electronic version of your article in Elsevier Web products, including ScienceDirect. Please supply 'stills' with your files: you can choose any frame from the video or animation or make a separate image. These will be used instead of standard icons and will personalize the link to your video data. For more detailed instructions please visit our video instruction pages. Note: since video and animation cannot be embedded in the print version of the journal, please provide text for both the electronic and the print version for the portions of the article that refer to this content.

Supplementary material
Supplementary material such as applications, images and sound clips, can be published with your article to enhance it. Submitted supplementary items are published exactly as they are received (Excel or PowerPoint files will appear as such online). Please submit your material together with the article and supply a concise, descriptive caption for each supplementary file. If you wish to make changes to supplementary material during any stage of the process, please make sure to provide an updated file. Do not annotate any corrections on a previous version. Please switch off the 'Track Changes' option in Microsoft Office files as these will appear in the published version.

Data linking
If you have made your research data available in a data repository, you can link your article directly to the dataset. Elsevier collaborates with a number of repositories to link articles on ScienceDirect with relevant repositories, giving readers access to underlying data that give them a better understanding of the research described.

There are different ways to link your datasets to your article. When available, you can directly link your dataset to your article by providing the relevant information in the submission system. For more information, visit the database linking page.

For supported data repositories a repository banner will automatically appear next to your published article on ScienceDirect.

In addition, you can link to relevant data or entities through identifiers within the text of your manuscript, using the following format: Database: xxxx (e.g., TAIR: AT1G01020; CCDC: 734053; PDB: 1XFN).

AudioSlides
The journal encourages authors to create an AudioSlides presentation with their published article. AudioSlides are brief, webinar-style presentations that are shown next to the online article on ScienceDirect. This gives authors the opportunity to summarize their research in their own words and to help readers understand what the paper is about. More information and examples are available. Authors of this journal will automatically receive an invitation e-mail to create an AudioSlides presentation after acceptance of their paper.

Interactive plots
This journal enables you to show an Interactive Plot with your article by simply submitting a data file. Full instructions.

AFTER ACCEPTANCE

Online proof correction

Corresponding authors will receive an e-mail with a link to our online proofing system, allowing annotation and correction of proofs online. The environment is similar to MS Word: in addition to editing text, you can also comment on figures/tables and answer questions from the Copy Editor. Web-based proofing provides a faster and less error-prone process by allowing you to directly type your corrections, eliminating the potential introduction of errors.

If preferred, you can still choose to annotate and upload your edits on the PDF version. All instructions for proofing will be given in the e-mail we send to authors, including alternative methods to the online version and PDF.

We will do everything possible to get your article published quickly and accurately. Please use this proof only for checking the typesetting, editing, completeness and correctness of the text, tables and figures. Significant changes to the article as accepted for publication will only be considered at this stage with permission from the Editor. It is important to ensure that all corrections are sent back to us in one communication. Please check carefully before replying, as inclusion of any subsequent corrections cannot be guaranteed. Proofreading is solely your responsibility.

Offprints

The corresponding author will, at no cost, receive a customized Share Link providing 50 days free access to the final published version of the article on ScienceDirect. The Share Link can be used for sharing the article via any communication channel, including email and social media. For an extra charge, paper offprints can be ordered via the offprint order form which is sent once the article is accepted for publication. Both corresponding and co-authors may order offprints at any time via Elsevier's Webshop. Corresponding authors who have published their article open access do not receive a Share Link as their final published version of the article is available open access on ScienceDirect and can be shared through the article DOI link.

AUTHOR INQUIRIES

Visit the Elsevier Support Center to find the answers you need. Here you will find everything from Frequently Asked Questions to ways to get in touch.

You can also check the status of your submitted article or find out when your accepted article will be published.